

REPORT DOCUMENTATION PAGE

Public reporting burden for this collection of information is estimated to average 1 hour per response, including the time for reviewing instructions, searching existing data sources, gathering the data needed, and completing and reviewing this collection of information. Send comments regarding this burden estimate or any other aspect of this collection of information, including suggestions for reducing this burden to Washington Headquarters Services, Directorate for Information Operations and Reports (0704-0188). Respondents should be aware that notwithstanding any other provision of law, no person shall be subject to any penalty for failing to comply with a collection of information if it does not display a currently valid OMB control number. PLEASE DO NOT RETURN YOUR FORM TO THE ABOVE ADDRESS.

AFRL-SR-AR-TR-02-

0797

1. REPORT DATE (DD-MM-YYYY) 31 - 05 - 2002		2. REPORT TYPE Final Technical Report		3. DATES COVERED (from - to) 01 Mar 1999 to 31 May 2002	
4. TITLE AND SUBTITLE Electromagnetic Scattering from Multiple Scale Geometries				5a. CONTRACT NUMBER 287th 02 F49620-99-C-0014	
				5b. GRANT NUMBER	
				5c. PROGRAM ELEMENT NUMBER	
6. AUTHOR(S) Maria Z Caponi Alain Sei				5d. PROJECT NUMBER FQ8671-9900630 G550/00	
				5e. TASK NUMBER	
				5f. WORK UNIT NUMBER	
7. PERFORMING ORGANIZATION NAME(S) AND ADDRESS(ES) AND ADDRESS(ES) TRW Space and Electronics Group 1, Space Park, MS R1-1008 Redondo Beach, CA 90278				8. PERFORMING ORGANIZATION REPORT NUMBER 1A570-0001-UT-01	
9. SPONSORING / MONITORING AGENCY NAME(S) AND ADDRESS(ES) USAF, AFMC Air Force Office of Scientific Research 801 North Randolph St, Room 732 Arlington, VA 22203-1977				10. SPONSOR/MONITOR'S ACRONYM(S)	
12. DISTRIBUTION / AVAILABILITY STATEMENT A - Approved for public release; distribution unlimited					
13. SUPPLEMENTARY NOTES					
14. ABSTRACT This final technical report describes the development, implementation, numerical validation and potential exploitation of an accurate and efficient scattering solvers to compute the horizontal (TE mode) and vertical (TM mode) polarization returns from multi-scale surfaces. This modeling effort was motivated by a large number of remote sensing applications that require the characterization by means of radar scattering measurements of the scattering surface configuration or variations in the surface patterns for detection or environmental purposes. The nature of the relevant scattering surfaces and the measured scattered fields drives the need for an extremely accurate scattering solver able to deal with multi-scale surfaces in an efficient manner. This objective was achieved by using a combination of perturbation and asymptotic expansions and an innovative and careful implementation of these expansions for full double precision accuracy. The Fourier series representations used in this problem allowed for very efficient computations due the relatively small order of these series in typical cases. HH and VV polarization have been implemented and allow the rigorous investigation of critical remote sensing problems.					
15. SUBJECT TERMS Electromagnetic Scattering, Rough Surface, Ocean scattering, Numerical Methods, High Frequency					
16. SECURITY CLASSIFICATION OF: UNCLASSIFIED			17. LIMITATION OF ABSTRACT UL	18. NUMBER OF PAGES	19a. NAME OF RESPONSIBLE PERSON
a. REPORT UNCLASSIFIED	b. ABSTRACT UNCLASSIFIED	c. THIS PAGE UNCLASSIFIED			19b. TELEPHONE NUMBER (include area code)

20020702 040

Electromagnetic Scattering from Multiple Scale Geometries

Executive Summary

This final report describes the development, implementation, numerical validation and potential exploitation of a highly accurate and efficient scattering solver to compute the horizontal (TE mode) and vertical (TM mode) polarized returns from multi-scale surfaces for ocean remote sensing applications. A large number of remote sensing applications require the characterization by means of radar scattering measurements of the scattering surface configuration or variations in the surface patterns for detection or environmental purposes. In particular, for applications associated with ocean remote sensing appropriate exploitation of the experimental measurements requires a detailed knowledge of the relation between the characteristics of surface waves and their variation with environmental parameters, and the properties of observables, such as polarized return power and Doppler spectrum. Relevant ocean geometries include more than one dominant scale and recent results have shown that the number of scales included in the problem and the accuracy of the computation can strongly affect the prediction of modeled polarized radar backscattering returns cf. [Sei et al, 1999]. The standard models used to predict ocean backscatter returns usually resort to simplified two-scale model and zero or first order computations [Valenzuela, 1978]. These models are unable to predict recent significant experimental results demonstrating that horizontally (TE mode) polarized radar backscatter returns can intermittently exceed vertical (TM mode) polarized returns at low grazing angles. Furthermore, the experimental measurements of the normalized backscattered returns are generally in the -60-dB to -100-dB range [Lee et al, 1997b], demonstrating the need for a scattering model with a relative accuracy of at least 10 digits. These requirements, the complexity and multitude of scales present on the application of interest as well as the absence of satisfactory scattering algorithms in the existing literature motivated this project and an approach that emphasizes the use of high order methods to achieve accurate and fast, versatile and user-friendly computations. The successful approach to the solution of such a numerical challenge is based on innovative mathematical methods as well as their very careful implementations to obtain double precision accuracy. The mathematical methods developed for this problem are based on a combination of high order asymptotic and perturbation methods and their implementation is based on the development of libraries for the manipulation of Taylor-Fourier series. This final report provides a complete description of the mathematical methods and their implementation as well as their potential exploitation for ocean remote sensing. Technical details will often be referred to already published work. Finally the source code as well as a guide for its compilation and implementation is provided in the accompanying floppy disk.

1.1 Introduction

A large number of remote sensing applications entail the characterization by means of radar scattering measurements of the scattering surface configuration or variations in the surface patterns for detection or environmental purposes. In particular, appropriate exploitation of sensor measurements for ocean remote sensing applications require an in depth knowledge of the relation between the characteristics of surface waves and their variation with environmental parameters, and the properties of observables, such as polarized return power and Doppler spectrum. The electromagnetic scattering from multiple scale geometries (ESMSG) project detailed in this report focuses on the development, implementation and numerical validation of highly accurate and efficient scattering solvers to compute the horizontal (TE mode) and vertical (TM mode) polarization returns from multi-scale surfaces for utilization in ocean radar remote sensing applications as well as potential extensions to terrain remote sensing. Specific ocean radar remote sensing applications of interest include ocean spectrum characterization for wind speed and direction prediction, ship wake detection and ocean bottom topography and or internal current determination.

Ocean specific pattern variations can occur when internal waves created by submerged objects or bottom topography interact with the ocean surface waves modifying the surface roughness. In turn, the wind generates short surface waves (of the order of cm) that are modulated by and superimposed on a continuum of longer waves ranging from 50 cm to 100's of meters. Depending on the wind and ocean currents, these waves can travel in various directions creating a complex 3-dimensional surface or approach a simpler 2- dimensional-like, but still multi-scale geometry. Although the centimeter-scale waves are mainly responsible for backscattering microwave radar signals, recent experiments have shown that specific characteristics of the finite amplitude long waves strongly affect the properties of the polarized backscattering radar return; bistatic returns are expected to be affected similarly. In general, the ocean surface backscattering cross sections are very low, resulting in ratios of radar return power to radar input power of the order of -80dB . Further, the time series measurements show spikes in the polarization ratios TE/TM (HH/VV) that can reach values larger than 1 for small grazing angles. Experimental analysis of the data indicates that the spikes are associated with the presence of asymmetric, large amplitude, long waves. These results cannot be explained with the currently used composite surface models because these models lack the accuracy necessary for quantitative predictions and neglect multipath effects. Further, these models strongly depend on an arbitrary separation of scales on the surface and therefore do not yield genuine results. Other scattering models that have been used to describe the experimental data are either not sufficiently accurate or can only model specific length scales or profiles.

In summary, the surfaces relevant to ocean surveillance applications of interest have roughness scales of the order of the radiation wavelength with fairly large slopes. These rough surfaces are modulated by and superimposed on variations with several length scales. These attributes have been shown to have a significant impact on the scattering return characteristics. Polarized ratios of the returns are particularly affected and it is necessary to model them accurately.

An appropriate model to interpret and predict radar returns for relevant ocean (as well as terrain) remote sensing applications should be able to:

- a) calculate the polarized returns from 3-dimensional, corrugated, large slope surfaces;
- a) evaluate the effects of disparate scales in the return; e.g. long scale modulations of short scale corrugations (of the order of the radiation wavelength),
- b) guaranty an accuracy greater than the smallest quantity of interest (returns can be as low as -100 dB, so the numerics must guaranty as least 10 digits)
- c) be sufficiently simple and fast so that parametric investigations of correlation between the surface characteristics and the polarized returns are easy to perform and
- d) be validated.

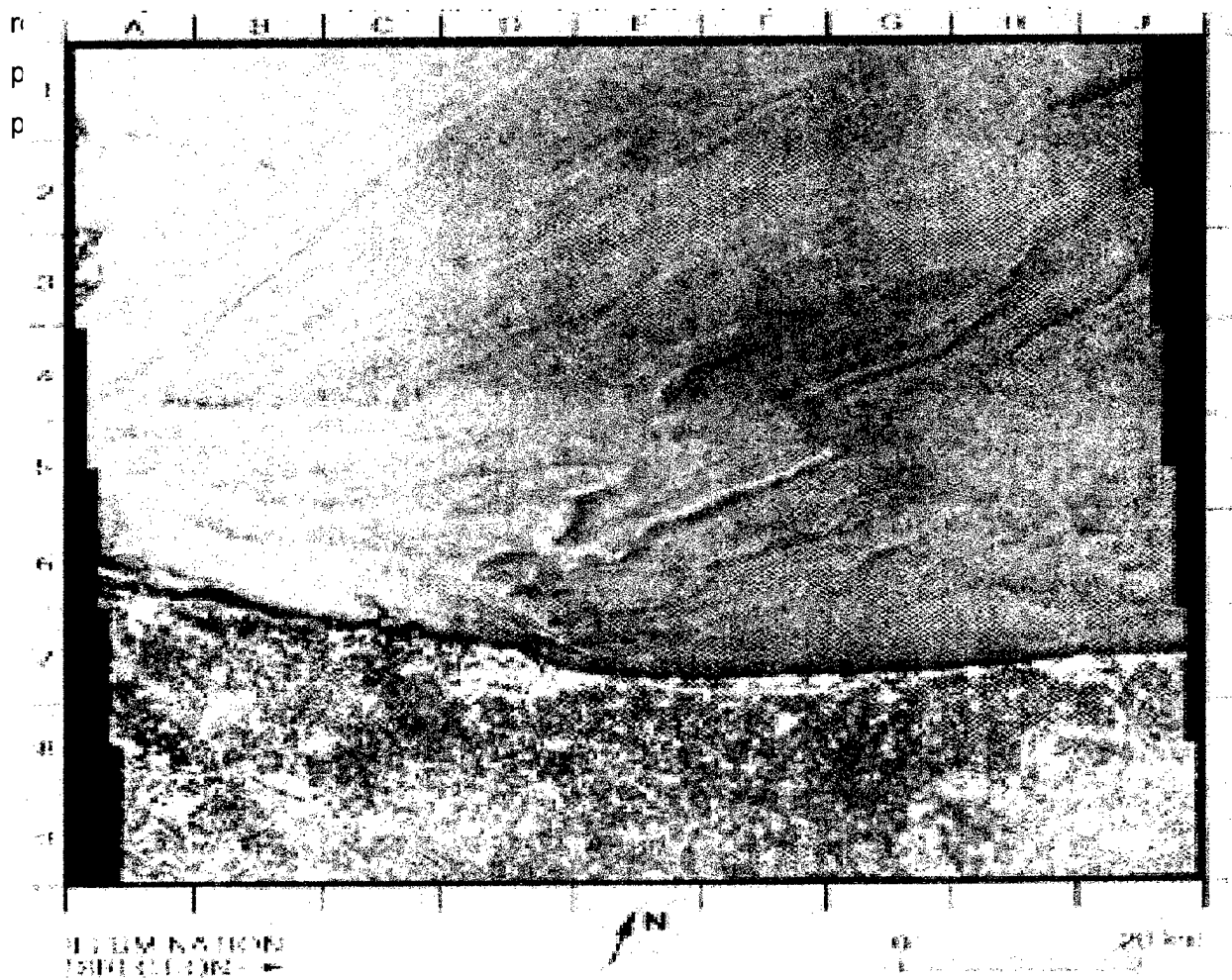
During the three years of this project, work has been focused in obtaining and implementing an algorithm with most of these characteristics. In particular, in order to guarantee a successful initial algorithm, the investigations focused on the development and implementation of a fast two-dimensional polarized scattering solver able to deal with complex multi-scale surfaces with 10-digit accuracy and perform efficient parametric studies.

1.2 Problem

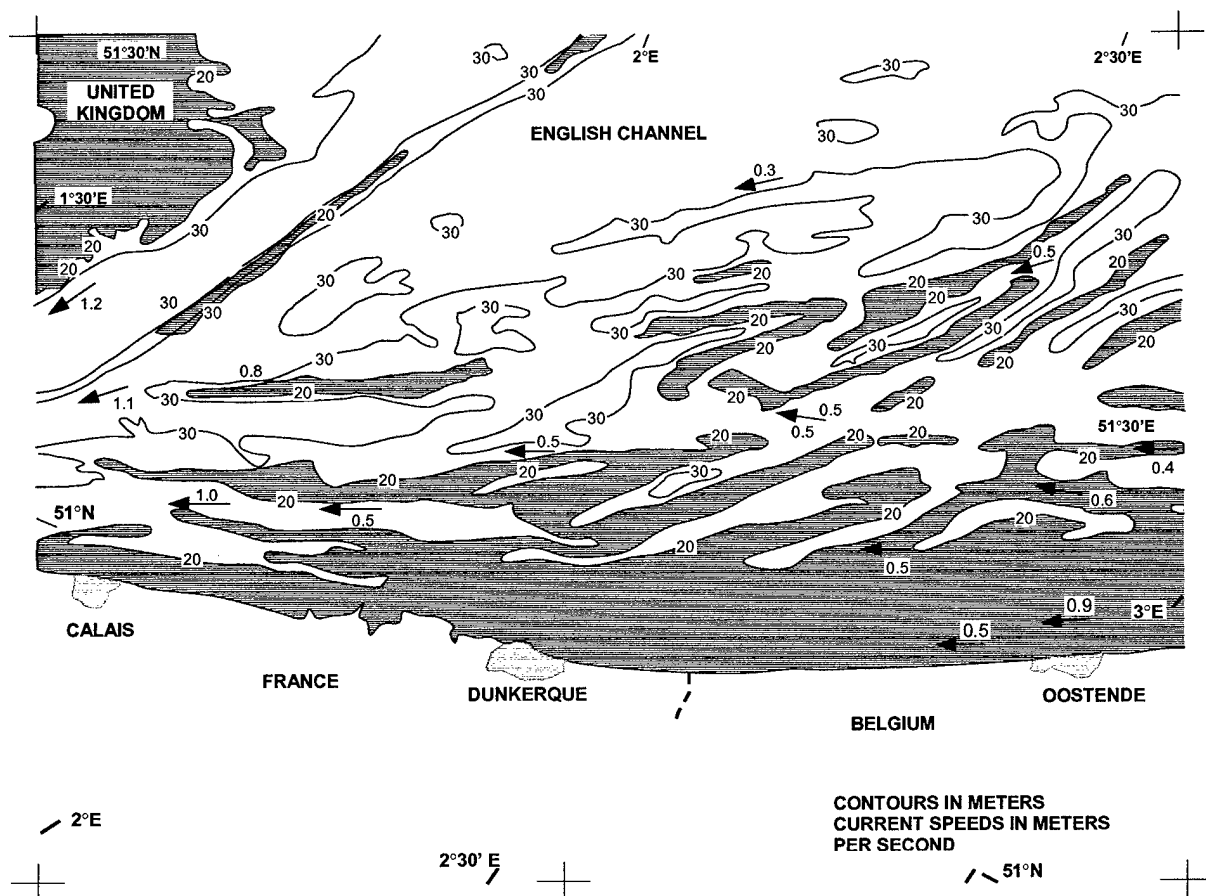
Historically, the electromagnetic scattering models used for ocean applications assumed that the dominant return from the ocean surface was due to constructive interference from those waves with period (λ_{water}) resonant with the radiation wavelength ($\lambda_{\text{radiation}}$). That is, water waves (so called Bragg waves) that satisfy the Bragg scattering condition, $\lambda_{\text{water}} = \lambda_{\text{radiation}} / 2 \sin \theta_i$, where θ_i is the radiation incidence angle cf. [Crombie, 1955]. In that case, the rough ocean surface was assumed to have very small slopes and the backscattered returns were computed by low order expansions in the height of the surface (small perturbation theory) of the scattered field. The computed vertical polarization (vertical transmit and vertical receive, VV) returns calculated with that model are proportional to the energy density of Bragg waves and for low

grazing (high incidence) angles they are always much larger than the horizontal (horizontal transmit and horizontal receive, HH) returns. For example, it can be shown cf. [Valenzuela, 1978] that the ratio HH/VV goes to 0 at 90 degrees incidence for a perfect conductor.

Late 70's experimental measurements demonstrated that short surface waves (~ 30 cm) could image long patterns (~ 1 Km) that could be associated with the ocean bottom topography. (Cf. Figure 1B). This result was interpreted as the modulation of the resonant (Bragg) short waves spatial distribution energy density by the long surface current gradients. Thus, in order to understand the experimental results it was necessary to include in the model the variation in the Bragg resonant waves due to the long wave tilt and composite models were developed to take this effect into account. These models also predicted large vertical to horizontal return ratios ($VV/HH \gg 1$) for small grazing angles. In addition the maximum of the Doppler spectra (power



(A)



(B)

Figure 1: Land Sat images of the English Channel. L band: 30-cm.

A) Radar image - B) Bottom topography contours.

New experimental results obtained during the early to mid 90's sparked a renewed interest in appropriate scattering models to interpret polarized radar data. For example, experimental observations with the TRW X-band radar mounted on the bow of a boat in a Loch Linnhe experiment [Lee et al, 1995, 1996] as well as complementary laboratory experiments [Lee et al, 1997a, 1997b] showed that for low grazing angles the horizontal returns could be larger than the vertical returns. Further, the regions where these events or spikes ($HH/VV > 1$) occurred were of an intermittent nature and the result of very low scattering returns, of the order of -60 to -100 dB range (See Figure 2 below). The measured Doppler spectra, also demonstrated that as the

grazing angle decreased, the maxima associated with the HH returns, moved towards faster velocities that no longer could be associated with Bragg waves. (See Figure 2A and 2B).

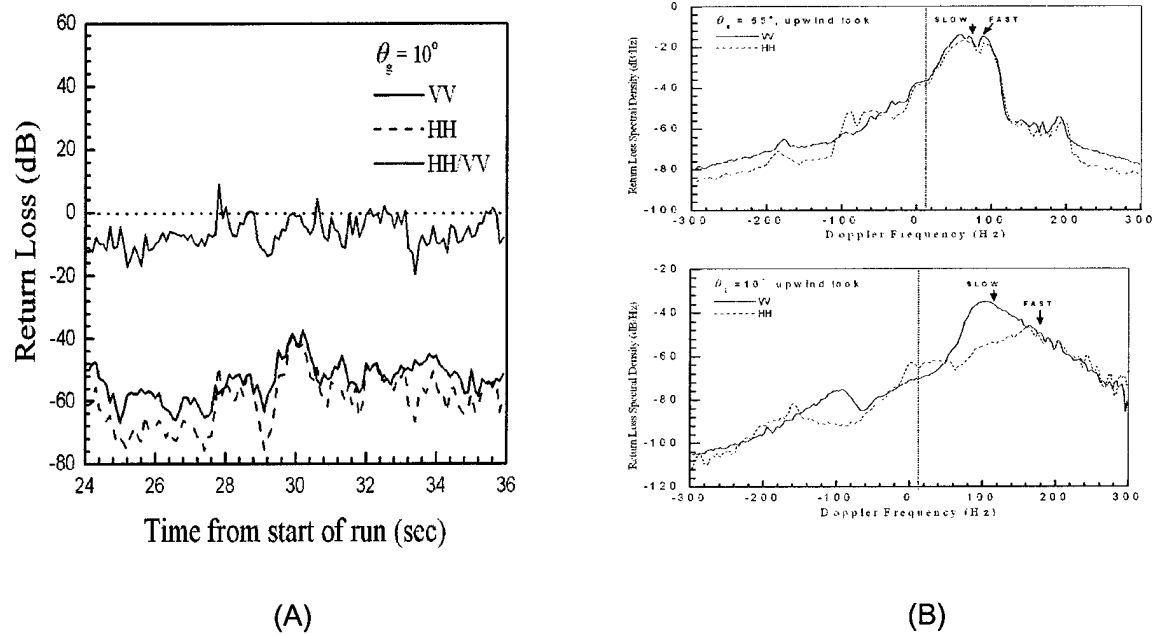


Figure 2: (A) A short sample of time-resolved, band-pass-filtered backscattered echoes at X-Band (B) Time-integrated Doppler spectra of wind waves (see [Lee et al, 1995] for details).

The paradigm was further complicated by differences in the vertical and horizontal radar images obtained under different weather conditions. For example, the JUSREX'92 experimental results [Gasparovic and Etkin, 1994] indicated that internal waves are well imaged by HH and VV for a stable boundary layer (longer wave spectrum), whereas they **are not** well imaged in VV for an unstable boundary layer (short wave spectrum). The short waves mask long wave patterns in VV but not in HH (cf. Fig. 3). These and other similar experimental results resulted in a different understanding of the dominant scattering mechanisms from ocean surfaces:

- a) returns are associated with the modulation of short waves (of the order of 1 – 30cm) by finite amplitude long waves (.5m – 3m) and/or the generation of large amplitude short waves in the front faces of almost breaking long waves;
- b) the strong horizontal polarization scattering returns are due mainly to “Non-Bragg mechanism” that are most likely dominated by specular and multibounce or multipath interference from incipient braking waves;
- c) the multi-scale nature of the ocean surfaces plays a dominant role for the horizontal returns;

- d) the difference between horizontal and vertical returns yields an additional insight in the interpretation of radar measurements.

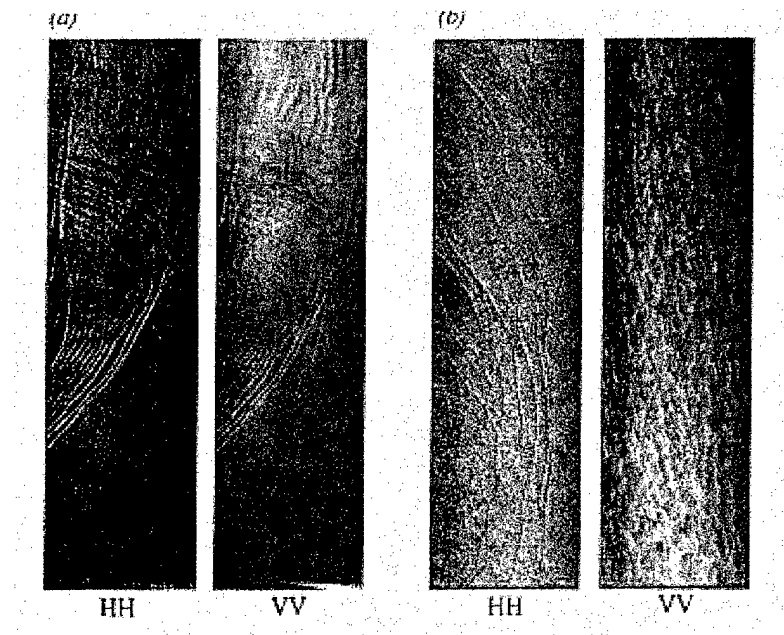


Figure 3: Radar images taken the JUSREX'92 experiment under (a) stable and (b) unstable boundary layer conditions (see [Churyumov and Kravtsov, 2000] for details).

Most important, the results also pointed out the need for an appropriate scattering model that could take into account the multi-scale nature of the surface, the larger slopes and could deal with the very low returns. Composite models using low order expansions or generally models with low accuracy or failing to take into account the large range of contributing scales will fail to predict the experimental results.

From a computational point of view the task of developing such a model (multi-scale, at least 10 digit accuracy, includes both TE and TM polarizations) seems rather formidable. In the following sections a description is given of the method employed in this project to successfully address this computational challenge. Section 1.3 summarizes the mathematical model. Section 1.4 discusses some of the problems encountered in its implementation and in Section 1.5 validation results are summarized. Potential exploitations of this algorithm are described in Section 1.6. More detailed descriptions of the points discussed in those sections are given in the Appendices as well as in the associated publications. A diskette with the algorithm and documentation is included with this Final report.

1.3 Mathematical model

The problem of evaluating scattering returns from rough surfaces is rather challenging --- owing to the multiple-scale nature of rough scatterers, whose spectra may span a wide range of length-scales cf. [Valenzuela, 1978]. A number of techniques have been developed to treat limiting cases of this problem. For example, the high frequency case, in which the wavelength λ of the incident radiation is much smaller than the characteristic surface length-scales, has been treated by means of low order asymptotic expansions, such as the Kirchhoff approximation. On the other hand, resonant problems where the incident radiation wavelength is of the order of the roughness scale have been treated by perturbation methods, typically first or second order expansions in the height h of the surface cf. [Rice, 1951; Mitzner, 1964; Shmelev, 1972; Voronovich, 1994]. However, when a multitude of scales is present on the surface none of these techniques is adequate, and attempts to combine them in so-called two-scale approaches have been given cf. [Kuryanov, 1963; McDaniel and Gorman, 1983; Voronovich, 1994; Gil'man et al, 1996]. The results provided by these methods are not always satisfactory, owing to the limitations imposed by the low orders of approximation used in both, the high frequency and the small perturbation methods.

A new approach to multi-scale scattering, based on use of expansions of very high order in both parameters λ and h , has been proposed recently cf. [Bruno et al, 2000]. These combined methods, which are based on complex variable theory and analytic continuation, require nontrivial mathematical treatments; the resulting approaches, however, do expand substantially on the range of applicability over low order methods, and can be used in some of the most challenging cases arising in applications. Perturbation series of very high-order in h have been introduced and used elsewhere to treat resonant problems --- in which the wavelength of radiation is comparable to the surface length-scales cf. [Bruno and Reitich, 1993; Sei et al, 1999].

This new method does not require separation of the surface length-scales into large and small, but instead it is able to deal with a continuum of scales on the surface. Indeed the high order expansions presented below have a common "overlap" region in the (h, λ) plane where both components are highly accurate. More precisely, there is a range of surface heights and incident wavelengths for which both methods produce results with machine accuracy. Therefore by dividing the scales of a surface at wavelength (or scale) in the overlap region we obtain a general method which is applicable to surfaces containing a continuum of length-scales --- which is ideal for evaluation of scattering from surfaces with spectral distributions of oceanic type.

We consider surfaces containing a continuum of scales but, as mentioned above, the existence of an overlap allows us to solve the complete multiple-scale problem by expressing an arbitrary surface

$$y = S(x)$$

as a sum

$$y = S_0(x) + F(x)$$

where $S_0(x)$ contains wavenumbers less than N_s , and $F(x)$ contains the complementary set of wavenumbers greater than N_s . Thus, our method uses a dichotomy in wave numbers but it does not assume a separation of scales. This feature is essential in the study of oceanic waves since many studies show that the wave spectrum spans a large range of wavenumbers (see for instance [Pierson and Moskowitz, 1964]).

The discussion here is restricted to the particular case of an HH configuration in two dimensions since the VV case can be treated similarly. The modifications necessary to treat the VV case will be pointed out as needed. The scattered field created by an incident H polarized plane wave impinging on the rough surface solves the Helmholtz equation with a Dirichlet boundary condition. Our approach to the solution of the general problem with rough surface $y = S(x)$ proceeds as follows:

- We consider the surface $S(x, \delta) = S_0(x) + \delta F(x)$, which will be used as a basis for a perturbative method in the parameter δ .
- The solution $u = u(x, \delta)$ associated with the surface $S(x, \delta)$ is obtained by perturbation theory around $\delta = 0$.
- The solution for the surface $S(x)$ is then recovered by setting $\delta=1$. (This evaluation usually leads to divergent series whose re-summation requires appropriate analytic continuation.)

In detail, writing:

$$(1) \quad \begin{cases} u(x, z, \delta) = \sum_{m=0}^{+\infty} u_m(x, z) \frac{\delta^m}{m!} \\ u_m(x, z) = \frac{\partial^m u}{\partial \delta^m}(x, z, \delta = 0) \end{cases}$$

The fact that, for every value of δ the field $u(x,z,\delta)$ solves the Helmholtz equation

$$(2) \quad \begin{cases} \Delta u(x, z; \delta) + k^2 u(x, z; \delta) = 0 \\ u(x, S(x, \delta); \delta) = -u^{inc}(x, S(x, \delta)) \end{cases}$$

implies that, for index m we have

$$(3) \quad \begin{cases} \Delta u_m(x, z) + k^2 u_m(x, z) = 0 \\ u_m(x, S_0(x)) = G[F, u_0, u_1, \dots, u_{m-1}](x, S_0(x)) \end{cases}$$

The interest in this equation arises from the fact that, although the right hand side in the boundary condition for u_m is highly oscillatory, the surface S_0 itself is not. *We therefore have reduced a problem on a highly oscillatory surface to a sequence of problems on a non-oscillatory surface.* For example the zeroth, first and second order Taylor coefficients u_0 , u_1 and u_2 in the expansion of $u(x,z,\delta)$ solve the following scattering problems:

$$(5) \quad \begin{cases} \Delta u_1(x, z) + k^2 u_1(x, z) = 0 \\ u_1(x, S_0(x)) = -F(x) \left(\frac{\partial u_0}{\partial z} + \frac{\partial u^{inc}}{\partial z} \right)(x, S_0(x)) \end{cases}$$

$$(4) \quad \begin{cases} \Delta u_0(x, z) + k^2 u_0(x, z) = 0 \\ u_0(x, S_0(x)) = -u^{inc}(x, S_0(x)) \end{cases}$$

$$(6) \quad \begin{cases} \Delta u_2(x, z) + k^2 u_2(x, z) = 0 \\ u_2(x, S_0(x)) = -F^2(x) \left(\frac{\partial^2 u_0}{\partial z^2} + \frac{\partial^2 u^{inc}}{\partial z^2} \right)(x, S_0(x)) \\ \quad - 2F(x) \frac{\partial u_1}{\partial z}(x, S_0(x)) \end{cases}$$

The general boundary condition for u_m in equation (3) (denoted by $G[F, u_0, u_1, \dots, u_{m-1}](x, S_0(x))$) can be computed by differentiation of order m with respect to δ of the exact boundary condition of equation (2). Note the boundary term for u_m involve all the previous Taylor coefficients u_j $j=0\dots m-1$. This is already obvious on equation (5) and (6).

From equation (4), (5) and (6), it is clear that the computation of each Taylor coefficients u_m involves solving a **high frequency problem** on a smooth surface. Typically u^{inc} is a plane wave with wave number $k=2\pi/\lambda$ and S_0 is a surface with characteristic length d much greater than λ . The characteristic length in our approach is the period of the surface as we have chosen a Fourier description of the surface. We are then faced with solving very accurately a high-frequency scattering problem.

Also equations (4), (5) and (6) show that the computation of the boundary condition involves z-derivatives of high-order of the previous Taylor coefficients. The simplest example is the boundary condition for u_1 involves the z-derivative of u_0 . Since we know u_0 on the surface (from equation (4)) knowing the z-derivative is equivalent to knowing the *normal derivative on the surface*. This involves therefore the computation of the **Dirichlet to Neumann map**. So the two main components of the algorithm are

- A High-frequency solver
- A Dirichlet to Neumann Map code

We give below an overview of each component. A detailed description of the high-frequency solver can be found in [Bruno et al., 2002].

1.3.1 High-Frequency Solver

1.3.1.1 Background

Our approach to the high-frequency problem uses an integral equation formulation, whose solution $v(x)$ is sought and obtained in the form of an asymptotic expansion

$$(7) \quad v(x, k) = e^{i\alpha x - \beta S_0(x)} \sum_{n=p}^{+\infty} \frac{v_n(x)}{k^n}$$

with $p=-1$ for TM polarization and $p=0$ for TE polarization. This expansion is similar in form to the geometrical optics

$$(8) \quad u(x, z, k) = e^{ikS(x, z)} \sum_{n=0}^{+\infty} \frac{u_n(x, z)}{k^n}$$

where $S=S(x, z)$ is the *unknown* phase of the scattered field. Note that the phase of the density $v(x)$ of (7) is determined directly from the geometry and the incident field and, unlike that in the geometrical optics field, it is not an unknown of the problem. In particular, the present approach

does not require solution of an eikonal equation (cf. [Vidale, 1988; VanTrier and Symes, 1991; Fatemi et al, 1995; Benamou, 1999], and it bypasses the complex nature of the field of rays, caustics, etc.

The validity of the expansion (8) has been extensively studied [Friedlander, 1946; Luneburg, 1949a; Luneburg, 1949b; Van Kampen, 1949; Luneburg, 1964]; in particular, it is known that equation (8) needs to be modified in the presence of singularities of the scattering surface. To treat edges and wedges, for example, an expansion containing powers of $k^{1/2}$ [Luneburg, 1949b; Van Kampen, 1949; Keller, 1958; Lewis and Boersma, 1969; Lewis and Keller, 1964] must be used; caustics and creeping waves also lead to similar modified expansions [Kravtsov, 1964; Brown, 1966; Ludwig, 1966; Lewis et al, 1967; Ahluwalia et al, 1968]. Proofs of the asymptotic nature of expansion (8) were given in cases where no such singularities occur [Miranker, 1957; Bloom and Kazarinoff, 1976]. In practice only expansions (8) of very low orders (one, or, at most two) have been used, owing in part to the substantial algebraic complexity required by high order expansions [Bouche et al, 1997]. First order versions of the expansion (7), on the other hand were treated in [Lee, 1975; Chaloupka and Meckelburg, 1985; Ansorge 1986,1987].

The region of validity of our expansion (7) the other hand corresponds to configurations where no shadowing occurs. At shadowing the wave vector of the incident plane wave is tangent to the surface at some point, which causes certain integrals to diverge; see [Bruno et al, 2002] for details. Thus, a different kind of expansion, in fractional powers of $1/k$, should be used to treat shadowing configurations: a first order version of such an expansion was discussed in [Hong, 1967]; see [Friedlander and Keller, 1955; Lewis and Keller, 1964; Brown 1966; Duistermaat, 1992] for the ray-tracing counterpart.

In [Bruno et al, 2002] we show that high order summations of expansion (7) can indeed be used to produce highly accurate results for surfaces and wavelengths of interest in applications for both TE and TM polarization. Results with machine precision accuracy, which were obtained from computations involving expansions of order as high as 20, are presented. Our algorithm is based on systematic use and manipulation of certain Taylor-Fourier series representations, which are discussed in detail in [Bruno et al, 2002].

1.3.1.2 Integral Equation

The scattered field $u=u(x,z)$ induced by an incident plane wave impinging on the rough surface $y=S_0(x)$ under TE polarization is the solution of the Helmholtz equation with a Dirichlet boundary condition. As is known [Voronovich, 1994] the field $u(x,z)$ can be computed as an

integral involving a surface density $v(x,k)$ and the Green's function $G(x,z,x',z')$ for the Helmholtz equation

$$(9) \quad u(x,z) = \int_{-\infty}^{+\infty} v(\xi,k) \frac{\partial G}{\partial n_\xi}(x,z,\xi,S_0(\xi)) \sqrt{1+S_0'(\xi)^2} d\xi$$

where $v(x,k)$ satisfies the boundary integral equation

$$(10) \quad \frac{v(\xi,k)}{2} + \int_{-\infty}^{+\infty} v(\xi,k) \frac{\partial G}{\partial n_\xi}(x,S_0(x),\xi,S_0(\xi)) \sqrt{1+S_0'(\xi)^2} d\xi = -e^{i\alpha x - i\beta S_0(x)}$$

with $\alpha = k \sin(\theta^{\text{inc}})$, $\beta = k \cos(\theta^{\text{inc}})$ and $k = 2\pi/\lambda$ is the wavenumber. θ^{inc} is the incidence angle measured counter-clockwise from the vertical axis. A useful form of the integral equation (10) results as we factor out the rapidly oscillating phase function

$$(11) \quad \mu(x,k) + \int_{-\infty}^{+\infty} \mu(\xi,k) \frac{\partial G}{\partial n_\xi}(x,S_0(x),\xi,S_0(\xi)) e^{-i\alpha(x-\xi) + i\beta(S_0(x) - S_0(\xi))} \sqrt{1+S_0'(\xi)^2} d\xi = -2$$

$$\mu(x,k) = e^{-i\alpha x + i\beta S_0(x)} v(x,k)$$

which cancels the fast oscillations in all non-integrated terms, and thus suggests use of an expansion of the form (7). Substitution of the expansion (7) into equation (11) then yields:

$$(12) \quad \sum_{n=p}^{+\infty} \frac{1}{k^n} \left(v_n(x) - \frac{i}{2} I^n(x,k) \right) = -2$$

$$(13) \quad I^n(x,k) = \int_{-\infty}^{+\infty} v_n(\xi) \frac{\partial G}{\partial n_\xi}(x,S_0(x),\xi,S_0(\xi)) e^{-i\alpha(x-\xi) + i\beta(S_0(x) - S_0(\xi))} \sqrt{1+S_0'(\xi)^2} d\xi$$

To solve equation (12) we use asymptotic expansions for the integrals $I^n(x,k)$, collect coefficients of each power of $1/k$, and then determine, recursively, the coefficients $v_n(x)$. We obtain in [Bruno et al, 2002], an expansion which gives $I^n(x,k)$ in terms of derivatives of $v_n(x)$.

$$(14) \quad \begin{cases} I^n(x,k) = \frac{1}{k} \sum_{q=0}^{+\infty} \frac{I_q^n(x)}{k^q} \\ I_q^n(x) = \sum_{\ell=0}^q \frac{\partial^\ell v_n(x)}{\partial x^\ell} B_{q-\ell}(x) \end{cases}$$

where the functions $B_{q-l}(x)$ are determined from the profile and incidence angle only. We then find a recursion which gives $v_n(x)$ as a linear combination of derivatives of the previous coefficients $v_{n-1-q}(x)$.

$$(15) \quad \begin{cases} v_0(x) = -2 \\ v_n(x) = \frac{i}{2} \sum_{q=0}^{n-1} I_q^{n-1-q}(x) \end{cases}$$

1.3.2 Dirichlet to Neumann Map

1.3.2.1 Reduction to first-order normal derivative

The boundary condition for an arbitrary order $u_m(x, z)$ can be derived by differentiating to order m the boundary condition for $u(x, y, \delta)$ and then setting $\delta=0$. In detail we find for the TE case

$$(16) \quad u_m(x, S_0(x)) = - \left(F^m(x) \frac{\partial^m u^{inc}}{\partial z^m} + \sum_{p=1}^m \frac{m! F^p(x)}{p!(m-p)!} \frac{\partial^p u_{m-p}}{\partial z^p} \right) (x, S_0(x))$$

and for the TM case

$$(17) \quad \frac{\partial u_m}{\partial n}(x, S_0(x)) = - \left(F^m(x) \frac{\partial^{m+1} u^{inc}}{\partial z^m \partial n} + \sum_{p=1}^m \frac{m! F^p(x)}{p!(m-p)!} \frac{\partial^{p+1} u_{m-p}}{\partial z^p \partial n} \right) (x, S_0(x))$$

The formulas above show that differentiation of high order is required. However using an argument similar to the one used in the proof of the Cauchy-Kowalesky theorem [Hadamard, 1964; Courant and Hilbert, 1962], we can set up the calculation recursively so that at any given stage only the Dirichlet and Neumann data are required.

For example in the TE case, the boundary condition for $u_2(x, z)$ given in formula (6), requires the second order derivative of $u_0(x, z)$ evaluated on the surface $z=S_0(x)$ with respect to z . That quantity can be computed if $u_0(x, S_0(x))$ and $\partial u_0 / \partial z(x, S_0(x))$ are known on the surface

$$(18) \quad \begin{cases} A(x) = u_0(x, S_0(x)) \\ B(x) = \frac{\partial u_0}{\partial z}(x, S_0(x)) \end{cases}$$

$z=S_0(x)$. Differentiating with respect to x (tangential derivative) we find

$$\begin{cases} A''(x) = \frac{\partial^2 u_0}{\partial x^2}(x, S_0(x)) + 2S_0'(x) \frac{\partial^2 u_0}{\partial z \partial x}(x, S_0(x)) + (S_0'(x))^2 \frac{\partial^2 u_0}{\partial z \partial z}(x, S_0(x)) + S_0''(x) \frac{\partial u_0}{\partial z}(x, S_0(x)) \\ B'(x) = \frac{\partial^2 u_0}{\partial z \partial x}(x, S_0(x)) + S_0'(x) \frac{\partial^2 u_0}{\partial z \partial z}(x, S_0(x)) \end{cases}$$

Using Helmholtz equation on the boundary yields

$$\frac{\partial^2 u_0}{\partial x \partial x}(x, S_0(x)) = -\frac{\partial^2 u_0}{\partial z \partial z}(x, S_0(x)) - k^2 u_0(x, S_0(x))$$

And finally

$$(19) \quad \frac{\partial^2 u_0}{\partial z \partial z}(x, S_0(x)) = \frac{-1}{1 + (S_0')^2} (A''(x) + k^2 A(x) - S_0''(x) B(x) + 2S_0'(x) B'(x))$$

Note that only x derivatives (that is tangential derivatives) are involved as long we known the first z -derivative (or normal derivative). This is a classical result of the theory of characteristics [Hadamard, 1949, chap 7].

To compute the m^{th} derivative of u_0 with respect to z , the same calculation can be repeated with

$$\begin{cases} A(x) = \frac{\partial^{m-2} u_0}{\partial z^{m-2}}(x, S_0(x)) \\ B(x) = \frac{\partial^{m-1} u_0}{\partial z^{m-1}}(x, S_0(x)) \end{cases}$$

Therefore by keeping two of the successive z derivatives of u_0 (resp u_p in general) we can compute the z -derivative of u_0 (resp u_p) to any order. The main remaining question is therefore the computation of the z (or normal) derivative of u_0 (resp u_p) given the Dirichlet data $u_0(x, S_0(x))$ (resp $u_p(x, S_0(x))$).

1.3.2.2 Evaluation of the first-order normal derivative

Our integral representation (9) of the scattered field u_0 (resp u_p) does not allow the calculation of $\partial u_0 / \partial n(x, z)$ for $z = S_0(x)$ by differentiation under the integral sign since it gives rise to non integrable terms. A detailed analysis of the origin of the non-integrable terms showed that they arose from the logarithmic behavior of the Green's function at the origin. So the main difficulty reduces to computing the normal derivative in the case where Green's function is the

logarithm. This corresponds to Laplace's equation, that is Helmholtz's equation with $k=0$. So we consider a "scattered" field of the form:

$$u(x, z) = \int_{-\infty}^{+\infty} v(\xi) \frac{\partial}{\partial n_\xi} \log(r(x, z, \xi, S_0(\xi))) \sqrt{1 + S_0'(\xi)^2} d\xi$$

$$r(x, z, \xi, S_0(\xi)) = \left[(x - \xi)^2 + (z - S_0(\xi))^2 \right]^{1/2}$$

Using the analyticity of the logarithm, the Cauchy-Riemann equations relate tangential and normal derivatives of the logarithm and its conjugate function.

In detail we have

$$\begin{cases} \frac{\partial \log}{\partial n_\xi} = \frac{\partial \theta}{\partial t_\xi} \\ \frac{\partial \theta}{\partial n_\xi} = -\frac{\partial \log}{\partial t_\xi} \end{cases} \quad \theta(x, z, \xi) = \tan^{-1} \left(\frac{z - S_0(\xi)}{x - \xi} \right)$$

Therefore we can write:

$$u(x, z) = \int_{-\infty}^{+\infty} v(\xi) \frac{\partial}{\partial t_\xi} \theta(x, z, \xi, S_0(\xi)) \sqrt{1 + S_0'(\xi)^2} d\xi$$

Noting that

$$\frac{\partial}{\partial t_\xi} \theta(x, z, \xi, S_0(\xi)) = \frac{1}{\sqrt{1 + S_0'(\xi)^2}} \frac{d}{d\xi} \theta(x, z, \xi, S_0(\xi))$$

After integration by parts, we obtain

$$u(x, z) = \int_{-\infty}^{+\infty} \frac{\partial v(\xi)}{\partial \xi} \theta(x, z, \xi, S_0(\xi)) d\xi$$

This expression can now be differentiated under the integral sign with respect to the normal at x

$$\begin{aligned} \frac{\partial u}{\partial n_x}(x, z) &= \int_{-\infty}^{+\infty} \frac{\partial v(\xi)}{\partial \xi} \frac{\partial \theta}{\partial n_x}(x, z, \xi, S_0(\xi)) d\xi \\ &= - \int_{-\infty}^{+\infty} \frac{\partial v(\xi)}{\partial \xi} \frac{\partial \log}{\partial t_x}(x, z, \xi, S_0(\xi)) d\xi \end{aligned}$$

and finally

$$\frac{\partial u}{\partial n_x}(x, z) = - \frac{\partial}{\partial t_x} \int_{-\infty}^{+\infty} \frac{\partial v(\xi)}{\partial \xi} \log(x, z, \xi, S_0(\xi)) d\xi$$

Therefore the normal derivative of a double layer potential has been expressed as the tangential derivative of a single layer (with a different density). The normal derivative on the surface can then be obtained by taking the limit when z tends to $S_0(x)$.

For the general case where $k \neq 0$, after isolating the logarithmic part of the Green's function, the remainder of the Green's function (which is the Hankel function minus the logarithm) is treated by differentiation under the integral sign, as it does not give rise to singular terms.

1.4 Implementation issues

Taylor-Fourier algebra

The implementation of the high-frequency solver as well as the Dirichlet to Neumann map is done without discretization points on the surface. Instead we represent the unknown coefficients of the various current densities of equation (7) as Fourier series. Therefore the densities themselves are Taylor-Fourier series that is Taylor series in $1/k$ whose coefficients are Fourier series. Thus, a Taylor-Fourier series $f(x,t)$ is given by an expression of the form

$$f(x,t) = \sum_{n=0}^{+\infty} f_n(x) t^n \quad f_n(x) = \sum_{p=-\infty}^{p=+\infty} f_{n,p} e^{ipx}$$

The manipulations required by our methods include sum, products, composition and as well as algebraic and functional inverses. These operations need to be implemented with care, as we show in what follows.

Compositions and inverses of Taylor-Fourier series require consideration of multiplication and addition, so we discuss the latter two operations first. Additions do not pose difficulties: naturally, they result from addition of coefficients. Multiplication and division of Taylor-Fourier series, on the other hand, could in principle be obtained by means of Fast Fourier Transforms [Press et al, 1992]. Unfortunately such procedures are not appropriate in our context. Indeed, as shown below, the very rapid decay of the Fourier and Taylor coefficients arising in our calculations is not well captured through convolutions obtained from FFTs. Since an accurate representation of this decay is essential in our method --- which, based on high order differentiation of Fourier-Taylor series, greatly magnifies high frequency components --- an alternate approach needs to be used.

Before describing our accurate algorithms for manipulation of Taylor-Fourier series we present an example illustrating the difficulties associated with use of FFTs in this context. We thus consider the problem of evaluating the subsequent derivatives of the function

$$S(x) = \left(\sum_{n=0}^{+\infty} \frac{\cos(kx)}{a^{|k|}} \right)^2$$

through multiplication and differentiation of Fourier series. For comparison purposes we note that S actually admits the closed form:

$$S(x) = \left(1 + 2 \frac{a \cos(x) - 1}{a^2 - 2a \cos(x) + 1} \right)^2$$

The value $a=10$ is used in the following tests. Table 1 below shows the errors resulting in the evaluation of a sequence of derivatives of the function S at $x=0$ through two different methods: FFT and direct summation of the convolution expression. (Here errors were evaluated by comparison with the corresponding values obtained from direct differentiation of the expression by means of an algebraic manipulator).

Differentiation Order	Exact value at $x=0$	20 modes		30 modes		40 modes	
		FFT	Conv	FFT	Conv	FFT	Conv
2	-7.376924249352232e-01	1.3e-12	5.4e-16	1.7e-11	2.7e-16	1.0e-11	2.7e-16
10	-4.361708943655447e+03	8.8e-07	1.2e-09	1.1e-03	6.9e-16	3.8e-03	6.9e-16
20	1.220898732494702e+12	3.1e-02	5.0e-05	1.4e+03	2.2e-11	1.3e+05	8.2e-16

Table 1: Values of the derivatives of the function $S(x)$ at $x=0$ for various orders of differentiation. The columns marked 20 Modes, 30 Modes and 40 Modes list the *relative errors* of the derivatives computed by summing differentiated Fourier series truncated at 20, 30 and 40 Modes, respectively. Columns FFT and Conv. resulted from use of Fourier coefficients obtained through FFTs and direct convolution, respectively.

We see that, as mentioned above, use of Fourier series obtained from FFTs lead to substantial accuracy losses. Indeed, FFTs evaluate the small high-order Fourier coefficients of a product through sums and differences of "large" function values, and thus, they give rise to large relative errors in the high-frequency components. These relative errors are then magnified by the differentiation process, and all accuracy is lost in high order differentiations: note the increasing loss of accuracy that results from use of larger number of Fourier modes in the FFT procedure. The direct convolution, on the other hand, does not suffer from this difficulty. Indeed, direct convolutions evaluate a particular Fourier coefficient a_n of a product of series through sums of terms of the same order of magnitude as a_n . The result is a series whose coefficients are fully accurate in relative terms, so that subsequent differentiations do not lead to accuracy losses. We point out that full double precision accuracy can be obtained for derivatives

of orders 20 and higher provided sufficiently many modes are used in the method based on direct convolutions.

In addition to sums and multiplications, our approach requires use of algorithms for composition and as well as algebraic and functional inverses of Taylor-Fourier series. In view of the previous considerations, a few comments will suffice to provide a complete prescription. Compositions result from iterated products and sums of Fourier series, and thus they do not present difficulties. As is known from the theory of formal power series [Cartan, 1963], functional inverses of a Taylor-Fourier series with $f_0 = 0$ results quite directly once the algebraic inverse of the Fourier series $f_1(x) \neq 0$ is known. We may thus restrict our discussion to evaluation of algebraic inverses of Fourier series. As in the case of the product of Fourier series, two alternatives can be considered for the evaluation of algebraic inverses. One of them involves point evaluations and FFTs; in view of our previous comments it is clear such an approach would not lead to accurate numerics. An alternative approach, akin to use of a direct convolution in evaluation of products, requires solution of a linear system of equations for the Fourier coefficients of the algebraic inverse. In view of the decay of the Fourier coefficients of smooth functions, such linear systems can be truncated and solved to produce the coefficients of inverses with high accuracy.

In sum, manipulations of Taylor-Fourier series should not use point-value discretizations if accurate values of functions and their derivatives are to be obtained. The approach described in this section calls, instead, for operations performed fully in Fourier space. In practice we have found the procedures described here produce full double precision accuracies for all operations between Taylor-Fourier series and their subsequent high-order derivatives in very short computing times.

1.5 Validation of the Code

1.5.1 High-Frequency Solver

In this section we present the results produced by our algorithm for the energy radiated in the various scattering directions. We use the periodic Green's function G of period d [Petit, 1980]

$$\tilde{G}(x, z) = \frac{1}{2id} \sum_{n=-\infty}^{+\infty} \frac{e^{i\alpha_n x - i\beta_n z}}{\beta_n} \quad \alpha_n = \alpha + n \frac{2\pi}{d} \quad \beta_n = \sqrt{k^2 - \alpha_n^2}$$

to obtain from the Rayleigh series for the scattered field

$$(20) \quad u(x, z) = \sum_{n=-\infty}^{+\infty} B_n e^{i\alpha_n x + i\beta_n z}$$

Here, the coefficients B_n are "Rayleigh amplitudes", which are given in TE polarization by

$$B_n = \frac{1}{2d} \int_0^d \left(-1 + \frac{\alpha_n}{\beta_n} S'_0(x)\right) v(x, k) e^{-i\alpha_n x - i\beta_n S_0(x)} dx$$

and in TM polarization by

$$B_n = \frac{1}{2id\beta_n} \int_0^d v(x, k) e^{-i\alpha_n x - i\beta_n S_0(x)} dx$$

The required integrals were computed by means of the trapezoidal rule, which for the periodic functions under consideration is spectrally accurate, and can be computed very efficiently by means of the FFT. Our numerical results show values and errors corresponding to the "scattering efficiencies" e_n , see [Petit, 1980], which are defined by

$$e_n = \frac{\beta_n}{\beta} |B_n|^2$$

and which give the fraction of the energy which is scattered in each one of the (finitely many) scattering directions. To test the accuracy of our numerical procedures the high-frequency (HF) results were compared to those of the method of variation boundaries [Bruno and Reitich, 1993] (MVB) in an "overlap" wavelength region --- in which both algorithms are very accurate. Additional results, in regimes beyond those that can be resolved by the boundary variation method are also presented in [Bruno et al, 2002].

Note that the HF and MVB methods are substantially different in nature: one is a high order expansion in $1/k$ whereas the other is a high order expansion in the height h of the profile. In the examples that follow we list relative errors for the computed values of scattered energies in the various scattering directions.

The results below show examples of accuracies reached by our high frequency solver. The scattering surface, the polarization and angle of the incident field and height to period ratio as well as the wavelength to period ratio are indicated above the table of results. Note the double precision accuracies reached with expansion of the order of 15. The order zero calculation corresponds to the classical Kirchhoff approximation (or tangent plane approximation). Note the substantial gain in accuracy provided by our solver over this classical approximation.

Scattering surface TE Polarization Normal Incidence



Scattering Direction #	Scattered Energy	Order 0	Order 1	Order 3	Order 5	Order 9	Order 11
0	4.843033211037387e-02	1.9e-3	4.8e-6	1.9e-8	4.2e-11	1.6e-15	0.0e-16
1	4.533269321280629e-02	2.3e-3	2.4e-6	8.3e-9	2.4e-11	1.8e-15	0.0e-16
2	8.263582066556663e-02	8.3e-4	3.0e-6	1.3e-8	3.5e-11	3.4e-16	0.0e-16
3	1.032017750281185e-03	1.8e-2	7.4e-5	3.7e-8	1.3e-10	9.7e-15	1.0e-15
4	1.019744820363490e-01	1.0e-3	1.3e-6	7.1e-10	1.6e-12	0.0e-16	0.0e-16
5	1.396970992023250e-01	1.2e-4	3.4e-6	5.1e-9	8.7e-12	0.0e-16	0.0e-16
6	7.578492663719054e-02	7.9e-4	6.5e-6	1.3e-8	2.6e-11	3.7e-16	0.0e-16
7	2.361867030378681e-02	1.3e-3	1.0e-5	2.3e-8	5.5e-11	8.8e-16	0.0e-16

The run time for the calculation of order 11 was 3 seconds on a Dec Alpha 600MHz.

Scattering surface TM Polarization Normal Incidence



Scattering Direction #	Scattered Energy	Order 0	Order 1	Order 3	Order 5	Order 9	Order 11
0	4.626620392423562e-02	9.3e-5	3.3e-7	2.5e-10	2.0e-13	0.0e-16	0.0e-16
1	4.784012804881663e-02	1.1e-4	2.0e-7	1.7e-10	5.6e-14	0.0e-16	0.0e-16
2	8.098026673047228e-02	7.2e-5	4.4e-7	3.6e-10	2.5e-14	0.0e-16	0.0e-16
3	1.530238230277614e-03	2.3e-5	9.3e-9	2.5e-12	1.7e-15	0.0e-16	0.0e-10
4	1.044707459140400e-01	1.1e-4	1.3e-7	2.6e-10	2.5e-13	0.0e-16	0.0e-16
5	1.392864901043021e-01	1.9e-5	4.4e-8	2.6e-10	2.6e-13	0.0e-16	0.0e-16
6	7.439074834360192e-02	6.0e-5	2.0e-7	4.9e-11	4.5e-14	0.0e-16	0.0e-16
7	2.290107975972599e-02	3.0e-5	1.3e-7	2.3e-11	3.7e-14	6.9e-18	0.0e-16

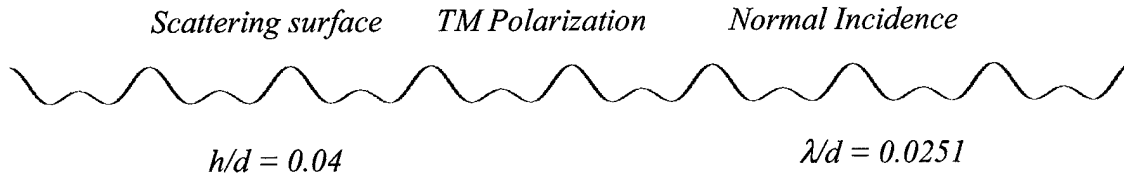
The run time for the calculation of order 11 was 3 seconds on a Dec Alpha 600MHz.

Scattering surface TE Polarization Normal Incidence



Scattering Direction #	Scattered Energy	Order 0	Order 1	Order 5	Order 9	Order 11	Order 15
0	1.983702874853860e-01	1.4e-3	6.7e-6	6.3e-10	1.8e-13	5.0e-15	0.0e-16
1	2.125625186015414e-02	4.3e-3	7.3e-6	8.6e-10	4.6e-14	4.9e-16	0.0e-16
2	5.109656298137152e-02	4.2e-3	5.3e-6	1.3e-9	3.5e-14	6.9e-15	0.0e-16
3	1.350594564861170e-01	1.1e-3	3.0e-6	1.8e-10	5.1e-14	6.9e-16	0.0e-16
4	1.670755436364386e-02	4.3e-3	9.0e-6	1.5e-9	1.8e-13	1.0e-14	0.0e-16
5	1.041839113172000e-01	8.7e-4	1.1e-5	4.7e-10	3.8e-14	0.0e-16	0.0e-16
6	3.029977474761340e-02	7.6e-4	1.1e-5	4.8e-10	1.0e-15	2.0e-15	0.0e-16
7	2.828409217693459e-02	2.5e-3	3.2e-5	1.8e-9	3.5e-14	4.6e-15	6.1e-16

The run time for the calculation of order 15 was 6 seconds on a Dec Alpha 600MHz.



Scattering Direction #	Scattered Energy	Order 0	Order 1	Order 5	Order 9	Order 11	Order 15
0	1.985778821348800e-01	2.6e-4	2.1e-6	1.1e-11	1.8e-15	1.0e-15	1.2e-15
1	2.203189065423864e-02	9.4e-5	1.3e-7	1.9e-13	4.5e-16	4.9e-16	4.7e-16
2	4.989624245086630e-02	1.5e-4	5.8e-7	6.8e-12	3.4e-16	4.2e-16	4.9e-16
3	1.363942224141270e-01	1.5e-4	4.1e-7	9.1e-12	1.5e-15	9.2e-16	9.2e-16
4	1.685456723960805e-02	7.2e-5	2.9e-7	2.5e-12	4.6e-16	2.5e-16	2.3e-16
5	1.040033802018770e-01	9.3e-5	1.0e-7	8.7e-12	3.1e-16	2.1e-16	3.1e-16
6	2.994981016528542e-02	2.3e-5	4.6e-8	5.6e-12	4.2e-17	3.2e-16	2.9e-16
7	2.795532080716518e-02	7.0e-5	4.3e-7	3.5e-13	9.0e-17	3.1e-17	4.1e-17

The run time for the calculation of order 15 was 5 seconds on a Dec Alpha 600MHz.

1.5.2 Dirichlet to Neumann Map

To test the accuracy of the Dirichlet to Neumann map, the Rayleigh expansion (20) of the scattered field was used again. Here we choose surfaces for which the Rayleigh hypothesis holds that is surfaces for which the Rayleigh expansion (20) is uniformly convergent up to the surface itself cf. [Petit and Cadilhac, 1966; Millar, 1969; Kyurkchan et al, 1996]. In that case the Rayleigh series can be differentiated with respect to the normal and the results from the Rayleigh series and the integral formulation described in section 1.3.2 can be compared. Just as in the previous section the coefficient B_n are obtained from the method of variation of boundary. In detail, since the normal derivative of the field on the surface is a periodic function of the tangential variable x , we compared the Fourier coefficient of that function as produced by the differentiation of the Rayleigh series and the methods of section 1.3.2. The results presented below show the absolute error for the first 9 Fourier coefficients of this function for two different surfaces. The agreement is quite satisfactory given that the accuracy of the coefficient B_n is 15~16 digits but they are multiplied by $k=2\pi/\lambda=2\pi/0.025 \sim 251$. So for example the relative error on the first (and largest) coefficient is $1.4e-12/251=5.6e-15$.

Scattering surface TE Polarization Normal Incidence



0	2.513274122871854e+02	1.4e-12
1	2.467789729688969e-01	4.1e-13
2	4.853137888184910e-04	4.6e-12
3	2.692275458156496e-06	2.6e-13
4	2.418002116077943e-08	2.1e-12
5	3.012222915203911e-10	2.5e-12
6	3.142218774380850e-12	1.5e-12
7	5.094686950567004e-13	5.1e-13
8	1.367272645883451e-13	1.4e-13
9	2.246949775547679e-14	2.2e-14

Scattering surface TE Polarization Normal Incidence



0	2.5132741228718315e+02	8.8e-13
1	9.8711672408589575e-02	7.1e-13
2	3.9503306957875781e-01	1.6e-13
3	7.0040665308186701e-04	7.9e-13
4	1.2489143602822332e-03	1.6e-13
5	9.6829269045451665e-06	2.4e-13
6	1.1239693826031570e-05	2.5e-13
7	1.9232684834524107e-07	2.6e-13
8	1.6608798644321709e-07	1.6e-13
9	4.9820286787390020e-09	6.8e-14

1.5.3 Multi-scale algorithm

Finally the multiple scale algorithms were integrated and very high accuracies were indeed obtained. We present below two examples of highly accurate multiple scale geometries scattering in TE illumination. The errors listed are the absolute error as compared to the method of variation of boundaries. The results were obtained by summation of the Taylor series (1) to the order in $1/k$ specified in the top row. The two scale results were obtained by using Kirchhoff approximation (that is order 0 in $1/k$) and a first order expansion in the roughness h . The

difference between the two scale column and the Order 1 column comes from the fact that we used an expansion of order 20 in the high-frequency solver for Order 1 as opposed to order 0 for the two scale case.

$$h/d = 0.0252$$

Scattering surface

$$\lambda/d = 0.025$$



Scattering Direction #	Scattered Energy	Two Scale	Order 1	Order 2	Order 4	Order 6	Order 8
0	4.833824308716315e-02	1.8e-4	9.2e-5	2.1e-8	2.3e-12	5.8e-14	6.0e-15
1	4.524676580264179e-02	2.0e-5	8.7e-5	2.0e-8	2.0e-12	4.0e-14	2.3e-15
2	8.248342098822989E-02	2.3e-4	1.6e-4	3.2e-8	3.2e-12	6.6e-14	8.8e-15
3	1.053390492569949E-03	1.7e-5	2.0e-6	2.2e-8	3.4e-12	8.9e-15	8.8e-16
4	0.101853442231311	8.7e-5	1.9e-4	2.3e-8	6.0e-12	3.0e-14	5.5e-15
5	0.139564830538028	2.8e-4	2.6e-4	6.3e-8	1.3e-11	2.7e-14	8.8e-15
6	7.574080330783492E-02	2.0e-4	1.4e-4	6.0e-8	1.1e-11	1.5e-14	8.9e-15
7	2.357615851308177E-02	7.5e-5	4.4e-5	8.6e-9	8.1e-13	2.4e-14	1.5e-14

The scattering surface was in that case defined by $z=0.025(\cos(2\pi x)+0.01\cos(20\pi x))$. The calculation of order 8, which yielded 14 digits of accuracy, took 1 hour 9 minutes 54 seconds on a 600 MHz machine. A result with 12 digits of accuracy was obtained for order 4 and took 5 minutes and 51 seconds on the same machine. The large difference in timing is due mainly to a reduction in number of Fourier modes used. Whereas 30 modes suffice for 12-digit accuracy, 100 modes are necessary for 15-digit accuracy.

$$h/d = 0.0101$$

Scattering surface

$$\lambda/d = 0.025$$



Scattering Direction #	Scattered Energy	Two Scale	Order 1	Order 2	Order 4	Order 6
0	0.198901761348164	2.1e-4	6.1e-5	4.3e-8	1.1e-12	3.5e-14
1	2.118863974374862E-02	8.4e-5	6.5e-6	4.9e-9	1.2e-13	3.1e-15
2	5.064428936060158E-02	2.3e-4	1.5e-5	3.4e-9	8.2e-13	2.4e-14
3	0.135474001366087	1.1e-4	4.1e-5	3.3e-9	8.2e-13	3.7e-14
4	1.614783623594695E-02	6.5e-5	5.0e-6	4.2e-9	9.9e-13	5.7e-14
5	0.104163054003108	1.2e-4	3.2e-5	8.1e-10	5.6e-14	2.6e-14
6	3.084758570010842E-02	3.2e-5	9.3e-6	4.2e-8	8.5e-13	1.9e-13
7	2.782604772500211E-02	7.8e-5	8.5e-6	3.2e-8	7.4e-13	6.3e-14

In this next example, the scattering surface was defined by $z=0.01*(\cos(2\pi x)+\cos(4\pi x)+0.025\cos(20\pi x))$. The calculation of order 6, which yielded 14 digits

of accuracy, took 55 minutes and 34 seconds on a 600 MHz machine. A result with 12 digits of accuracy obtained for order 4 took 13 minutes and 17 seconds on the same machine.

1.6 Exploitation and Follow on

A natural transition program is to correlate polarized radar backscattering returns to relevant surface characteristics, with specific focus on ocean surfaces, through the utilization of an appropriately validated highly efficient and accurate algorithm specially designed for the solution of scattering problems from multiple scale surfaces. The overall objective is to improve the interpretation and predictive capabilities from radar remote sensing returns.

1.6.1 Modeling of Doppler spectrum

The time evolution of the polarized scattering returns is of great use in analyzing the distribution and evolution of scatterers on the ocean surface. Indeed, the power spectrum of the polarized backscattered returns, also known as the Doppler spectrum, is routinely used in experiments for diagnostic and analysis of the distribution and speed of the scatterers on the moving surface, cf. [Lee et al, 1997a; Rozenberg et al, 1996; Lee et al, 1996; Lee et al, 1997b; Liu et al, 1998; Lee et al, 1995; Ja et al, 2001; Duncan et al, 1999].

TRW's Ocean technology department, a world-renown center of excellence for ocean hydrodynamics, has developed many ocean simulation tools based on the formulations described in [Longuet-Higgins and Cokelet, 1976] and [Zhakarov, 1968]. These algorithms are design to model the hydrodynamic evolution of a variety of scales on the water surface. The coupling of these hydrodynamic models to the TRW high-order high frequency multi-scale electromagnetic numerical solver will provide a powerful, efficient and extremely accurate algorithm for the modeling and analysis of Doppler spectra. The high accuracy delivered by the scattering solver is necessary due to the range of scattering returns typically observed to be between -60 dB to -100 dB. This means that to compute reliably simulation results, an accuracy of 10 digits is necessary at the very least.

Once the Doppler spectrum code is implemented, a series of hypothesis regarding the cause and nature of the HH/VV ratio intermittent spiking can be addressed. In particular, the broadening of the velocity distribution introduced by the scattering process can be analyzed. Indeed, since the propagation of water waves will be performed numerically the distribution of velocities at every point along the profile can be evaluated as a function of time. The power spectrum of this distribution of velocities can then be compared to the power spectrum of the scattering returns for each polarization (the Doppler spectrum). To our knowledge, the basic

understanding of the relationship between the distribution of velocities on the water surface and the associated Doppler spectrum for HH and VV polarization obtained from the scattering returns has never been undertaken. It will be of immediate interest to the ocean scattering and remote-sensing communities that seeks to interpret measured Doppler spectra in terms of surface characteristics.

1.6.2 Return from statistically described rough surfaces

The computational speed of our multi-scale algorithm allows the investigation of the surface configuration mechanisms responsible for distinct radar return signatures. In particular, detailed parametric studies can be performed about the dependence of the scattering returns on the surface statistical characteristics such as their spectral distribution cf. [Pierson and Moskowitz, 1964; Donelan and Pierson, 1987; Jahne and Riemer, 1990; Apel, 1994 and Elfouhaily et al, 1997]. One outstanding, yet unsolved, problem in that field concerns the retrieval of wind speed and direction from radar measurements. A number of empirical models have been proposed cf. [Apel, 1994] and more recent measurements have been made cf. [Chaudry and Moore, 1984; Masuko et al, 1986; Woiceshyn et al, 1986; Carswell et al, 1994].

However the establishment of a reliable empirical relationship between radar cross section and wind speed and direction remains elusive cf. [Rufenach, 1998; Phillips, 1988]. The discrepancy can be attributed to two main factors. First the computations of the radar cross section are all based on two-scale models. These models rely on the distribution of short "Bragg" waves, which spectrum is still a matter of active research cf. [Pierson and Moskowitz, 1964; Donelan and Pierson, 1987; Jahne and Riemer, 1990; Apel, 1994 and Elfouhaily et al, 1997]. Of course, the interpretation of measured data and the retrieval of wind characteristics require a model of the dependence of the radar returns on the wind characteristics.

We propose to alleviate the errors introduced by the two-scale scattering model by replacing the scattering module by our highly accurate solver. The expected outcome of that study is the evaluation of current ocean spectra with full electromagnetic account of all scales on the surface at X-band. Furthermore accurate scattering computations will permit to test the current functional forms of the backscattered cross section as a function of wind speed and to determine their range of validity. This will help the wind retrieval (inverse) problem, which is poorly understood at this point cf. [Rufenach, 1998].

It is of interest to note here that the recent studies we carried out with a simplified version of our algorithm, for periodic surfaces with slopes in the range 0.01-0.3, have already yielded results not expected from the predictions of classical theories cf. [Sei et al., 1999]. In

particular, these results provide the first rigorous theoretical evidence of anomalous absorption of polarized EM radiation. This result is potentially of strong relevance to the ocean scattering community. Our results show that significant effects on the backscattering polarization ratio (HH/VV or TE/TM) can arise from modulated short waves, that is, corrugated surfaces with features similar to those abundant in ocean surfaces (cf. Figure 4 and [Sei et al., 1999]). The effects depend on incidence angle, dielectric constant and specific configuration characteristics.

Figure 2 shows an instance of the results we have obtained. It illustrates the increase in the ratio of HH/VV, obtained for the specific wavetrain of Figure 4, for a particular region of slope values ($ka = \pi h/d$, where h is the height and d the period of the wavetrain). The figure also shows the constant, and orders of magnitude smaller, value of HH/VV that would have been predicted by either first order theories or the classical theory of Rice. These results are all the more relevant in view of the recent experimental measurements that have demonstrated the strong contribution to the radar return from incipient or actively breaking water waves cf. [Lee et al, 1997; Liu et al, 1998].

These waves are nonlinear by nature, with large slopes ($ka \sim .1$) consisting of wavetrains of different scales and can be directionally modulated. The experimental results show "sea spikes" in potential agreement with our calculation. The "sea spikes" are regions of large HH/VV polarization ratios and sporadically high HH returns for near grazing angles in direct contradiction with first order perturbation theories.



Figure 4. Periodic modulated wave train

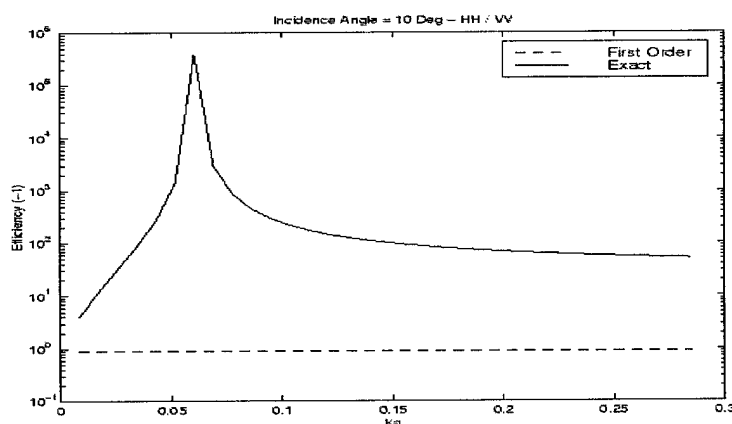


Figure 5. Simulated scattering returns for surface shown in Fig. 4 and comparison with first order and classical theories.

1.7 Bibliography

- M. Abramowitz and I. Stegun, *Handbook of mathematical functions with formulas, graphs, and mathematical tables*, US Dept Commerce, June, 1964.
- D. S. Ahluwalia, R. M. Lewis and J. Boersma, *Uniform asymptotic theory of diffraction by a plane screen*, SIAM J. Appl. Math., 16 (4), 783-807, 1968.
- J. R. Apel, *An improved model for the ocean surface wave vector spectrum and its effects on radar backscatter*, J. Geophys. Res., 99, 16,269-26,291, 1994.
- H. Ansoerge, *Electromagnetic reflection from a curved dielectric interface*, IEEE Trans. Ant. Prop., 34,842-845, 1986.
- H. Ansoerge, *First order corrections to reflection and transmission at a curved dielectric interface with emphasis on polarization properties*, Radio science, 22, 993-998, 1987.
- J. D. Benamou, *Direct computations of multivalued phase space solutions for Hamilton-Jacobi equations*, Comm. Pure Appl. Math., 52, 1443-1475, 1999.
- N. Bleistein and R. A. Handelsman, *Asymptotic expansions of integrals*, Dover Publications, New York, 1986.
- C. O. Bloom and N. D. Kazarinoff, *Short wave radiation problems in inhomogeneous media: asymptotic solutions*, Lecture Notes in Mathematics 522, Springer-Verlag, Berlin, 1976.
- D. Bouche, F. Molinet and R. Mittra, *Asymptotic methods in electromagnetics*, Springer-Verlag, Berlin, 1997.
- W. P. Brown, *On the asymptotic behavior of electromagnetic fields from convex cylinders near grazing incidence*, J. of Math. Anal. and App., 15, 355-385, 1966.
- O. Bruno and F. Reitich, *Numerical solution of diffraction problems: a method of variation of boundaries I, II, III*, J. Opt. Soc. A 10, 1168-1175, 2307-2316, 2551-2562, 1993.
- O. Bruno, A. Sei and M. Caponi, *Rigorous multi-scale solver for rough-surface scattering problems: high-order-high-frequency and variation of boundaries*, Proceedings of the NATO Sensors and Electronics Technology (SET) Symposium on "Low Grazing angle clutter: Its Characterization, Measurement, and Application", JHU/APL, Laurel, MD, April 25-27 2000.

- O. Bruno, A. Sei and M. Caponi, *High-order high-frequency solutions of rough surface scattering problems, to appear in Radio Science*, 2002. See also Appendix A1.
- J. R. Carswell, S. C. Carson, R. E. McIntosh, K. K. Li, G. Neumann, D. J. McLaughlin, J. C. Wilkerson, P. G. Black and V. Nghiem, *Airborne scatterometers: Investigating ocean backscatter under low- and high-wind conditions*, Proc. IEEE, 82, 1835-1860, 1994.
- H. Cartan, *Elementary theory of analytic functions of one or several complex variables*, Addison-Wesley, Reading, Mass., 1963.
- H. Chaloupka and H. J. Meckelburg, *Improved high-frequency current approximation for curved conducting surfaces*, AEU, Arch. Elektron. Ubertragungstech, 39, 245-250, 1985.
- A. H. Chaudhry and R. K. Moore, *Tower-based backscatter measurements of the sea*, IEEE J. Ocean. Eng., OE-9, 309-316, 1984.
- A. N. Churyumov and Y.A. Kravtsov, *Microwave backscatter from mesoscale breaking waves on the sea surface*, Waves in Random media, 10, 1-15, 2000.
- R. Courant and D. Hilbert, *Methods of Mathematical Physics*, Interscience Publishers, 1962.
- D.D. Crombie, *Doppler spectrum of sea echo at 13.6 Mc/s*, Nature, 175, 681-682, 1955.
- M. A. Donelan and W. J. Pierson, *Radar scattering and equilibrium ranges in wind-generated waves with application to scatterometry*, J. Geophys. Res., 92, 4971-5029, 1987.
- J. J. Duistermaat, *Huygens' principle for linear partial differential equations, Huygens' principle, 1690-1990: theory and applications*, H. Blok Ed, Elsevier, 1992.
- J.H. Duncan, H. Qiao, V. Philomin and A. Wentz, *Gentle spilling breakers: Crest profile evolution*, J. Fluid Mech., 379, 191-222, 1999.
- T. Elfouhaily, B. Chapron and K. Katsaros, *A unified directional spectrum for long and short wind-driven waves*, J. Geophys. Res., 102, 15,781-15,796, 1997.
- E. Fatemi, B. Engquist and S. Osher, *Numerical solution of the high frequency asymptotic expansion for the scalar wave equation*, J. Comp. Phys., 120, 145-155, 1995.
- F. G. Friedlander, *Geometrical Optics and Maxwell's equations*, Proc. Cambridge Philos. Soc., 43 (2), 284-286, 1946.
- F. G. Friedlander and J. B. Keller, *Asymptotic expansion of solutions of $(\Delta + k^2) u = 0$* , Comm. Pure Appl. Math., 8, 387-394, 1955.

- R.F. Gasparovic and V.S. Etkin, *An overview of the joint US/Russia internal wave remote sensing experiment*, Proc. IGARSS'94, 741-743, 1994.
- M. A. Gil'Man, A. G. Mikheyev and T. L. Tkachenko, *The two-scale model and other methods for the approximate solution of the problem of diffraction by rough surfaces*, Comp. Maths Math. Phys., 36, 1429-1442, 1996.
- J. Hadamard, *La théorie des équations aux dérivées partielles*, Editions Scientifiques, Pekin, 1964.
- J. Hadamard, *Leçons sur la propagation des ondes et les équations de l'hydrodynamique*, Chelsea Publishing Company, New-York, 1949.
- S. Hong, *Asymptotic theory of electromagnetic and acoustic diffraction by smooth convex surfaces of variable curvature*, J. Math. Phys., 8, 1223-1232, 1967.
- M.C. Hutley, *Diffraction gratings*, Academic Press, San Diego, Calif., 1982.
- S.J. Ja, J.C. West, H. Qiao and J.H. Duncan, *Mechanisms of low-grazing-angle scattering from spilling breaker water waves*, Radio Science, 36, 981-998, 2001.
- B. Jahne and K. S. Riemer, *Two-dimensional wave number spectra of small-scale water surface waves*, J. Geophys. Res., 95, 11,531-11546, 1990.
- J. B. Keller, *A geometric theory of diffraction*, AMS Calculus of variations and its applications, L.M. Graves ed., McGraw-Hill, New York, 1958.
- B. Kinsman, *Wind waves, their generation and propagation on the ocean surface*, Englewood Cliffs, New Jersey, Prentice-Hall, 1965.
- Y. A. Kravtsov, *A modification of the geometric optics method*, Radiofizika, 7, 664-673, 1964.
- B. F. Kuryanov, *The scattering of sound at a rough surface with two types of irregularity*, Soviet Physics-Acoustic, 8 (3), 252-257, Jan. 1963.
- A.G. Kyurkchan, B.Y. Sternin and V.E. Shatalov, *Singularities of continuation of wave fields*, Physics-Uspekhi, 30 (12), 1221-1242, 1996.
- P. Lee, J.D. Barter, K.L. Beach, C.L. Hindman, B.M. Lake and H. Rungaldier, *X-band microwave backscattering from ocean waves*, J. Geo. Res. 100, 2591-2611, 1995.
- P. Lee, J.D. Barter, E. Caponi, M. Caponi, C.L. Hindman, B.M. Lake and H. Rungaldier, *Wind-speed dependence of small grazing angle microwave backscatter from sea surfaces*, IEEE Trans. Ant. Prop. 44, 333-340, 1996.

- P. Lee, J.D. Barter, K.L. Beach, C.L. Hindman, B.M. Lake, H.R. Thompson and R. Yee, *Experiments on Bragg and non-Bragg scattering using single-frequency and chirped radars*, Radio. Sci. 32, 1725-1744, 1997a.
- P. H. Y. Lee, J. D. Barter, K. L. Beach *et al.*, *Scattering from breaking waves without wind*, IEEE Trans. Ant. Prop., 46 (1), 14-26, 1997b.
- S. W. Lee, *Electromagnetic reflection from a conducting surface: geometrical optics solution*, IEEE Trans. Ant. Prop., 23, 184-191, 1975.
- R. M. Lewis and J. Boersma, *Uniform theory of edge diffraction*, J. Math. Phys., 10 (12), 2291-2305, 1969.
- R. M. Lewis and J. B. Keller, *Asymptotic methods for partial differential equations: The reduced wave equation and Maxwell's equations*, Research Report EM-194, New York University, 1964. (Reprinted in *Surveys in Applied Mathematics*, Vol. 1, 1-82, Plenum Press, New York, 1995).
- R. M. Lewis, N. Bleistein and D. Ludwig, *Uniform asymptotic theory of creeping waves*, Comm. Pure Appl. Math., 20, 295-320, 1967.
- Yong Liu, Stephen J. Frazier, and Robert E. McIntosh, *Measurement and Classification of Low-Grazing-Angle Radar Sea Spikes*, IEEE Transactions on Antennas and Propagation 46 (1), 27-40, 1998.
- M. S. Longuet-Higgins and E. D. Cokelet, *The deformation of steep surface waves on water I: A numerical method of computation*, Proc. R. Soc. A., 350, 1-26, 1976.
- R. K. Luneburg, *Mathematical theory of Optics*, Brown University, 1944. (Reprinted by University of California Press, Berkeley, 1964).
- R. K. Luneburg, *Asymptotic expansion of steady state electromagnetic fields*, Research Report EM-14, New York University, July 1949.
- R. K. Luneburg, *Asymptotic evaluation of diffraction integrals*, Research Report EM-15, New York University, October 1949.
- D. Ludwig, *Uniform asymptotic expansion at a caustic*, Comm. Pure Appl. Math., 19, 215-250, 1966.
- S. T. McDaniel and A. D. Gorman, *An examination of the composite-roughness scattering model*, J. Acoust. Soc. Am., 73, 1476-1486, 1983.
- H. Masuko, K. Okamoto, M. Shimada and S. Niwa, *Measurement of microwave backscattering signatures of the ocean surface using X-Band and Ka-Band airborne scatterometers*, J. Geophys. Res., 91, 13,065-13,083, 1986.

- R.F. Millar, *On the Rayleigh assumption in scattering by a periodic surface*, Proc. Camb. Phil. Soc., 65, 773-791, 1969.
- W. L. Miranker, *Parametric theory of $\Delta u + k^2 u$* , Arch. Ratl. Mech. Anal., 1, 139-152, 1957.
- K. M. Mitzner, *Effect of small irregularities on electromagnetic scattering from an interface of arbitrary shape*, J. Math. Phys., 5, 1776-1786, 1964.
- R. K. Moore and A. K. Fung, *Radar determination of winds at sea*, P. IEEE, 67 (11), 1504-1521, 1979.
- O. M. Phillips, *Remote sensing of the sea surface*, Ann. Rev. Fluid Mech., 20, 80-109, 1988.
- R. Petit, *Electromagnetic theory of Gratings*, Springer-Verlag, Berlin, 1980.
- R. Petit and M. Cadilhac, *Sur la diffraction d'une onde plane par un réseau infiniment conducteur*, C. R. Acad. Sci. Paris, Ser A-B, 262, 468-471, 1966.
- W.J. Pierson and L. Moskowitz, *A proposed spectral form for fully developed wind seas based on the similarity theory of S.A. Kitaigorodskii*, J. Geo. Res. 69, 5181—5190, 1964.
- W. H. Press, S. A. Teukolsky, W. T. Vetterling and B. P. Flannery, *Numerical Recipes*, Cambridge University Press, 1992.
- S. O. Rice, *Reflection of electromagnetic waves from slightly rough surfaces*, Comm. Pure Appl. Math., 4, 351-378, 1951.
- A. D. Rozenberg, D. C. Quigley, and W. Kendall Melville, *Laboratory Study of Polarized Microwave Scattering by Surface Waves at Grazing Incidence: The Influence of Long Waves*, IEEE Transactions on Geoscience and Remote Sensing 34 (6), 1331-1342, 1996.
- C. Rufenach, *Comparison of four ERS-1 scatterometer wind retrieval algorithms with buoy measurements*, J. Atmos. Oceanic Technol., 15, 304-313, 1998.
- A. Sei, O. P. Bruno and M. Caponi, *Study of polarization scattering anomalies with application to oceanic scattering*, Radio Science, 34 (2), 385-411, 1999.
- A. B. Shmelev, *Wave scattering by statistically uneven surfaces*, Soviet Physics uspekhi, 15 (2), 173-183, Sept. 1972.
- G.R. Valenzuela, *Theories for the interaction of electromagnetic and oceanic waves - A review*, Boundary-layer Meteor. 13, 61-85, 1978.
- N. G. Van Kampen, *An asymptotic treatment of diffraction problems*, Physica 14 (9), 575-589, January 1949.

- J. Vidale, *Finite difference calculation of traveltimes*, B. Seismol. Am., 78, 2062-2076, 1988.
- A. G. Voronovich, *Wave scattering from rough surfaces*, Springer-Verlag, Berlin, 1994.
- J. VanTrier and W. W. Symes, *Upwind finite- difference calculation of traveltimes*, Geophysics, 56, 812-821, 1991.
- P. M. Woiceshyn, M. G. Wurtele, D. H Boggs, L. F. McGoldrick and S. Peteherych, *The necessity for a new parametrization of an empirical model for wind/ocean scatterometry*, J. Geophys. Res., 91, 2273-2288, 1986.
- V. E. Zhakarov, *Stability of periodic waves of finite amplitude on the surface of a deep fluid*, J. Appl. Mech. Tech. Phys. (Engl. Transl.), 9, 190-194, 1968.

APPENDICES

The appendices list the published work in the course of this project, the patent application filed with the US Patent office as a result of this work and the annual progress reports produced in the course of this project.

Appendix A1:

High-Order High Frequency solutions of rough surface scattering problem, to appear in Radio Science, 2002.

Appendix A2:

Polarization ratios anomalies of 3D rough surface scattering as second order effects, IEEE AP-S International symposium, Boston, Massachusetts, July 2001.

Appendix A3:

Rigorous multi-scale solver for rough-surface scattering problems: high-order-high-frequency and variation of boundaries, Proceedings of the NATO Sensors and Electronics Technology (SET) Symposium on "Low Grazing angle clutter: Its Characterization, Measurement, and Application", JHU/APL, Laurel, MD, April 2000.

Appendix A4:

High-Order High Frequency solutions of rough surface scattering problem, Fifth International Conference on Mathematical and Numerical Aspects of Wave Propagation, Santiago de Compostella, Spain, July 2000.

Appendix A5:

An innovative high-order method for electromagnetic scattering from rough surfaces, National Radio Science Meeting, Boulder, Colorado, January 2000.

Appendix B1:

US Patent application: *High-Order High-Frequency rough surface scattering solver*

Appendix C1: Progress report for 03/01/1999 – 07/31/1999

Appendix C2: Progress report for 07/31/1999 – 07/31/2000

Appendix C3: Progress report for 07/31/2000 – 07/31/2001

Appendix C4: Progress report for 07/31/2001 – 12/31/2001

Appendix A1:

High-Order High Frequency solutions of rough surface scattering problem, to appear in
Radio Science, 2002.

High-Order High-Frequency Solutions of Rough Surface Scattering Problems

Oscar P. Bruno

Applied Mathematics, California Institute of Technology, Pasadena Ca, 91125

Alain Sei

Ocean Technology Department, TRW, 1 Space Park, Redondo Beach, Ca. 90278

Maria Caponi

Ocean Technology Department, TRW, 1 Space Park. Redondo Beach. Ca. 90278

Abstract. A new method is introduced for the solution of problems of scattering by rough surfaces in the high-frequency regime. It is shown that high order summations of expansions in inverse powers of the wavenumber can be used within an integral equation framework to produce highly accurate results for surfaces and wavelengths of interest in applications. Our algorithm is based on systematic use and manipulation of certain Taylor-Fourier series representations and explicit asymptotic expansions of oscillatory integrals. Results with machine precision accuracy are presented which were obtained from computations involving expansions of order as high as twenty.

1. Introduction

Computations of electromagnetic scattering from rough surfaces play important roles in a wide range of applications, including remote sensing, surveillance, non destructive testing, etc. The problem of evaluating such scattering returns is rather challenging — owing to the multiple-scale nature of rough scatterers, whose spectra may span a wide range of length-scales [Valenzuela, 1978].

A number of techniques have been developed to treat limiting cases of this problem. For example, the high frequency case, in which the wavelength λ of the incident radiation is much smaller than the characteristic surface length-scales, has been treated by means of low order asymptotic expansions, such as the Kirchhoff approximation. On the other hand, resonant problems where the incident radiation wavelength is of the order of the roughness scale have been treated by perturbation methods, typically first or second order expansions in the height h of the surface [Rice, 1951; Shmelev, 1972; Mitzner, 1964; Voronovich, 1994]. However, when a multitude of scales is present on the surface none of these techniques is adequate, and attempts to combine them in a so-called two-scale approaches have been given [Kuryanov, 1963; McDaniel and Gorman, 1983; Voronovich, 1994; Gil'Man et al., 1996]. The results provided by these methods are not always satisfactory, owing to the limitations imposed by the low orders of approximation used in both, the high-frequency and the small perturbation methods.

A new approach to multi-scale scattering, based on use of expansions *of very high order* in both parameters λ and h , has been proposed recently [Bruno et al., 2000]. These combined methods, which are based on complex variable theory and analytic continuation, require nontrivial mathematical treatments; the resulting approaches, however, do expand substantially on the range of applicability over low order methods, and can be used in some of the most challenging

cases arising in applications. Perturbation series of very high-order in h have been introduced and used elsewhere to treat resonant problems — in which the wavelength of radiation is comparable to the surface length-scales [Bruno and Reitich, 1993; Sei et al., 1999]. In this paper we focus on our high-order perturbation series in the wavelength λ , which, as we shall show, exhibits excellent convergence in the high-frequency, small wavelength regime. The combined (h, λ) perturbation algorithms for multiscale surfaces, which require as a main component the accurate high frequency solvers presented in this paper, are described in [Bruno et al., 2000].

Our approach to the present high-frequency problem uses an integral equation formulation, whose solution ν is sought and obtained in the form of an asymptotic expansion

$$\nu(x, k) = e^{i\alpha x - i\beta f(x)} \sum_{n=p}^{+\infty} \frac{\nu_n(x)}{k^n}, \quad (1)$$

with $p = -1$ for TM polarization and $p = 0$ for TE polarization. This expansion is similar in form to the geometrical optics series [Lewis and Keller, 1964]

$$u(x, y, k) = e^{ikS(x, y)} \sum_{n=0}^{+\infty} \frac{u_n(x, y)}{k^n}, \quad (2)$$

where $S = S(x, y)$ is the *unknown* phase of the scattered field. Note that the phase of the density ν of (1) is determined directly from the geometry and the incident field and, unlike that in the geometrical optics field, it is not an unknown of the problem. In particular, the present approach does not require solution of an eikonal equation [Vidale, 1988; VanTrier and Symes, 1991; Fatemi et al., 1995; Benamou, 1999], and it bypasses the complex nature of the field of rays, caustics, etc.

The validity of the expansion (2) has been extensively studied [Friedlander, 1946; Luneburg, 1949a; Luneburg, 1949b; Van Kampen, 1949; Luneburg, 1964]; in particular, it is known that equation (2) needs to be modified in the presence of singularities of the scattering surface.

To treat edges and wedges, for example, an expansion containing powers of $k^{-1/2}$ [Luneburg, 1949b; Van Kampen, 1949; Keller, 1958; Lewis and Boersma, 1969; Lewis and Keller, 1964] must be used; caustics and creeping waves also lead to similar modified expansions [Kravtsov, 1964; Brown, 1966; Ludwig, 1966; Lewis et al., 1967; Ahluwalia et al., 1968]. Proofs of the asymptotic nature of expansion (2) were given in cases where no such singularities occur [Miranker, 1957; Bloom and Kazarinoff, 1976]. In practice only expansions (2) of very low orders (one, or, at most two) have been used — owing in part to the substantial algebraic complexity required by high order expansions [Bouche et al., 1997]. First order versions of the expansion (1), on the other hand were treated in [Lee, 1975; Chaloupka and Meckelburg, 1985; Ansorge, 1986; Ansorge, 1987].

The region of validity of our ansatz (1), on the other hand, corresponds to configurations where no shadowing occurs. At shadowing the wave vector of the incident plane wave is tangent to the surface at some point, which causes certain integrals to diverge; see Section 4. Thus, a different kind of expansion, in fractional powers of $1/k$, should be used to treat shadowing configurations: a first order version of such an expansion was discussed in [Hong, 1967]; see [Friedlander and Keller, 1955; Lewis and Keller, 1964; Brown, 1966; Duistermaat, 1992] for the ray-tracing counterpart.

In this paper we show that high order summations of expansion (1) can indeed be used to produce highly accurate results for surfaces and wavelengths of interest in applications for both TE and TM polarizations; in Section 7, for example, we present results with machine precision accuracy, which were obtained from computations involving expansions of order as high as 20. Our algorithm is based on systematic use and manipulation of certain Taylor-Fourier series representations, which we discuss in Section 5. Operations such as product, composition and

inversion of Taylor-Fourier series lie at the core of our algebraic treatment; as shown in Section 5 certain numerical subtleties associated with these operations require a careful treatment for error control.

In order to streamline our discussion we first treat, in sections 2 to 5, the complete formalism in the TE case; the changes necessary for the TM case are then described in Section 6. In detail, in Section 2 we present our basic recursive formula for the evaluation of the coefficients $\nu_n(x)$ of equation (1) for the TE case. These coefficients depend on certain explicit asymptotic expansions of integrals, which we present in Sections 3 and 4. A discussion of the Taylor-Fourier algebra then ensues in Section 5. As we said, the modifications necessary for the TM case are discussed in Section 6. A variety of numerical results for both TE and TM polarizations, finally, are presented in Section 7.

2. High-Frequency Integral Equations — TE case

The scattered field $u = u(x, y)$ induced by an incident plane wave impinging on the rough surface $y = f(x)$ under TE polarization is the solution of the Helmholtz equation with a Dirichlet boundary condition. As is known [Voronovich, 1994] the field $u(x, y)$ can be computed as an integral involving a surface density $\nu(x, k)$ and the Green's function $G(x, y, x', y')$ for the Helmholtz equation

$$u(x, y) = \int_{-\infty}^{+\infty} \nu(x', k) \frac{\partial G}{\partial n'}(x, y, x', f(x')) \sqrt{1 + (f'(x'))^2} dx' \quad (3)$$

where ν satisfies the boundary integral equation

$$\frac{\nu(x, k)}{2} + \int_{-\infty}^{+\infty} \frac{\partial G}{\partial n'}(x, f(x), x', f(x')) \sqrt{1 + (f'(x'))^2} \nu(x', k) dx' = -e^{i\alpha x - i\beta f(x)}. \quad (4)$$

In what follows we will use the relations

$$\frac{\partial G}{\partial n'}(x, f(x), x', f(x'))\sqrt{1 + (f'(x'))^2} = -\frac{i}{4}h(kr)g(x, x')$$

$$r = \sqrt{(x' - x)^2 + (f(x') - f(x))^2} \quad h(t) = tH_1^1(t) \quad H_1^1 \text{ Hankel function}$$

$$g(x, x') = \frac{f(x') - f(x) - (x' - x)f'(x')}{r^2} \quad \alpha = k \sin(\theta) \quad \beta = k \cos(\theta),$$

where θ is the incidence angle measured counter-clockwise from the vertical axis, and $k = 2\pi/\lambda$ is the wavenumber.

A useful form of the integral equation (4) results as we factor out the rapidly oscillating phase function $e^{i\alpha x - i\beta f(x)}$

$$\left(e^{-(i\alpha x - i\beta f(x))} \nu(x, k) \right) - \frac{i}{2} \int_{-\infty}^{+\infty} h(kr)g(x, x') \left(e^{-(i\alpha x' - i\beta f(x'))} \nu(x', k) \right) dx' = -2, \quad (5)$$

which cancels the fast oscillations in all non-integrated terms, and thus suggests use of an ansatz of the form

$$\nu(x, k) = e^{i\alpha x - i\beta f(x)} \sum_{n=0}^{+\infty} \frac{\nu_n(x)}{k^n}. \quad (6)$$

Substitution of the ansatz (6) into equation (5) then yields

$$\sum_{n=0}^{+\infty} \frac{1}{k^n} \left(\nu_n(x) - \frac{i}{2} I^n(x, k) \right) = -2 \quad (7)$$

where

$$I^n(x, k) = \int_{-\infty}^{+\infty} h(kr)g(x, x') e^{i\alpha(x' - x) - i\beta(f(x') - f(x))} \nu_n(x') dx'.$$

To solve equation (7) we use asymptotic expansions for the integrals $I^n(x, k)$, collect coefficients of each power of $1/k$, and then determine, recursively, the coefficients $\nu_n(x)$. In detail, we obtain in Section 3 an expansion which gives $I^n(x, k)$ in terms of derivatives of $\nu_n(x)$

$$I^n(x, k) = \frac{1}{k} \sum_{q=0}^{+\infty} \frac{I_q^n(x)}{k^q} \quad \text{where} \quad I_q^n(x) = \sum_{\ell=0}^q \frac{\partial^\ell \nu_n(x)}{\partial x^\ell} B_{q-\ell}(x) \quad (8)$$

where the functions $B_{q-\ell}(x)$ are determined from the profile and incidence angle only. (We point out, however, that our algebraic treatment yields an expression for $I_q^n(x)$ which, although equivalent to that of (8), is different in form; see Remark 1 and equation (25).) From (7) and (8) we then find a recursion which gives $\nu_n(x)$ as a linear combination of derivatives of the previous coefficients $\nu_{n-1-q}(x)$

$$\begin{cases} \nu_0(x) &= -2 \\ \nu_n(x) &= \frac{i}{2} \sum_{q=0}^{n-1} I_q^{n-1-q}(x). \end{cases} \quad (9)$$

Use of the Taylor-Fourier algebra of Section 5 allows us to perform accurately the high order differentiations required by our high-order expansions; the needed expansion (8) of the integral I^n , in turn, is the subject of the next section.

3. Asymptotic expansion of $I^n(x, k)$

We first split the integral I^n as a sum $I^n = I_-^n + I_+^n$ where

$$I_-^n(x, k) = \int_{-\infty}^x h(kr)g(x, x')e^{i\alpha(x'-x)-i\beta(f(x')-f(x))}\nu_n(x')dx'$$

$$I_+^n(x, k) = \int_x^{+\infty} h(kr)g(x, x')e^{i\alpha(x'-x)-i\beta(f(x')-f(x))}\nu_n(x')dx'$$

We evaluate in detail the asymptotic expansion for $I_+^n(x, k)$; the corresponding expansion for I_-^n then follows analogously.

Using $t = x' - x$ we obtain

$$I_+^n(x, k) = \int_0^{+\infty} h(k\phi_+(x, t))g(x, x+t)e^{i\alpha t-i\beta(f(x+t)-f(x))}\nu_n(x+t)dt \quad (10)$$

where

$$\phi_+(x, t) = \sqrt{t^2 + (f(x+t) - f(x))^2}.$$

For the treatment presented here, $f(x)$ is assumed to satisfy the condition

$$\phi'_+(x, t) = \frac{\partial \phi_+(x, t)}{\partial t} > 0 \quad \text{for } t \geq 0 \quad (11)$$

so that the map $t \mapsto \phi_+(x, t)$ is invertible. (This condition is generally satisfied by rough surfaces considered in practice: for a sinusoidal profile $f(x) = a \cos(x)$, for example, the inequality (11) holds as long as $a < 1$.) Then setting

$$u = \phi_+(x, t) \quad \Longleftrightarrow \quad t = \phi_+^{-1}(x, u)$$

equation (10) becomes

$$I_+^n(x, k) = \int_0^{+\infty} h(ku) \frac{g(x, x + \phi_+^{-1}(x, u))}{\phi'_+(x, \phi_+^{-1}(x, u))} \nu_n(x + \phi_+^{-1}(x, u)) e^{i\alpha\phi_+^{-1}(x, u) - i\beta(f(x + \phi_+^{-1}(x, u)) - f(x))} du.$$

Calling

$$\begin{cases} F_+^n(x, u) &= \frac{g(x, x + \phi_+^{-1}(x, u))}{\phi'_+(x, \phi_+^{-1}(x, u))} \nu_n(x + \phi_+^{-1}(x, u)) \\ \psi_+(x, u) &= \left(f(x + \phi_+^{-1}(x, u)) - f(x) \right) \cos(\theta) - \phi_+^{-1}(x, u) \sin(\theta), \end{cases} \quad (12)$$

$I_+^n(x, k)$ reduces to

$$I_+^n(x, k) = \int_0^{+\infty} F_+^n(x, u) h(ku) e^{-ik\psi_+(x, u)} du.$$

Remark 1 The unknown $\nu_n(x)$ is contained as a factor in the function $F_+^n(x, u)$. Notation (12) is useful in that it helps present the integrand as a product of two distinct factors: a non-oscillatory component $F_+^n(x, u)$ and an oscillatory component $h(ku)e^{-ik\psi_+(x, u)}$.

In addition to (11) we assume the profile $y = f(x)$ is an analytic function — so that the map $u \mapsto F_+^n(x, u)$ is analytic as well. Using the Taylor series

$$F_+^n(x, u) = \sum_{m=0}^{+\infty} \frac{\partial^m F_+^n(x, 0)}{\partial u^m} \frac{u^m}{m!} = \sum_{m=0}^{+\infty} p_{n,m}^+(x) u^m \quad (13)$$

the integral $I_+^n(x, k)$ takes the form

$$\begin{aligned} I_+^n(x, k) &= \sum_{m=0}^{+\infty} p_{n,m}^+(x) \int_0^{+\infty} u^m h(ku) e^{-ik\psi^+(x,u)} du \\ &= \sum_{m=0}^{+\infty} \frac{p_{n,m}^+(x)}{k^{m+1}} \int_0^{+\infty} v^m h(v) e^{-ik\psi^+(x, \frac{v}{k})} dv. \end{aligned} \quad (14)$$

Thus, the $1/k$ expansion of I_+^n results from the corresponding expansions of the integrals

$$A^+(k, m, x) = \int_0^{+\infty} v^m h(v) e^{-ik\psi^+(x, \frac{v}{k})} dv. \quad (15)$$

These non-convergent integrals must be re-interpreted by means of analytic continuation — in a manner similar to that used in the definition and manipulation of Mellin transforms [Bleistein and Handelsman, 1986]. An explicit expansion of $A^+(k, m, x)$ is given in the following section.

3.1. Expansion of the integrals I_+^n and I_-^n

Using the Taylor expansion of $\psi^+(x, u) = \sum_{m=0}^{+\infty} \psi_m^+(x) \frac{u^m}{m!}$ in the variable u together with the identity $\psi^+(x, 0) = 0$, expansion of the function $\exp(-i(k\psi^+(x, \frac{v}{k}) - \psi_1^+(x)v))$ leads to the expression

$$e^{-ik\psi^+(x, \frac{v}{k})} = e^{-i\psi_1^+(x)v} \left(1 + \sum_{n=1}^{+\infty} k^{-n} \sum_{\ell=1}^n \frac{a_{\ell,n}^+(x)}{\ell!} v^{n+\ell} \right) \quad (16)$$

for certain (function) coefficients $a_{\ell,n}^+(x)$. Then, defining

$$A_0^+(p, x) = \int_0^{+\infty} v^p h(v) e^{-i\psi_1^+(x)v} dv \quad (17)$$

and

$$A_n^+(m, x) = \sum_{\ell=0}^n \frac{a_{\ell,n}^+(x)}{\ell!} A_0^+(m+n+\ell, x) \quad (18)$$

we obtain

$$A^+(k, m, x) = A_0^+(m, x) + \sum_{n=1}^{+\infty} \frac{A_n^+(m, x)}{k^n}, \quad (19)$$

and the series

$$I_+^n(x, k) = \sum_{q=0}^{+\infty} \left(\sum_{\ell=0}^q p_{n,q-\ell}^+(x) A_\ell^+(q-\ell, x) \right) k^{-q-1} \quad (20)$$

for I_+^n results. We see that this expansion is given in terms of the integrals (17) which, like those of the previous section, are non-convergent and require analytic continuation. An explicit expression for this integral as a function of p and x is given in Section 4.

The case of $I_-^n(x, k)$ can be treated similarly: we use $t = x - x'$ and the definitions

$$\phi_-(x, t) = \sqrt{t^2 + (f(x-t) - f(x))^2}$$

$$F_-^n(x, u) = \frac{g(x, x - \phi_-^{-1}(x, u))}{\phi'_-(x, \phi_-^{-1}(x, u))} \nu_n(x - \phi_-^{-1}(x, u))$$

$$\psi^-(x, u) = \left(f(x - \phi_-^{-1}(x, u)) - f(x) \right) \cos(\theta) - \phi_-^{-1}(x, u) \sin(\theta).$$

Then, letting $a_{\ell,n}^-(x)$ be the coefficients in the expansion of $e^{-ik\psi^-(x, \frac{v}{k})}$

$$e^{-ik\psi^-(x, \frac{v}{k})} = e^{-i\psi_1^-(x)v} \left(1 + \sum_{n=1}^{+\infty} k^{-n} \sum_{\ell=1}^n \frac{a_{\ell,n}^-(x)}{\ell!} v^{n+\ell} \right),$$

calling

$$A_0^-(p, x) = \int_0^{+\infty} v^p h(v) e^{-i\psi_1^-(x)v} dv$$

and defining the functions $A_n^-(m, x)$ by

$$A_n^-(m, x) = \sum_{\ell=0}^n \frac{a_{\ell,n}^-(x)}{\ell!} A_0^-(m+n+\ell, x). \quad (21)$$

we obtain the expansion for the integral I_-^n :

$$I_-^n(x, k) = \sum_{q=0}^{+\infty} \left(\sum_{\ell=0}^q p_{n,q-\ell}^-(x) A_\ell^-(q-\ell, x) \right) k^{-q-1}. \quad (22)$$

3.2. A simplified expression for the integral $I^n(x, k)$

The expansions for $I_+^n(x, k)$ and $I_-^n(x, k)$ can be combined into an expression which depends only on the functions $p_{n,\ell}^+(x)$, $a_{\ell,n}^+(x)$ and

$$S(q, x) = A_0^+(q, x) + (-1)^q A_0^-(q, x). \quad (23)$$

Indeed, using the identity $\phi^-(x, t) = \phi^+(x, -t)$ we find

$$\psi_\ell^-(x) = (-1)^\ell \psi_\ell^+(x), \quad a_{\ell,n}^-(x) = (-1)^{\ell+n} a_{\ell,n}^+(x), \quad \text{and} \quad p_{n,\ell}^-(x) = (-1)^\ell p_{n,\ell}^+(x). \quad (24)$$

The $1/k$ -expansion of $I^n(x, k)$ now follows from (20), (22) and (24)

$$\begin{aligned} I^n(x, k) &= I_+^n(x, k) + I_-^n(x, k) \\ &= \sum_{q=0}^{+\infty} \left(\sum_{\ell=0}^q p_{n,q-\ell}^+(x) A_\ell^+(q-\ell, x) + p_{n,q-\ell}^-(x) A_\ell^-(q-\ell, x) \right) k^{-q-1} \\ &= \sum_{q=0}^{+\infty} \sum_{\ell=0}^q p_{n,q-\ell}^+(x) \left(A_\ell^+(q-\ell, x) + (-1)^{q-\ell} A_\ell^-(q-\ell, x) \right) k^{-q-1} \end{aligned}$$

Using (18), (21) and (24) we thus obtain our key formula

$$I^n(x, k) = \sum_{q=0}^{+\infty} \frac{I_q^n(x)}{k^{q+1}}, \quad \text{where} \quad (25)$$

$$I_q^n(x) = \sum_{\ell=0}^q p_{n,q-\ell}^+(x) \left(\sum_{j=0}^{\ell} \frac{a_{j,\ell}^+(x)}{\ell!} S(q+j, x) \right).$$

As we have seen, the function $S(m, x)$ is defined by divergent integrals; an explicit expression for this function is given in the following section. The coefficients $a_{j,m}^+$ and $p_{n,m}^+$, in turn, are defined as products, quotients, compositions and inverses of certain power series expansions; accurate methods for such manipulations of power series are given in Section 5. Note that

$a_{j,\ell}^+(x)$ and $S(q+j, x)$ depend on the scattering profile and incidence angle only; the coefficient $p_{n,m}^+$ depends on the geometry and the derivatives of the coefficient ν_n of order $\leq m$.

4. Computation of $S(q, x)$.

Interestingly, a closed form expression can be given for the function $S(q, x)$. Indeed, since $\psi_1^-(x) = \psi_1^+(x)$ we may write

$$\begin{aligned} S(q, x) &= A_0^+(q, x) + (-1)^q A_0^-(q, x) \\ &= \int_0^{+\infty} v^q h(v) \left(e^{-i\psi_1^+(x)v} + (-1)^q e^{i\psi_1^+(x)v} \right) dv, \end{aligned}$$

or,

$$S(q, x) = \begin{cases} 2 \int_0^{+\infty} v^{q+1} H_1^1(v) \cos(\psi_1^+(x)v) dv & q \text{ even} \\ -2i \int_0^{+\infty} v^{q+1} H_1^1(v) \sin(\psi_1^+(x)v) dv & q \text{ odd.} \end{cases}$$

Using formulae (11.4.19) and (11.4.16) in [Abramowitz and Stegun, 1964] together with the Taylor expansion of $\sin(x)$ and $\cos(x)$, we then obtain the closed form expression

$$S(q, x) = \begin{cases} 2^{q+2} \sum_{k=0}^{+\infty} (-1)^k \frac{(2\psi_1^+(x))^{2k}}{(2k)!} \frac{\Gamma(\frac{2k+q+3}{2})}{\Gamma(\frac{1-2k-q}{2})} & q \text{ even} \\ -i 2^{q+2} \sum_{k=0}^{+\infty} (-1)^k \frac{(2\psi_1^+(x))^{2k+1}}{(2k+1)!} \frac{\Gamma(\frac{2k+q+4}{2})}{\Gamma(\frac{-2k-q}{2})} & q \text{ odd.} \end{cases} \quad (26)$$

Thus $S(q, x)$ is a series in powers of $\psi_1^+(x)$, whose coefficients can be evaluated explicitly in terms of the Γ function.

Remark 2 *It is easy to see that the radius of convergence of the power series in equation (26) is 1, and that the series actually diverges for $\psi_1^+ = 1$. This condition has an interesting physical*

interpretation; since

$$\psi_1^+(x) = \frac{f'(x) \cos(\theta) - \sin(\theta)}{\sqrt{1 + f'(x)^2}}$$

the condition $\psi_1^+(x) = 1$ is equivalent to

$$f'(x) = -\cot(\theta)$$

or, equivalently, that some rays in the incident plane wave are tangent to the scattering surface.

Alternatively, using the asymptotic expansion

$$H_1^1(v) \sim \sqrt{\frac{2}{\pi v}} e^{i\left(v - \frac{3\pi}{4}\right)}$$

we see that the oscillatory term in $A_0^+(p, x)$ is $e^{i(1-\psi_1^+(x))v}$, which becomes non-oscillatory for $\psi_1^+(x) = 1$, and thus causes the integral to diverge. Therefore, as mentioned in the introduction, the present algorithm applies only to configurations for which no shadowing occurs. Extension of these methods to configurations including shadowing are forthcoming.

Remark 3 In addition to the infinite series (26), the function S admits a finite closed form representation, namely:

$$S(q, \psi) = (1 - \psi^2)^{-(q+3/2)} P_q(\psi)$$

where $P_q(x)$ is a polynomial of degree equal to the integer part of $q/2$. These polynomials can be computed easily and efficiently through a Taylor expansion of the product $S(q, \psi)(1 - \psi^2)^{(q+3/2)}$.

For example, the first few values of q we have

$$\begin{aligned}
S(0, \psi) &= (1 - \psi^2)^{-3/2} \cdot 2 \\
S(1, \psi) &= (1 - \psi^2)^{-5/2} \cdot (-6) \\
S(2, \psi) &= (1 - \psi^2)^{-7/2} \cdot (-6 + 24\psi) \\
S(3, \psi) &= (1 - \psi^2)^{-9/2} \cdot (90 + 120\psi) \\
S(4, \psi) &= (1 - \psi^2)^{-11/2} \cdot (90 + 1080\psi + 720\psi^2) \\
S(5, \psi) &= (1 - \psi^2)^{-13/2} \cdot (-3150 - 12600\psi - 5040\psi^2)
\end{aligned}$$

5. Computation of $p_{n,q-\ell}^+$ and $a_{j,\ell}^+$: Taylor-Fourier algebra

As indicated previously, the functions $p_{n,q-\ell}^+$ and $a_{j,\ell}^+$ in equations (12), (13) and (16) can be obtained through manipulations of Taylor-Fourier series, which we define, quite simply, as Taylor series whose coefficients are Fourier series. Thus, a Taylor-Fourier series $f(x, t)$ is given by an expression of the form

$$f(x, t) = \sum_{n=0}^{+\infty} f_n(x) t^n \quad f_n(x) = \sum_{\ell=-\infty}^{\infty} f_{n\ell} e^{i\ell x} \quad (27)$$

The manipulations required by our methods include sum, products, composition and as well as algebraic and functional inverses. These operations need to be implemented with care, as we show in what follows.

Compositions and inverses of Taylor-Fourier series require consideration of multiplication and addition, so we discuss the latter two operations first. Additions do not pose difficulties: naturally, they result from addition of coefficients. Multiplications and divisions of Taylor-Fourier series, on the other hand, could in principle be obtained by means of Fast Fourier Transforms [Press et al., 1992]. Unfortunately such procedures are not appropriate in our context. Indeed, as we show below, the very rapid decay of the Fourier and Taylor coefficients arising

in our calculations is not well captured through convolutions obtained from FFTs. Since an accurate representation of this decay is essential in our method — which, based on high order differentiations of Fourier-Taylor series, greatly magnifies high frequency components — an alternate approach needs to be used.

Before describing our accurate algorithms for manipulation of Taylor-Fourier series we present an example illustrating the difficulties associated with use of FFTs in this context. We thus consider the problem of evaluating the subsequent derivatives of the function

$$S(x) = \left(\sum_{k=-\infty}^{\infty} \frac{\cos(kx)}{a^{|k|}} \right)^2$$

through multiplication and differentiation of Fourier series. For comparison purposes we note that S actually admits the closed form

$$S(x) = \left(1 + 2 \frac{a \cos(x) - 1}{a^2 - 2a \cos(x) + 1} \right)^2; \quad (28)$$

the value $a = 10$ is used in the following tests.

In Table 1 below we present the errors resulting in the evaluation of a sequence of derivatives of the function S at $x = 0$ through two different methods: FFT and direct summation of the convolution expression. (Here errors were evaluated by comparison with the corresponding values obtained from direct differentiation of the expression (28) by means of an algebraic manipulator.) We see that, as mentioned above, use of Fourier series obtained from FFTs lead to substantial accuracy losses. Indeed, FFTs evaluate the small high-order Fourier coefficients of a product through sums and differences of “large” function values, and thus, they give rise to large relative errors in the high-frequency components. These relative errors are then magnified by the differentiation process, and all accuracy is lost in high order differentiations: note the increasing loss of accuracy that results from use of larger number of Fourier modes in the FFT procedure.

The direct convolution, on the other hand, does not suffer from this difficulty. Indeed, direct convolutions evaluate a particular Fourier coefficient a_n of a product of series through sums of terms of the same order of magnitude as a_n . The result is a series whose coefficients are fully accurate in relative terms, so that subsequent differentiations do not lead to accuracy losses. We point out that full double precision accuracy can be obtained for derivatives of orders 20 and higher provided sufficiently many modes are used in the method based on direct convolutions.

In addition to sums and multiplications, our approach requires use of algorithms for composition and as well as algebraic and functional inverses of Taylor-Fourier series. In view of the previous considerations, a few comments will suffice to provide a complete prescription. Compositions result from iterated products and sums of Fourier series, and thus they do not present difficulties. As is known from the theory of formal power series [Cartan, 1963], functional inverses of a Taylor-Fourier series (27) with $f_0 = 0$ results quite directly once the algebraic inverse of the Fourier series $f_1(x) \neq 0$ is known. We may thus restrict our discussion to evaluation of algebraic inverses of Fourier series.

As in the case of the product of Fourier series, two alternatives can be considered for the evaluation of algebraic inverses. One of them involves point evaluations and FFTs; in view of our previous comments it is clear such an approach would not lead to accurate numerics. An alternative approach, akin to use of a direct convolution in evaluation of products, requires solution of a linear system of equations for the Fourier coefficients of the algebraic inverse. In view of the decay of the Fourier coefficients of smooth functions, such linear systems can be truncated and solved to produce the coefficients of inverses with high accuracy.

In sum, manipulations of Taylor-Fourier series should not use point-value discretizations if accurate values of functions and their derivatives are to be obtained. The approach described

in this section calls, instead, for operations performed fully in Fourier space. In practice we have found the procedures described here produce full double precision accuracies for all operations between Taylor-Fourier series and their subsequent high-order derivatives in very short computing times.

6. High-Frequency Integral Equations — TM case

In the transverse magnetic (TM) polarization, the scattered field $u = u(x, y)$ induced by an incident plane wave impinging on the rough surface $y = f(x)$ is the solution of the Helmholtz equation with a Neumann boundary condition. The field $u(x, y)$ can be computed [Voronovich, 1994] as an integral involving a surface density $\nu(x, k)$ and the Green's function $G(x, y, x', y')$ for the Helmholtz equation

$$u(x, y) = \int_{-\infty}^{+\infty} \nu(x', k) G(x, y, x', f(x')) \sqrt{1 + (f'(x'))^2} dx' \quad (29)$$

where ν satisfies the boundary integral equation

$$-\frac{\nu(x, k)}{2} + \int_{-\infty}^{+\infty} \frac{\partial G}{\partial n}(x, f(x), x', f(x')) \sqrt{1 + (f'(x'))^2} \nu(x', k) dx' = -\frac{\partial u^{inc}}{\partial n}(x, f(x)). \quad (30)$$

In what follows we will use the relations

$$\begin{aligned} u^{inc}(x, y) &= e^{i\alpha x - i\beta y} & \frac{\partial G}{\partial n}(x, f(x), x', f(x')) &= -\frac{i}{4} h(kr) g(x, x') \\ r &= \sqrt{(x' - x)^2 + (f(x') - f(x))^2} & h(t) &= t H_1^1(t) & H_1^1 &\text{Hankel function} \\ g(x, x') &= \frac{f(x) - f(x') - f'(x)(x - x')}{r^2} & \alpha &= k \sin(\theta) & \beta &= k \cos(\theta), \end{aligned}$$

where θ is the incidence angle measured counter-clockwise from the vertical axis, and $k = 2\pi/\lambda$ is the wavenumber. Since

$$\frac{\partial u^{inc}}{\partial n}(x, f(x)) = -\frac{i\alpha f'(x) + i\beta}{\sqrt{1 + (f'(x))^2}} e^{i\alpha x - i\beta f(x)},$$

calling $\tilde{\nu}(x, k) = \nu(x, k) \sqrt{1 + (f'(x))^2}$ we can rewrite equation (30) as follows:

$$\frac{\tilde{\nu}(x, k)}{2} - \int_{-\infty}^{+\infty} \tilde{\nu}(x', k) h(kr) g(x, x') dx' = (i\alpha f'(x) + i\beta) e^{i\alpha x - i\beta f(x)} \quad (31)$$

As in Section 2, a useful form of the integral equation (31) results as we factor out the rapidly oscillating phase function $e^{i\alpha x - i\beta f(x)}$

$$\left(e^{-(i\alpha x - i\beta f(x))} \tilde{\nu}(x, k) \right) - \frac{i}{2} \int_{-\infty}^{+\infty} h(kr) g(x, x') \left(e^{-(i\alpha x - i\beta f(x))} \tilde{\nu}(x', k) \right) dx' = 2(i\alpha f'(x) + i\beta), \quad (32)$$

which cancels the fast oscillations in all non-integrated terms. Using an expansion for the function $\tilde{\nu}(x, k)$ similar to (6)

$$\tilde{\nu}(x, k) = e^{i\alpha x - i\beta f(x)} \sum_{n=-1}^{+\infty} \frac{\nu_n(x)}{k^n}. \quad (33)$$

in (32) then yields

$$\sum_{n=-1}^{+\infty} \frac{1}{k^n} \left(\tilde{\nu}_n(x) - \frac{i}{2} I^n(x, k) \right) = 2k(i \sin(\theta) f'(x) + i \cos(\theta)) \quad (34)$$

where

$$I^n(x, k) = \int_{-\infty}^{+\infty} h(kr) g(x, x') e^{i\alpha(x' - x) - i\beta(f(x') - f(x))} \tilde{\nu}_n(x') dx'.$$

The solution of equation (34) requires asymptotic expansions for the integrals $I^n(x, k)$. These expansions are obtained, as in the TE case, by the methods of Section 3. In particular we obtain the following expressions for the coefficients $\tilde{\nu}_n(x)$:

$$\begin{cases} \tilde{\nu}_{-1}(x) = 2(i \sin(\theta) f'(x) + i \cos(\theta)) \\ \tilde{\nu}_n(x) = \frac{i}{2} \sum_{q=0}^n I_q^{n-q-1}(x). \end{cases} \quad (35)$$

7. Numerical results

Our numerical method proceeds to obtain the integral densities $\nu(x, k)$ through equation (6) in TE polarization and equation (33) in TM polarization, with coefficients ν_n and $\tilde{\nu}_n$ obtained from (9) and (35) respectively, and with I_q^n given by (25). The Taylor-Fourier expansions required in equation (12) for the functions ϕ_+^{-1} and g/ϕ'_+ are precomputed, as they depend only on the profile f and they are independent of wave numbers, incidence angles, etc. The precomputation time was 0.5 seconds for the profile of Figure 1(a) and Figure 1(b) and 0.7 seconds for the profile of Figure 1(c). (This and all subsequent calculations were performed in a DEC Alpha workstation (600MHz)). Once the density has been obtained all field related quantities can be evaluated easily from equation (3) in the TE case and equation (29) in the TM case.

In this section we present the results produced by our algorithm for the energy radiated in the various scattering directions. To do this, we use the periodic Green's function \tilde{G} of period d [Petit et al., 1980]

$$\tilde{G}(x, y) = \frac{1}{2id} \sum_{n=-\infty}^{+\infty} \frac{e^{i\alpha_n x + i\beta_n y}}{\beta_n}, \quad \alpha_n = \alpha + n \frac{2\pi}{d}, \quad \beta_n = \sqrt{k^2 - \alpha_n^2}$$

to obtain from (3) (TE) or from (29) (TM), the Rayleigh series for the scattered field

$$u(x, y) = \sum_{n=-\infty}^{+\infty} B_n e^{i\alpha_n x + i\beta_n y}.$$

Here, the coefficients B_n are "Rayleigh amplitudes", which are given in TE polarization by

$$B_n = \frac{1}{2d} \int_0^d \left(-1 + \frac{\alpha_n}{\beta_n} f'(x) \right) \nu(x, k) e^{-i\alpha_n x - i\beta_n f(x)} dx;$$

and in TM polarization by

$$B_n = \frac{1}{2id\beta_n} \int_0^d \tilde{\nu}(x, k) e^{-i\alpha_n x - i\beta_n f(x)} dx.$$

The required integrals were computed by means of the trapezoidal rule, which for the periodic functions under consideration is spectrally accurate, and can be computed very efficiently by means of the FFT.

Our numerical results show values and errors corresponding to the “scattering efficiencies” e_n , see [Petit et al., 1980], which are defined by

$$e_n = \frac{\beta_n}{\beta} |B_n|^2,$$

and which give the fraction of the energy which is scattered in each one of the (finitely many) scattering directions. To test the accuracy of our numerical procedures we compare our high-frequency (HF) results to those of the method of variation boundaries [Bruno and Reitich, 1993] (MVB) in an “overlap” wavelength region — in which both algorithms are very accurate; additional results, in regimes beyond those that can be resolved by the boundary variation method are also presented. Note that the HF and MVB methods are substantially different in nature: one is a high order expansion in $1/k$ whereas the other is a high order expansion in the height h of the profile. In the examples that follow we list *relative errors* for the computed values of scattered energies in the various scattering directions. The figures given in the columns denoted by Order 0-19 are the relative errors for the values of the scattered energy calculated from the high frequency code to orders 0-19 in the corresponding scattering direction. In all cases errors were evaluated through comparison with a highly accurate reference solution; in Tables 2 to 8 the reference solution was produced by means of the boundary variations code mentioned above; in Tables 9 and 10, the reference solution was obtained through a higher-order application of our high frequency algorithm (Order 15). The first term in the high-frequency expansion happens to coincide with the classical Kirchhoff approximation. Note that the Kirchhoff approximation can also be obtained as the zeroth order term of the Neumann

series for equation (4). We emphasize, however, that the high-frequency method used in this paper is of a completely different nature to that arising from use of Neumann series.

Our first example, presented in Table 2, corresponds to the profile in Figure 1(a) illuminated by a TE polarized plane wave with $h = 0.025$, $\lambda = 0.025$ and an incidence angle $\theta = 30^\circ$. The run time was 10 seconds for the calculation of order 17; we see that, as claimed, the present approach produces results with full double precision accuracy in short computing times.

The results for the profile in Figure 1(a) under TM polarization are given in Table 3. Here we take $h = 0.025$, $\lambda = 0.0251$, with an incidence angle $\theta = 30^\circ$. Our choice of wavelength in the present TM case, which is slightly different from the value $\lambda = 0.025$ we used in the TE case, was made to avoid the Wood anomaly [Hutley, 1982] that occurs at the latter value, for which the test boundary variation code fails. Our high-frequency method however does not suffer from that drawback and results for the profile in Figure 1(a) with $h = 0.025$, $\lambda = 0.025$ and an incidence angle $\theta = 30^\circ$ are given in Table 4. The reference solution in this case is the high-order high-frequency solution of order 21. The convergence of our expansion in this case is similar to the convergence observed to the previous case where $\lambda/d = 0.0251$. Again, full double precision accuracies are reached in a 10 second calculation.

Our method is not restricted to sinusoidal surfaces, of course. In Table 5, for instance we present results corresponding to the profile of Figure 1(b) with $h = 0.01$, $\lambda = 0.025$ and $\theta = 0^\circ$ in TE polarization. The run time was 5 seconds for the order 11 calculation. Table 6 shows results for the same profile under TM polarization with $h = 0.01$, $\lambda = 0.0251$ and $\theta = 0^\circ$. The run time was 4 seconds for the order 11 calculation.

We next consider the third order ‘‘Stokes’’ wave [Kinsman, 1965] shown in Figure 1(c). The results presented in Table 7 assumed the parameter values $h = 0.02$, $\lambda = 0.04$ and $\theta = 0^\circ$ and TE

polarization. The run time in this case was 27 seconds for the calculation of order 19. Table 8 shows the results for TM polarization and $h = 0.02$, $\lambda = 0.041$ and $\theta = 0^\circ$. The run time was 23 seconds for the order 19 calculation.

Table 9, presents results for a low grazing angle example for the profile of Figure 1(a) with $h = 0.025$, $\lambda = 0.001$ and $\theta = 70^\circ$ (20° grazing) in TE polarization. As mentioned above, for reference in this case we used the high-frequency solution of order 15. The run time for the order 9 calculation was 12 seconds. The results for the profile of Figure 1(a) under TM polarization with $h = 0.025$, $\lambda = 0.0011$ and $\theta = 70^\circ$ are given in Table 10. The run time was 19 seconds for the order 9 calculation.

A final remark concerning the order of the Fourier series used in the examples above is now in order. For the examples given in Tables 2-8 no more than 30 Fourier modes were used. The number of Fourier modes needed depends on the incidence angle, height of the profile, the order of the high-frequency expansion used and the accuracy required; in the cases considered in Tables 9 and 10, for example, it was necessary to use 45 Fourier coefficients to achieve the accuracies reported.

8. Conclusions

We have shown that high order summations of expansions of the type (1) can be used to produce highly accurate results for problems of scattering by rough surfaces in the high-frequency regime in TE and TM polarizations. Our algorithm is based on analytic continuation of divergent integrals and careful algebraic manipulation of Taylor-Fourier series representations. Our results show accuracies which improve substantially over those given by classical methods such as the Kirchhoff approximation. As shown recently [Sei et al., 1999], such accuracies are needed to

capture important aspects of rough surface scattering involving very low scattering returns and occurrences of unusual polarization ratios. Further, the results of [Bruno and Reitich, 1993] clearly suggest that a multiscale perturbation algorithm of the type proposed in [Bruno et al., 2000] should yield the required accuracies for multiscale surfaces provided an accurate high-frequency solver, such as the one presented in this paper, is used. This paper thus extends the range of applicability of classical asymptotic methods producing a versatile, highly accurate and efficient high-frequency numerical solver.

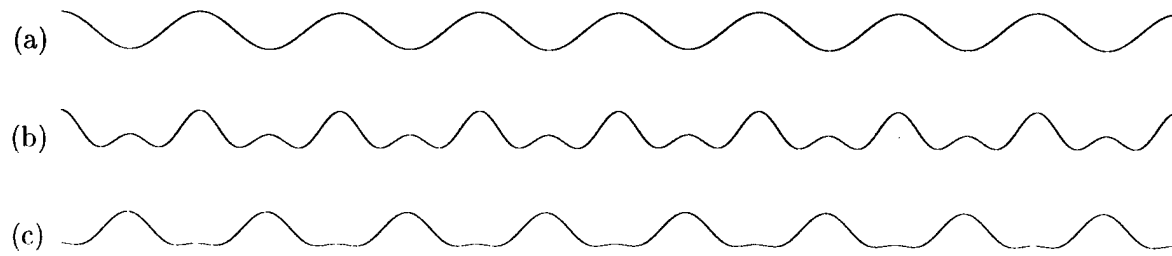


Figure 1. Various profiles considered in the text:

$$(a) \ f(x) = \frac{h}{2} \cos(2\pi x)$$

$$(b) \ f(x) = \frac{h}{2} (\cos(2\pi x) + \cos(4\pi x))$$

$$(c) \ f(x) = \frac{h}{2} (-\cos(2\pi x) + 0.35 \cos(4\pi x) - 0.035 \cos(6\pi x))$$

Table 1. Values of the derivatives of the function $S(x)$ at $x = 0$ for various orders of differentiation. The columns marked 20 Modes, 30 Modes and 40 Modes list the *relative errors* of the derivatives computed by summing differentiated Fourier series truncated at 20, 30 and 40 Modes, respectively. Columns FFT and Conv. resulted from use of Fourier coefficients obtained through FFTs and direct convolution, respectively.

Order	Exact value at 0	20 Modes		30 Modes		40 Modes	
		FFT	Conv.	FFT	Conv.	FFT	Conv.
2	-7.376924249352232e-01	1.3e-12	5.4e-16	1.7e-11	2.7e-16	1.0e-11	2.7e-16
4	2.377008924791275e+00	6.8e-11	3.0e-14	4.2e-09	2.9e-15	9.8e-10	2.9e-15
6	-1.702966504696142e+01	5.5e-10	1.8e-12	4.6e-07	0.0e-00	1.7e-07	0.0e-00
8	2.184589621949499e+02	2.7e-08	5.8e-11	2.9e-05	2.3e-15	4.1e-05	2.3e-15
10	-4.361708943655447e+03	8.8e-07	1.2e-09	1.1e-03	6.9e-16	3.8e-03	6.9e-16
12	1.248619506829422e+05	1.4e-05	1.7e-08	3.1e-02	0.0e-00	2.2e-01	8.0e-16
14	-4.844671808314213e+06	1.4e-04	1.8e-07	6.5e-01	6.0e-15	8.7e+00	1.0e-15
16	2.445839768254340e+08	1.1e-03	1.5e-06	1.0e+01	1.3e-13	2.7e+02	1.6e-15
18	-1.557531553377787e+10	6.5e-03	9.4e-06	1.3e+02	1.9e-12	6.6e+03	0.0e-00
20	1.220898732494702e+12	3.1e-02	5.0e-05	1.4e+03	2.2e-11	1.3e+05	8.2e-16

Table 2. Results for the profile of Figure 1(a) in TE polarization with $h = 0.025$, $\lambda = 0.025$ and incidence angle $\theta = 30^\circ$. The run time was 10 seconds for the calculation of order 17.

Efficiency #	Scattered Energy	Order 0	Order 1	Order 5	Order 11	Order 17
0	7.538669511479800e-04	3.8e-02	6.3e-05	1.1e-08	5.0e-12	2.4e-13
1	1.194293110668300e-01	2.0e-04	3.1e-06	4.9e-09	2.8e-13	2.2e-14
2	4.713900020760300e-03	1.5e-02	1.7e-05	2.7e-08	6.5e-13	3.3e-14
3	9.472951023686101e-02	2.4e-03	5.8e-05	1.7e-09	1.2e-13	4.0e-15
4	1.606247510782500e-01	1.2e-04	8.9e-05	2.8e-10	7.3e-14	8.6e-15
5	8.121747375826800e-02	1.5e-03	1.3e-04	2.3e-08	3.5e-14	7.9e-15
6	2.068175899532900e-02	2.7e-03	1.9e-04	1.2e-08	3.1e-13	4.4e-15
7	3.171379802403400e-03	3.9e-03	2.5e-04	3.5e-08	1.5e-13	5.3e-15

Table 3. Results for the profile of Figure 1(a) in TM polarization with $h = 0.025$, $\lambda = 0.0251$ and incidence angle $\theta = 30^\circ$. The run time was 10 seconds for the calculation of order 17.

Efficiency #	Scattered Energy	Order 0	Order 1	Order 5	Order 11	Order 17
0	1.148002904781718e-03	3.1e-02	3.4e-05	2.6e-09	7.2e-13	4.0e-13
1	1.196487185464779e-01	1.5e-04	1.1e-05	2.2e-11	1.8e-14	3.3e-14
2	3.930863630633380e-03	1.6e-02	2.9e-05	2.8e-10	1.5e-13	1.1e-13
3	9.729981709870275e-02	2.4e-03	2.3e-05	2.6e-10	4.3e-14	3.7e-14
4	1.603959300090739e-01	1.4e-04	4.0e-05	3.6e-10	1.9e-14	2.4e-14
5	7.991729015156721e-02	1.5e-03	6.5e-05	2.8e-10	1.3e-14	6.9e-15
6	2.011674295356339e-02	2.7e-04	9.8e-05	3.4e-10	4.0e-14	1.3e-14
7	3.052813099869383e-03	3.9e-03	1.4e-04	2.5e-09	4.4e-14	9.6e-14

Table 4. Results for the profile of Figure 1(a) in TM polarization with $h = 0.025$, $\lambda = 0.025$ and incidence angle $\theta = 30^\circ$. The run time was 10 seconds for the calculation of order 17.

Efficiency #	Scattered Energy	Order 0	Order 1	Order 5	Order 11	Order 17
0	6.978718873398379e-004	4.0e-02	4.8e-05	3.2e-09	4.0e-13	1.6e-15
1	1.193803726254851e-001	2.1e-04	1.1e-05	1.9e-11	1.3e-14	9.3e-16
2	4.854671479355886e-003	1.5e-02	2.5e-05	2.6e-10	3.9e-14	5.4e-16
3	9.427330239288337e-002	2.4e-03	2.3e-05	2.5e-10	6.8e-15	2.9e-16
4	1.606619051666006e-001	1.1e-04	3.9e-05	3.5e-10	4.3e-15	5.2e-16
5	8.146471443830940e-002	1.5e-03	6.4e-05	2.8e-10	4.3e-15	0.0e-16
6	2.079411505463193e-002	2.7e-04	9.6e-05	3.1e-10	2.2e-14	1.0e-15
7	3.195973191313253e-003	3.9e-03	1.4e-04	2.3e-09	1.4e-13	1.9e-15

Table 5. Results for the profile of Figure 1(b) in TE polarization with $h = 0.01$, $\lambda = 0.025$ and $\theta = 0^\circ$. The run time was 5 seconds for the order 11 calculation.

Efficiency #	Scattered Energy	Order 0	Order 1	Order 5	Order 9	Order 11
0	1.983702874853860e-01	1.4e-03	6.7e-06	6.3e-10	1.8e-13	9.8e-16
1	2.125625186015414e-02	4.3e-03	7.3e-06	8.6e-10	4.6e-14	1.5e-14
2	5.109656298137152e-02	4.2e-03	5.3e-06	1.3e-09	3.5e-14	1.1e-14
3	1.350594564861170e-01	1.1e-03	3.0e-06	1.8e-10	5.1e-14	6.6e-15
4	1.670755436364386e-02	4.3e-03	928e-06	1.5e-09	1.8e-13	2.7e-15
5	1.041839113172000e-01	8.7e-04	1.1e-05	4.7e-10	3.8e-14	2.9e-15
6	3.029977474761340e-02	7.6e-04	1.1e-05	4.8e-10	1.0e-15	9.0e-15
7	2.828409217693459e-02	2.5e-03	3.2e-05	1.8e-09	3.5e-14	9.4e-15

Table 6. Results for the profile of Figure 1(b) in TM polarization with $h = 0.01$, $\lambda = 0.025$ and $\theta = 0^\circ$. The run time was 4 seconds for the order 11 calculation.

Efficiency #	Scattered Energy	Order 0	Order 1	Order 5	Order 9	Order 11
0	1.985778821348800e-01	1.3e-03	1.1e-05	5.6e-11	9.1e-15	5.0e-15
1	2.203189065423864e-02	4.3e-03	6.1e-06	8.5e-12	2.0e-14	2.2e-14
2	4.989624245086630e-02	4.2e-03	1.2e-05	1.3e-10	6.8e-15	8.3e-15
3	1.363942224141270e-01	1.1e-03	3.0e-06	6.6e-11	1.1e-14	6.7e-15
4	1.685456723960805e-02	4.3e-03	1.7e-05	1.5e-10	2.7e-14	1.5e-14
5	1.040033802018770e-01	8.9e-04	9.9e-07	8.4e-11	2.9e-15	2.0e-15
6	2.994981016528542e-02	7.8e-04	1.5e-06	1.9e-10	1.4e-15	1.0e-14
7	2.795532080716518e-02	2.5e-03	1.5e-05	1.2e-11	3.2e-15	1.1e-15

Table 7. Results for the profile of Figure 1(c) in TE polarization with $h = 0.02$, $\lambda = 0.04$ and $\theta = 0^\circ$. The run time was 27 seconds for the calculation of order 19.

Efficiency #	Scattered Energy	Order 0	Order 1	Order 5	Order 11	Order 19
0	2.762105662320035e-01	1.9e-3	1.6e-5	7.4e-9	6.5e-14	2.4e-15
1	5.735818584364873e-02	3.1e-3	2.0e-5	1.9e-8	1.3e-12	6.0e-16
2	9.154897389472935e-02	3.7e-3	5.1e-6	8.2e-9	1.4e-12	6.7e-15
3	1.051875097051952e-01	4.6e-4	5.1e-6	1.6e-9	1.0e-12	9.2e-16
4	6.713521833646909e-02	1.7e-3	2.7e-5	1.4e-11	3.6e-12	2.1e-16
5	2.830374622545111e-02	3.9e-3	7.3e-5	1.4e-8	2.2e-13	6.7e-15
6	9.270117932865375e-03	5.9e-3	1.3e-4	3.2e-8	1.1e-11	3.0e-15
7	2.435385416440963e-03	7.9e-3	2.2e-4	8.4e-8	4.1e-12	1.8e-16

Table 8. Results for the profile of Figure 1(c) in TM polarization with $h = 0.02$, $\lambda = 0.041$ and $\theta = 0^\circ$. The run time was 23 seconds for the calculation of order 19.

Efficiency #	Scattered Energy	Order 0	Order 1	Order 5	Order 11	Order 19
0	1.291589358261453e-01	2.2e-03	1.6e-05	2.7e-10	2.1e-12	9.5e-14
1	1.662663939465338e-01	1.7e-03	5.1e-05	2.8e-10	1.6e-12	4.1e-14
2	3.920583564991646e-03	8.5e-03	5.3e-06	7.0e-09	1.3e-11	6.2e-13
3	1.878743087516774e-02	1.5e-02	2.7e-06	2.6e-09	6.9e-12	1.5e-13
4	7.416580102755271e-02	3.7e-03	2.8e-05	4.6e-09	6.7e-12	9.4e-15
5	7.840714643630796e-02	2.4e-04	2.0e-05	6.5e-09	6.6e-13	2.4e-14
6	5.345392880491968e-02	2.6e-03	1.6e-05	6.5e-09	9.6e-12	4.9e-14
7	2.611186407051911e-02	5.1e-03	6.8e-05	4.3e-09	8.6e-13	5.1e-14

Table 9. Results for the profile of Figure 1(a) in TE polarization with $h = 0.025$, $\lambda = 0.001$ and $\theta = 70^\circ$. The run time was 12 seconds for the order 9 calculation.

Efficiency #	Scattered Energy	Order 0	Order 1	Order 3	Order 7	Order 9
0	9.405896918172547e-03	9.1e-06	2.3e-07	1.2e-10	1.7e-14	6.1e-16
1	4.691450406852652e-03	1.2e-05	1.1e-07	8.4e-11	2.3e-16	2.2e-16
2	4.977619850889408e-03	1.2e-05	1.3e-07	7.3e-11	7.5e-15	9.1e-17
3	8.970028199252082e-03	1.1e-05	2.1e-07	1.8e-10	5.5e-15	3.6e-16
4	1.591650541515982e-03	8.4e-06	4.2e-08	2.5e-11	5.2e-17	3.9e-16
5	1.151449525094811e-02	6.0e-06	2.7e-07	2.7e-10	3.8e-15	5.7e-17
6	1.509705192413105e-04	2.8e-06	4.9e-09	8.3e-13	1.2e-15	2.0e-16
7	1.232860573339191e-02	6.3e-07	2.9e-07	3.5e-10	4.2e-15	7.6e-16

Table 10. Results for the profile of Figure 1(a) in TM polarization with $h = 0.025$, $\lambda = 0.0011$ and $\theta = 70^\circ$. The run time was 19 seconds for the order 9 calculation.

Efficiency #	Scattered Energy	Order 0	Order 1	Order 3	Order 7	Order 9
0	4.663322085313096e-03	2.9e-03	1.8e-05	1.4e-08	8.5e-14	9.9e-15
1	5.732453099268077e-03	2.4e-03	2.0e-05	1.5e-08	1.2e-14	1.0e-14
2	9.742422239435774e-03	1.4e-03	1.9e-05	1.5e-08	5.0e-14	2.7e-15
3	1.692802029774497e-03	5.8e-03	2.2e-05	1.7e-08	5.1e-16	2.9e-15
4	1.271613899298100e-02	5.4e-04	1.9e-05	1.7e-08	4.9e-14	2.5e-15
5	9.550848574956618e-05	2.7e-02	3.1e-05	2.7e-08	1.7e-13	8.7e-15
6	1.351161517190391e-02	2.2e-05	2.0e-05	1.9e-08	6.8e-14	5.3e-15
7	1.898341280339258e-04	2.0e-02	1.1e-05	9.9e-09	2.9e-13	7.6e-14

Acknowledgment and Disclaimer: Effort sponsored by DARPA/AFOSR under contract number F49620-99-C-0014, the Air Force Office of Scientific Research, Air Force Materials Command, USAF, under grant numbers F49620-99-1-0010 and F49620-99-1-0193, and through NSF contracts No. DMS-9523292 and DMS-9816802). The US Government is authorized to reproduce and distribute reprints for governmental purposes notwithstanding any copyright notation thereon. The views and conclusions contained herein are those of the authors and should not be interpreted as necessarily representing the official policies or endorsements, either expressed or implied, of the Air Force Office of Scientific Research or the US Government.

References

- M. Abramowitz and I. Stegun, *Handbook of mathematical functions with formulas, graphs, and mathematical tables*, US Dept Commerce, June, 1964.
- D. S. Ahluwalia, R. M. Lewis and J. Boersma, *Uniform asymptotic theory of diffraction by a plane screen*, SIAM J. Appl. Math., **16** (4), 783-807, 1968.
- H. Ansoorge, *Electromagnetic reflection from a curved dielectric interface*, IEEE Trans. Ant. Prop., **34**, 842-845, 1986.
- H. Ansoorge, *First order corrections to reflection and transmission at a curved dielectric interface with emphasis on polarization properties*, Radio science, **22**, 993-998, 1987.
- J. D. Benamou, *Direct computations of multivalued phase space solutions for Hamilton-Jacobi equations*, Comm. Pure Appl. Math., **52**, 1443-1475, 1999.
- N. Bleistein and R. A. Handelsman, *Asymptotic expansions of integrals*, Dover Publications, New York, 1986.
- C. O. Bloom and N. D. Kazarinoff, *Short wave radiation problems in inhomogeneous media : asymptotic solutions*, Lecture Notes in Mathematics 522, Springer-Verlag, Berlin, 1976.
- D. Bouche, F. Molinet and R. Mittra, *Asymptotic methods in electromagnetics*, Springer-Verlag, Berlin, 1997.
- W. P. Brown, *On the asymptotic behavior of electromagnetic fields from convex cylinders near grazing incidence*, J. of Math. Anal. and App., **15**, 355-385, 1966.
- O. Bruno and F. Reitich, *Numerical solution of diffraction problems: a method of variation of boundaries I, II, III*, J. Opt. Soc. A **10**, 1168-1175, 2307-2316, 2551-2562, 1993.

- O. Bruno, A. Sei and M. Caponi, *Rigorous multi-scale solver for rough-surface scattering problems: high-order-high-frequency and variation of boundaries*, To appear in the Proceedings of the NATO Sensors and Electronics Technology (SET) Symposium on "Low Grazing angle clutter: Its Characterization, Measurement, and Application", JHU/APL, Laurel, MD, April 25-27 2000.
- H. Cartan, *Elementary theory of analytic functions of one or several complex variables*, Addison-Wesley, Reading, Mass., 1963.
- H. Chaloupka and H. J. Meckelburg, *Improved high-frequency current approximation for curved conducting surfaces*, AEU, Arch. Elektron. Ubertragungstech, **39**, 245-250, 1985.
- J. J. Duistermaat, *Huygens' principle for linear partial differential equations*, Huygens' principle, 1690-1990 : theory and applications, H. Blok Ed, Elsevier, 1992.
- E. Fatemi, B. Engquist and S. Osher, *Numerical solution of the high frequency asymptotic expansion for the scalar wave equation*, J. Comp. Phys., **120**, 145-155, 1995.
- F. G. Friedlander, *Geometrical Optics and Maxwell's equations*, Proc. Cambridge Philos. Soc., **43** (2), 284-286, 1946.
- F. G. Friedlander and J. B. Keller, *Asymptotic expansion of solutions of $(\nabla^2 + k^2)u = 0$* , Comm. Pure Appl. Math., **8**, 387-394, 1955.
- M. A. Gil'Man, A. G. Mikheyev and T. L. Tkachenko, *The two-scale model and other methods for the approximate solution of the problem of diffraction by rough surfaces*, Comp. Maths Math. Phys., **36**, 1429-1442, 1996.
- S. Hong, *Asymptotic theory of electromagnetic and acoustic diffraction by smooth convex surfaces of variable curvature*, J. Math. Phys., **8**, 1223-1232, 1967.
- M.C. Hutley *Diffraction gratings*, Academic Press, San Diego, Calif., 1982.
- J. B. Keller, *A geometric theory of diffraction*, AMS Calculus of variations and its applications, L.M. Graves ed., McGraw-Hill, New York, 1958.
- B. Kinsman, *Wind waves, their generation and propagation on the ocean surface*, Englewood Cliffs, N.J., Prentice-Hall, 1965.
- Y. A. Kravtsov, *A modification of the geometric optics method*, Radiofizika, **7**, 664-673, 1964.
- B. F. Kuryanov, *The scattering of sound at a rough surface with two types of irregularity*, Soviet Physics-Acoustic, **8** (3), 252-257, Jan. 1963.
- S. W. Lee, *Electromagnetic reflection from a conducting surface: geometrical optics solution*, IEEE Trans. Ant. Prop., **23**, 184-191, 1975.

- R. M. Lewis and J. Boersma, *Uniform theory of edge diffraction*, J. Math. Phys., **10** (12), 2291-2305, 1969.
- R. M. Lewis and J. B. Keller, *Asymptotic methods for partial differential equations: The reduced wave equation and Maxwell's equations*, Research Report EM-194, New York University, 1964. (Reprinted in *Surveys in Applied Mathematics*, 1-82, Plenum Press, New York, 1995).
- R. M. Lewis, N. Bleistein and D. Ludwig, *Uniform asymptotic theory of creeping waves*, Comm. Pure Appl. Math., **20**, 295-320, 1967.
- R. K. Luneburg, *Mathematical theory of Optics*, Brown University, 1944. (reprinted by University of California Press, Berkeley, 1964).
- R. K. Luneburg, *Asymptotic expansion of steady state electromagnetic fields*, Research Report EM-14, New York University, July 1949.
- R. K. Luneburg, *Asymptotic evaluation of diffraction integrals*, Research Report EM-15, New York University, October 1949.
- D. Ludwig, *Uniform asymptotic expansion at a caustic*, Comm. Pure Appl. Math., **19**, 215-250, 1966.
- S. T. McDaniel and A. D. Gorman, *An examination of the composite-roughness scattering model*, J. Acoust. Soc. Am., **73**, 1476-1486, 1983.
- W. L. Miranker, *Parametric theory of $\Delta u + k^2 u$* , Arch. Ratl. Mech. Anal., **1**, 139-152, 1957.
- K. M. Mitzner, *Effect of small irregularities on electromagnetic scattering from an interface of arbitrary shape*, J. Math. Phys., **5**, 1776-1786, 1964.
- R. Petit, ed. *Electromagnetic theory of Gratings*, Springer-Verlag, Berlin, 1980.
- W. H. Press, S. A. Teukolsky, W. T. Vetterling and B. P. Flannery, *Numerical Recipes*, Cambridge University Press, 1992.
- S. O. Rice, *Reflection of electromagnetic waves from slightly rough surfaces*, Comm. Pure Appl. Math., **4**, 351-378, 1951.
- A. Sei, O. P. Bruno and M. Caponi, *Study of polarization scattering anomalies with application to oceanic scattering* Radio Science, **34** (2), 385-411, March 1999.
- A. B. Shmelev, *Wave scattering by statistically uneven surfaces*, Soviet Physics uspekhi, **15** (2), 173-183, Sept. 1972.
- G.R. Valenzuela, *Theories for the interaction of electromagnetic and oceanic waves - A review*, Boundary-layer Meteor. **13**, 61-85, 1978.
- N. G. Van Kampen, *An asymptotic treatment of diffraction problems*, Physica **14** (9), 575-589, January 1949.

- J. Vidale, *Finite difference calculation of traveltimes*, B. Seismol. Am., **78**, 2062-2076, 1988.
- A. G. Voronovich, *Wave scattering from rough surfaces*, Springer-Verlag, Berlin, 1994.
- J. VanTrier and W. W. Symes, *Upwind finite- difference calculation of traveltimes*, Geophysics, **56**, 812-821, 1991.

(Received _____)

Copyright 2001 by the American Geophysical Union.

Paper number .

:

:

:

:

:

:

:

:

:

Appendix A2:

Polarization ratios anomalies of 3D rough surface scattering as second order effects,
IEEE AP-S International symposium, Boston, Massachusetts, July 2001.

Polarization ratios anomalies of 3D rough surface scattering as second order effects

Alain Sei and Maria Caponi

Ocean Technology Department, TRW, 1 Space Park, Redondo Beach, Ca, 90278

Oscar Bruno

Applied Mathematics, California Institute of Technology, Pasadena Ca, 91125

Abstract. In the present paper a detailed analysis of the behaviour of the electromagnetic scattering from various corrugated bi-dimensional surfaces is presented. We show that rigorous electromagnetic computations on two dimensional surfaces can in fact yield HH/VV polarization ratios greater than one, with values consistent with those observed experimentally. Furthermore we show that HH/VV ratios greater than one are ubiquitous in the case of surfaces of the form $f(x, y) = f_1(x) + f_2(y)$, known as crossed grating in optics. As demonstrated theoretically and numerically below these surfaces produce backscattered returns for which the first order Rice/Valenzuela term vanishes for off axis incidence. Further, the second order term becomes dominant and has the property that HH returns exceed VV returns for a significant range of incident angles. Our approach is based on the methods of [Bruno and Reitich, 1993] which yield accurate results for a large range of values of the surface height. In particular, these methods can be used well beyond the domain of applicability of the first order theory of [Rice, 1951]. The error in our calculations is guaranteed to be several orders of magnitude smaller than the computed values. The high order expansions provided by these methods are essential to determine the role played by the second order terms as they show that these terms indeed dominate most of the backscattering returns for the surfaces mentioned above. Classically, large HH/VV ratios were sought by means of first order approximations on one dimensional sinusoidal profiles. As we show below, in that case the first order terms do not vanish and the first order theories predict the behaviour of the backscattered returns, for small values of the height to period ratio. However, in the case of a two dimensional bisinusoidal surface, strong polarization dependent anomalies appear in the scattering returns as a *result* of the contributions of second order terms since, in that case, the first order contributions vanish.

1 Introduction

Recently, in the framework of remote sensing, experimental data [Trizna et al., 1991, Lee et al., 1997] has drawn attention to a peculiar feature of polarization effects of oceanic scattering. It was observed that radar cross sections for HH polarization (transmit H and receive H) can exceed radar cross sections for VV polarization (transmit V and receive V) in so called super-events. In the present paper we show that rigorous electromagnetic computations on two dimensional surfaces can yield HH/VV ratios greater than one, with values consistent with those observed experimentally. Furthermore we show that HH/VV ratios greater than one are ubiquitous in the case of surfaces of the form $f(x, y) = f_1(x) + f_2(y)$, (known as crossed grating in optics). As demonstrated below these surfaces produce

backscattered returns for which the first order (Rice/Valenzuela) term vanishes for off axis incidence. Further, the second order term becomes dominant and has the property that HH returns exceed VV returns for a significant range of incident angles.

2 Perturbation expansions

We consider a time harmonic incident plane wave impinging on the doubly periodic surface $z = f(x, y)$, with x-axis period d_x and y-axis period d_y . We have: $f(x + d_x, y + d_y) = f(x, y)$. The incident electric field with wave vector \mathbf{k} is :

$$\mathbf{E}^{inc} = \mathbf{A} \exp [i(\alpha x + \beta y - \gamma z)] \quad (1)$$

where the vector $\mathbf{A} = (A^1, A^2, A^3)$ specifies the state of polarization of the incident wave and \mathbf{k} is determine from the incident angles ψ and θ as follows:

$$\mathbf{k} = \begin{pmatrix} \alpha = k \cos(\psi) \sin(\theta) \\ \beta = k \sin(\psi) \sin(\theta) \\ -\gamma = -k \cos(\theta) \end{pmatrix} \quad (2)$$

The angle θ is the angle between the vector \mathbf{k} and the z-axis and the angle ψ is the angle between the projection of the vector \mathbf{k} and the x-axis and $k = |\mathbf{k}| = 2\pi/\lambda$ where λ is wavelength of the incident radiation. The time harmonic Maxwell's equations for the scattered electric field \mathbf{E} reduce to the following equations in the case of a perfect conductor:

$$\begin{cases} \Delta \mathbf{E}(x, y, z) + k^2 \mathbf{E}(x, y, z) = 0 & \nabla \cdot \mathbf{E}(x, y, z) = 0 \\ \mathbf{n} \times \mathbf{E}(x, y, f(x, y)) = -\mathbf{n} \times \mathbf{E}^{inc}(x, y, f(x, y)) \end{cases} \quad (3)$$

where \mathbf{n} is the normal to the surface $z = f(x, y)$. To derive a perturbation series for the solution of this scattering problem we introduce the surface $f_\delta(x, y) = \delta f(x, y)$ where δ is a complex number, see [Bruno and Reitich, 1993]. The scattered field $\mathbf{E}(x, y, z; \delta)$ associated to the surface $f_\delta(x, y)$ can be written and computed as a Taylor series expansion in powers of δ , as follows:

$$\mathbf{E}(x, y, z; \delta) = \mathbf{E}(x, y, z; 0) + \mathbf{E}_\delta(x, y, z; 0)\delta + \mathbf{E}_{\delta\delta}(x, y, z; 0)\frac{\delta^2}{2} + \dots \quad (4)$$

Solving the scattering problem for the surface $z = f(x, y)$ then amounts to evaluating the series (4) at $\delta = 1$.

As is known, see [Petit, 1980], the field scattered from a bi-periodic surface can be represented outside the groove region (that is for $z > \max f(x, y)$) as a sum of outgoing plane waves with certain amplitudes $\mathbf{B}_{p,q}$ as follows $\mathbf{E}(x, y, z) = \sum_{p,q} \mathbf{B}_{p,q} e^{i\alpha_p x + i\beta_q y - \gamma_{p,q} z}$ where

$$\alpha_\ell = \alpha + \ell K_x \quad \beta_m = \beta + m K_y \quad \gamma_{\ell,m} = \sqrt{k^2 - \alpha_\ell^2 - \beta_m^2} \quad (5)$$

and where the surface $z = f(x, y)$ is given by its Fourier series:

$$f(x, y) = \sum_{\ell, m=-P}^P f_{\ell, m} e^{i\ell K_x x + im K_y y} \quad K_x = \frac{2\pi}{d_x} \quad K_y = \frac{2\pi}{d_y}$$

The outgoing (p, q) plane wave $e^{i\alpha_p x + i\beta_q y + \gamma_{p,q} z}$ will contribute backscattering returns if the following 3D Bragg conditions are satisfied:

$$\alpha_p = -\alpha \quad \beta_q = -\beta \quad \gamma_{p,q} = \gamma \quad (6)$$

From the definitions (2) and (5), the conditions (6) are equivalent to the following:

$$\frac{\lambda}{d_x} = \frac{2 \sin(\theta)}{\sqrt{p^2 + \left(\frac{d_x}{d_z}\right)^2 q^2}} \quad \tan(\psi) = \frac{q}{p} \frac{d_x}{d_y} \quad (7)$$

For a given incidence (θ, ψ) , for which p and q satisfy (7), it can be shown that the first order backscattered field is given by:

$$\mathbf{E}_\delta(x, y, z, ; 0) = \begin{pmatrix} 2i(\gamma A^1 + 2\alpha A^3) \\ 2i(\gamma A^2 + 2\beta A^3) \\ -2i(\alpha A^1 + \beta A^2) + 4i\frac{A^3}{\gamma}(\alpha^2 + \beta^2) \end{pmatrix} f_{p,q} e^{i\alpha_p x + i\beta_q y + \gamma_{p,q} z} \quad (8)$$

3 Numerical Results - Perfectly conducting surfaces

We consider the simplest two dimensional surface namely a bisinusoid surface with periods $d_x = d_y = 1$ and height h defined by:

$$f(x, y) = \frac{h}{4} (\cos(2\pi x) + \cos(2\pi y)) \quad (9)$$

The fact that the surface $f(x, y)$ is of the form $f(x, y) = f_1(x) + f_2(y)$ implies that the Fourier coefficients $f_{\ell,m}$ of $f(x, y)$ are such that $f_{p,q} = 0$ for $p \cdot q \neq 0$. In this case, formula (8) shows that unless $p = 0$ or $q = 0$, that is unless $\psi = 0$ or $\psi = \frac{\pi}{2}$, the first order backscattered field vanishes. When the incident field is aligned with the x or y axis, that is when $\psi = 0$ or $\psi = \frac{\pi}{2}$, then the ratio of HH to VV backscattered returns turns out to be:

$$\frac{\sigma_{HH}(\theta, 0)}{\sigma_{VV}(\theta, 0)} = \frac{\sigma_{HH}(\theta, \pi/2)}{\sigma_{VV}(\theta, \pi/2)} = \left(\frac{\cos(\theta)^2}{1 + \sin(\theta)^2} \right)^2 \quad (10)$$

which is the classical first order result found in [Valenzuela, 1978] for a perfect conductor (take the limit $\varepsilon \rightarrow +\infty$ in formulas 4.10 and 4.11 on page 211). When $\psi \neq 0$ or $\psi \neq \frac{\pi}{2}$, that is for $p \cdot q \neq 0$, the first order term vanishes (since $f_{p,q} = 0$ for $p \cdot q \neq 0$) and the second order term becomes dominant. This is illustrated in Figure 1 where the second order calculation is compared to a high order (21) converged reference solution (see [Bruno and Reitich, 1993, Sei et al., 1999] for details on the accuracy of the numerical algorithm used). Most interestingly, the second order term has the striking feature that HH returns exceed VV returns for a large range of incidence angles as illustrated in Figure 2, in sharp contrast to the first order returns. As expected from formula (8) the fact that the second order term is dominant is not a special feature of the bisinusoid surface (9); similar results were obtained for arbitrary surfaces of the form $f(x, y) = f_1(x) + f_2(y)$.

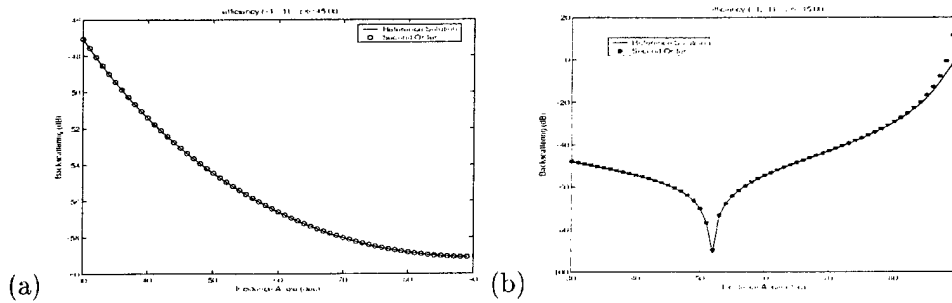


Figure 1: Comparison of the second order calculation to the exact high order calculation for the surface (9) with $h = 0.03$, $\psi = 45^\circ$ and $30^\circ \leq \theta \leq 89^\circ$. (a) HH polarization. (b) VV Polarization.

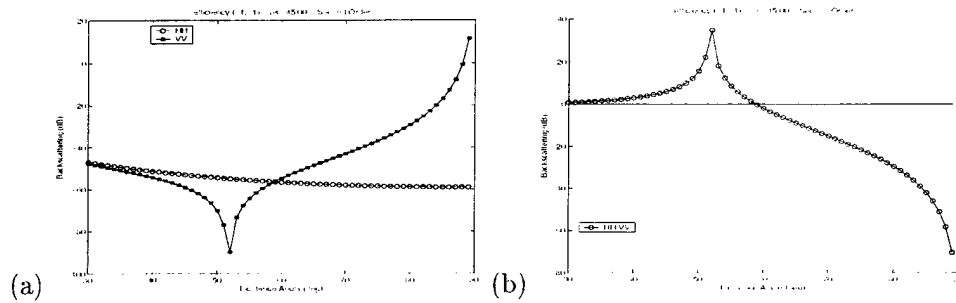


Figure 2: HH and VV backscattered returns for the surface (9) with $h = 0.03$, $\psi = 45^\circ$ and $30^\circ \leq \theta \leq 89^\circ$ (a). Corresponding HH to VV ratios (b).

Acknowledgements: The authors gratefully acknowledge support from TRW internal research fund.

References

- [Bruno and Reitich, 1993] O. Bruno and F. Reitich, *Numerical-solution of diffraction problems III - a method of variation of boundaries .3. doubly periodic gratings*, J. Opt. Soc. A **10**, 2551-2562, 1993.
- [Lee et al., 1997] P. Lee, J.D. Barter, K.L. Beach, C.L. Hindman, B.M. Lake, H.R. Thompson and R. Yee *Experiments on Bragg and non-Bragg scattering using single-frequency and chirped radars*, Radio. Sci. **32**, 1725-1744, 1997.
- [Petit, 1980] R. Petit, *Electromagnetic theory of gratings*, Springer-Verlag, 1980.
- [Rice, 1951] S.O. Rice, *Reflection of electromagnetic waves from slightly rough surfaces*, Comm. Pure Appl. Math. **4**, 351-378, 1951.
- [Sei et al., 1999] A. Sei, O.P. Bruno and M. Caponi, *Study of polarization dependent scattering anomalies with application to oceanic scattering*, Radio Science, **34**, 385-411, 1999.
- [Trizna et al., 1991] D.B. Trizna, J.P. Hansen, P. Hwang and J. Wu, *Laboratory studies of radar sea spikes at low grazing angles*, J. Geo. Res. **96**, 12529-12537, 1991.
- [Valenzuela, 1978] G.R. Valenzuela, *Theories for the interaction of electromagnetic and oceanic waves - A review*, Boundary-layer Meteor. **13**, 61-85, 1978.

Appendix A3:

Rigorous multi-scale solver for rough-surface scattering problems: high-order-high-frequency and variation of boundaries, Proceedings of the NATO Sensors and Electronics Technology (SET) Symposium on ``Low Grazing angle clutter: Its Characterization, Measurement, and Application", JHU/APL, Laurel, MD, April 2000.

NORTH ATLANTIC TREATY ORGANIZATION



RESEARCH AND TECHNOLOGY ORGANIZATION

BP 25, 7 RUE ANCELLE, F-92201 NEUILLY-SUR-SEINE CEDEX, FRANCE

RTO MEETING PROCEEDINGS 60

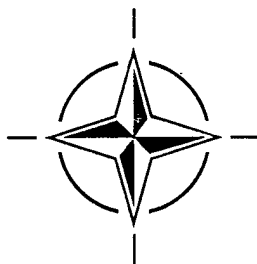
Low Grazing Angle Clutter: Its Characterization, Measurement and Application

(le Fouillis à incidence rasante, caractérisation, mesure et application)

Papers presented at the RTO Sensors and Electronics Technology Panel (SET) Symposium, held in Laurel, Maryland, USA, 25-27 April 2000.

This document should be announced and supplied only to NATO, Government Agencies of NATO nations and their bona fide contractors, and to other recipients approved by the RTO National Coordinators.

Ce document ne doit être notifié et distribué qu'à l'OTAN, qu'aux instances gouvernementales des pays de l'OTAN et à leurs organismes dépendants, ainsi qu'à leurs contractants dûment habilités et aux autres demandeurs agréés par les Coordonnateurs Nationaux pour la RTO.



Rigorous Multi-scale Solver for Rough-surface Scattering Problems: High-order-high-frequency and Variation of Boundaries

Oscar Bruno

Applied Mathematics 217-50, Caltech, Pasadena, CA 91125, USA

Alain Sei

Ocean Technology Department, TRW, Building R1/Rm 1008
Redondo Beach, CA 90278, USA

Maria Caponi

Ocean Technology Department, TRW, Building R1/Rm 1008
Redondo Beach, CA 90278, USA

1 Introduction

The electromagnetic scattering from the surface of the ocean plays an important role in a wide range of applications, including SAR imaging, remote sensing, detection, etc. The analysis of the scattering processes involved in these applications poses a rather challenging scientific problem as it requires description and understanding of diffraction by complicated surfaces [1]. Computationally, the main difficulty arises from the multiple-scale nature of the scattering surfaces, whose spectrum spans a wide range of lengthscales. A number of techniques have been developed to treat associated limiting cases. For example, the high frequency case, in which the wavelength λ of the incident radiation is much smaller than the surface lengthscales, can be handled by asymptotic methods such as geometrical optics or physical optics approximations. On the other hand, resonant problems where the incident radiation is of the order of the surface scale are treated by perturbation methods, typically first or second order expansions in the height h of the surface (cf. [2, 3, 35]).

However, when a multitude of scales is present on the surface none of the techniques above is adequate, and attempts to combine them in a so-called two-scale approaches [2, 4, 5] have been given. The two-scale models imply a splitting of the surface into a large and small scale, see e.g. [5, 6], where typically

a first order approximation in wavelength (Kirchhoff approximation) is used to treat smooth components of a surface and a first order in surface height (Rayleigh-Rice method [35]) is used to deal with the rough components of the surface. The results provided by these methods are not always satisfactory — precisely as a result of the limitations imposed by the low orders of approximation used in both, the high-frequency approximation and the small perturbation methods. (See e.g. [5] where the loss of accuracy of the two-scale model at low grazing angles is demonstrated.)

To alleviate these drawbacks, our approach to multi-scale scattering is based on use of expansions of *very high order* in both parameters λ and h — which leads to algorithms based on complex variable theory and analytic continuation. The resulting approach expands substantially on the range of applicability over low order methods, and can be used in some of the most challenging cases arising in practice. Furthermore, as demonstrated below, this new method does not require separation of the length-scales in the surface into large and small, but instead it is able to deal with a continuum of scales on the surface. Indeed the high order expansions presented below have a common “overlap” region in the (λ, h) plane where both components are highly accurate. More precisely, there is a range of surface heights and incident wavelengths for which both methods produce results with

machine accuracy. Therefore by dividing the scales of a surface at a point in the overlap region we obtain a general method which is applicable to surfaces containing a continuum of length-scales — which is ideal for evaluation of scattering from surfaces with spectral distributions of oceanic type.

High accuracy as is exhibited by our algorithms is essential in a wide range of important oceanic applications — whose return losses are typically in the -60 dB to -100 dB range. In particular, in order to provide credible results numerical methods must be able to insure accuracies of the order of up to 10 digits in some cases; see [37] for a case in point.

In the present paper we provide a description of our general approach, and we focus on the two basic elements of the general method, namely the high-order perturbation expansion in the wavelength λ and the high-order perturbation in height h . For simplicity we restrict our theoretical discussion to problems of scattering from a perfectly conducting rough surface of a transverse electric polarized wave (HH Polarization); numerical results will be given for both transverse electric and transverse magnetic polarizations, for three-dimensional problems, and for low to very low grazing angles. In particular we present results for a surface obtained from a Longuet-Higgins hydrodynamic code, for which our solver produced full double precision accuracy for grazing angles as low as 1° .

2 Multi-scale solver

Our multi-scale solver is based on the method of variation of boundaries [14–17]. We consider surfaces containing a continuum of scales but, as mentioned above, the existence of an overlap allows us to solve the complete multiple-scale problem by expressing an *arbitrary* surface $y = S(x)$ as a sum $y = S_0(x) + F(x)$ where $S_0(x)$ contains wave numbers $\leq N_S$, and $F(x)$ contain the complementary set of wave numbers $> N_S$. *Thus, our method uses a dichotomy in wave numbers but it does not assume a separation of scales.* This feature is essential in the study of oceanic waves since many studies show that the wave spectrum spans a large range of wavenum-

ber (see for instance [33]).

As mentioned above, we restrict our presentation to the particular case of an HH configuration in two dimensions; the scattered field created by an incident plane wave impinging on the rough surface thus solves the Helmholtz equation with a Dirichlet boundary condition. Our approach to the solution of the general problem with rough surface $y = S(x)$ proceeds as follows:

1. We consider the surface $S(x, \delta) = S_0(x) + \delta F(x)$, which will be used as a basis for a perturbative method in the parameter δ .
2. The solution $u = u(x, \delta)$ associated with the surface $S(x, \delta)$ is obtained by perturbation theory around $\delta = 0$.
3. The solution for the surface $S(x)$ is then recovered by setting $\delta = 1$. (As explained in Section 4 below, this evaluation usually leads to divergent series whose re-summation requires appropriate methods of analytic continuation.)

In detail, writing

$$(1) \quad \begin{cases} u(x, z; \delta) = \sum_{m=0}^{+\infty} u_m(x, z) \frac{\delta^m}{m!} \\ u_m = \frac{\partial^m u}{\partial \delta^m}(x, z; \delta = 0) \end{cases}$$

the fact that, for every fixed value of δ the field $u(x, z; \delta)$ solves the Helmholtz equation

$$(2) \quad \begin{cases} \Delta u(x, z; \delta) + k^2 u(x, z; \delta) = 0 \\ u(x, S(x, \delta); \delta) = -u^{inc}(x, S(x, \delta)) \end{cases}$$

then tells us that, for every fixed value of m we have

$$(3) \quad \begin{cases} \Delta u_m(x, z) + k^2 u_m(x, z) = 0 \\ u_m(x, S_0(x)) = G[F, u^{inc}, \dots, u_{m-1}](x, S_0(x)) \end{cases}$$

The interest in this equation arises from the fact that, although the right hand side in the boundary condition for u_m is highly oscillatory, *the surface S_0 itself*

is not. We therefore have reduced a problem on a highly oscillatory surface to a sequence of problems on a non-oscillatory surface. For example the zeroth and first order coefficient in the expansion of $u(x, z; \delta)$ solve the following scattering problems:

$$(4) \quad \begin{cases} \Delta u_0(x, z) + k^2 u_0(x, z) = 0 \\ u_0(x, S_0(x)) = -u^{inc}(x, S_0(x)). \end{cases}$$

and

$$(5) \quad \begin{cases} \Delta u_1(x, z) + k^2 u_1(x, z) = 0 \\ u_1(x, S_0(x)) = F(x) \left(\frac{\partial u^{inc}}{\partial z} + \frac{\partial u_0}{\partial z} \right) (x, S_0(x)). \end{cases}$$

The general boundary condition of (3) can be computed up to any order by differentiation with respect to δ of the boundary condition of (2), as in equation (5), and the general solution to arbitrary order can be found.

3 Variation of boundaries - previous work

In the particular case where the surface $y = S_0(x)$ is a plane, which allows for exact solution of each of the scattering problems (3), this perturbation method has been studied in detail [15-17]. Earlier uses of perturbation theory in these contexts had been limited to low-order methods; the new high order perturbation theory on the other hand, relies on expansions of very high order in powers of a deviation parameter, denoted here by δ , and techniques of analytic continuation in the complex δ -plane. Specifically, Taylor series for the field quantities are obtained through differentiation of the Maxwell system with respect to δ . The possible (and common) divergence of the resulting series is handled through re-summation techniques that exploit the analytic structure of the solution.

The resulting algorithms can resolve scattering returns with accuracies that are several orders of magnitude better than those given by classical methods [15-17]. Such accuracies can play an important

role in applications. For instance the fine resolution provided by our algorithms has recently helped settle a long-standing controversy relating to polarized back-scattering returns from rough surfaces—which amount to very small fractions of the incident energy [37].

As shown in the various papers cited in this section, this solver is extremely accurate for a wide range of surface heights and incidence angles. Thus, the accuracy of the multi-scale method proposed in the previous section is determined by the corresponding accuracy of the high-frequency solutions for equation (3). Such an accurate solver for high-frequency problems, in turn, is provided in the following section. The performance of both the boundary variation and high-frequency methods is studied numerically in Section 5.

4 High-order-high-frequency method

The scattered field can be computed from the surface current density ν induced on the surface $f(x)$ by the incident plane wave [2]. The function ν solves the integral equation

$$(6) \quad \nu(x, k) - \frac{i}{2} \int_{-\infty}^{+\infty} h(kMM') g(x, x') \nu(x', k) dx' = -e^{i\alpha x - i\beta f(x)}$$

where

$$\begin{aligned} MM' &= \sqrt{(x' - x)^2 + (f(x') - f(x))^2} \\ h(t) &= tH_1^1(t) \quad H_1^1 \text{ Hankel function} \\ g(x, x') &= (f(x') - f(x) - (x' - x)f'(x'))/MM'^2 \\ \alpha &= k \sin(\theta) \quad \beta = k \cos(\theta). \end{aligned}$$

To solve this equation we use an asymptotic expansion of high order around $k = \infty$. Our asymptotic expansion results from the geometrical optics type ansatz

$$(7) \quad \nu(x, k) = e^{i\alpha x - i\beta f(x)} \sum_{n=0}^{+\infty} \frac{\nu_n(x)}{k^n}$$

From equations (6) and (7) we obtain

$$(8) \quad \sum_{n=0}^{+\infty} \frac{1}{k^n} \left(\nu_n(x) - \frac{i}{2} I^n(x, k) \right) = -2$$

where

$$I^n(x, k) = \int_{-\infty}^{+\infty} h(kMM') g(x, x') e^{-ik\psi(x, x')} \nu_n(x') dx'$$

$$\psi(x, x') = \sin(\theta)(x' - x) - \cos(\theta)(f(x') - f(x))$$

To obtain the coefficients $\nu_n(x)$ we must produce the asymptotic expansion of $I^n(x, k)$ in powers of $1/k$. To do this we use two separate integration regions and we define

$$I_-^n(x, k) = \int_{-\infty}^x h(kMM') g(x, x') e^{-ik\psi(x, x')} \nu_n(x') dx'$$

$$I_+^n(x, k) = \int_x^{+\infty} h(kMM') g(x, x') e^{-ik\psi(x, x')} \nu_n(x') dx'$$

We focus first on an asymptotic expansion for $I_+^n(x, k)$. Using $t = x' - x$ we can write

$$I_+^n(x, k) = \int_0^{+\infty} h(k\phi_+(x, t)) g(x, x+t) e^{-ik\psi(x, t)} \nu_n(x+t) dt \quad (9)$$

where $\phi_+(x, t) = \sqrt{t^2 + (f(x+t) - f(x))^2}$ and $\psi(x, t) = \sin(\theta)t - \cos(\theta)(f(x+t) - f(x))$. For the simplest treatment we present here we assume that $f(x)$ satisfies the condition

$$\phi'_+(x, t) = \frac{\partial \phi_+(x, t)}{\partial t} > 0 \quad \text{for } t \geq 0$$

so that the map $t \mapsto \phi_+(x, t)$ is invertible; this condition is generally satisfied by rough surfaces relevant to the applications under consideration. Then setting

$$u = \phi_+(x, t) \iff t = \phi_+^{-1}(x, u)$$

we can rewrite equation (9) in the form

$$I_+^n(x, k) = \int_0^{+\infty} h(ku) F_n^+(x, u) e^{-ik\psi^+(x, u)} du.$$

with

$$F_n^+(x, u) = \frac{g(x, x + \phi_+^{-1}(x, u))}{\phi'_+(x, \phi_+^{-1}(x, u))} \nu_n(x + \phi_+^{-1}(x, u))$$

$$\psi^+(x, u) = (f(x + \phi_+^{-1}(x, u)) - f(x)) \cos(\theta) - \phi_+^{-1}(x, u) \sin(\theta)$$

(10)

We can now use the Taylor series of $u \mapsto F_n^+(x, u)$ around $u = 0$

$$F_n^+(x, u) = \sum_{m=0}^{+\infty} \frac{\partial^m F_n^+(x, 0)}{\partial u^m} \frac{u^m}{m!} = \sum_{m=0}^{+\infty} p_{n,m}^+(x) u^m$$

$$p_{n,m}^+(x) = \frac{1}{m!} \frac{\partial^m F_n^+(x, 0)}{\partial u^m}$$

to express $I_+^n(x, k)$ in the form

$$I_+^n(x, k) = \sum_{m=0}^{+\infty} p_{n,m}^+(x) \int_0^{+\infty} u^m h(ku) e^{-ik\psi^+(x, u)} du$$

$$= \sum_{m=0}^{+\infty} \frac{p_{n,m}^+(x)}{k^{m+1}} \int_0^{+\infty} v^m h(v) e^{-ik\psi^+(x, \frac{v}{k})} dv$$

$$= \sum_{m=0}^{+\infty} \frac{p_{n,m}^+(x)}{k^{m+1}} A^+(k, m, x) \quad (11)$$

where we have set

$$(12) \quad A^+(k, m, x) = \int_0^{+\infty} v^m h(v) e^{-ik\psi^+(x, \frac{v}{k})} dv$$

(These non-convergent integrals must be re-interpreted by means of analytic continuation — in a manner similar to that use in the definition and manipulation of Mellin transforms. We do not provide details about this analytic continuation procedure here; see [7] for a complete treatment in the case of the Mellin transform.)

To complete our expansion of $I_+^n(x, k)$ we need to produce a corresponding expansion of the quantity $A^+(k, m, x)$ in powers of $1/k$. With $\varepsilon = 1/k$ we call

$$\tilde{A}^+(\varepsilon, m, x) = A^+(k, m, x) = \int_0^{+\infty} v^m h(v) e^{i\psi^+(x, \varepsilon v)/\varepsilon} dv \quad (13)$$

By evaluation of the successive derivatives of $\tilde{A}^+(\varepsilon, m, x)$ with respect to ε at $\varepsilon = 0$ it is easy

to check that the coefficients of the Taylor series of $\tilde{A}^+(\varepsilon, m, x)$ with respect to ε can be obtained directly if all the integrals in the sequence

$$\tilde{A}^+(m, x) = \int_0^{+\infty} v^m h(v) e^{-i \frac{\partial \psi^+}{\partial u}(x, 0)} dv,$$

are known; for example, the first derivative is given

by (with $\psi_n^+(x) = \frac{\partial^n \psi^+}{\partial u^n}(x, u=0)$)

$$\left. \frac{\partial \tilde{A}^+(\varepsilon, m, x)}{\partial \varepsilon} \right|_{\varepsilon=0} = -i \frac{\psi_2^+(x)}{2} \tilde{A}^+(m+2, x)$$

Using equations (11) and (13) the expansion for $I_+^n(x, k)$ results; clearly, the expansion of $I_-^n(x, k)$ can be obtained through a similar derivation. The combined expansion for $I^n(x, k)$ involves combinations of quantities such as $p_{n,m}^+(x)$, $\psi_l^+(x)$, $p_{n,m}^-(x)$, $\psi_l^-(x)$, $\tilde{A}^+(m, x)$, $\tilde{A}^-(m, x)$. It can be shown that all of these quantities — and therefore the integrals $\tilde{A}^\pm(m, x)$ for all m — can be obtained from the integrals

$$\int_0^{+\infty} v^{m+1} H_1^1(v) \cos(av) dv \quad \text{if } m \text{ even}$$

$$\int_0^{+\infty} v^{m+1} H_1^1(v) \sin(av) dv \quad \text{if } m \text{ odd}$$

for which closed form formulas are available [8].

5 Numerical results

To test the accuracy of our numerical procedures we compare our results for the high-frequency and boundary variation methods in an "overlap" wavelength region — in which, as we show, both algorithms are very accurate. Note that these two methods are substantially different in nature: one is a high order expansion in λ whereas the other is a high order expansion in the height h of the profile. In the examples that follow we list relative errors for the computed values of the corresponding scattered energy (efficiency) shown; the results given in the columns denoted by Order 0-21 are the relative errors for the values of the scattered energy calculated from the

high frequency code to orders 0-21 in the scattering direction listed.

We start with a classical test example: a sinusoidal profile $f(x) = \frac{h}{2} \cos(2\pi x)$. In this example we have $h = 0.025$, $\lambda = 0.025$ and an incidence angle of 40° . The errors given in this table were computed through comparison with the results given by the boundary variations code. The convergence of the high frequency method is nicely illustrated by this example which, in fact, validates both the high frequency and the boundary variations calculation. We note that an approximation of order 21 in powers of $1/k$ is accurate to machine precision.

Scattering Direction #	Order 0	Order 5	Order 15	Order 21
0	2.0e-4	8.5e-10	4.1e-13	1.3e-14
1	3.1e-4	3.6e-9	1.6e-13	4.0e-15
2	2.5e-4	7.5e-9	8.7e-14	2.9e-16
3	2.6e-4	3.0e-9	1.8e-14	2.9e-16
4	1.8e-4	1.1e-10	4.6e-15	9.2e-16
5	2.1e-4	4.2e-10	5.6e-15	5.6e-16
6	1.4e-4	2.9e-9	1.6e-14	3.3e-16

Our next example corresponds to the same profile as above with $h = 0.025$, $\lambda = 0.001$ and an incidence angle of 70° (that is, 20° from grazing). This *high frequency problem* lies outside the domain of applicability of the method of variation of boundaries. Our errors here were computed through comparison with a calculation of higher order (Order 15). Again we see that the accuracy of the method is excellent in this case as well.

Scattering Direction #	Order 0	Order 3	Order 7	Order 11
0	9.7e-4	1.3e-8	4.0e-13	3.7e-16
1	2.5e-3	1.8e-8	5.6e-14	1.8e-16
2	2.4e-3	1.5e-8	5.4e-13	5.2e-16
3	1.2e-3	2.0e-8	9.1e-14	5.8e-16
4	5.3e-3	1.6e-8	9.5e-13	2.3e-15
5	5.2e-4	2.4e-8	5.8e-14	4.5e-16
6	1.9e-2	6.0e-9	3.4e-12	5.3e-15

For reference it is useful to indicate the times required by these computations: the calculation of order 21 shown in the first table resulted from a 17 second run on a DEC Alpha workstation (500MHz). The order 11 run shown on the second table took 9 seconds.

The scattering surface in our next example was produced by a hydrodynamic simulation of ocean waves. The numerical technique used for this simulation was directly inspired from the paper by Longuet-Higgins and Cokelet [10].

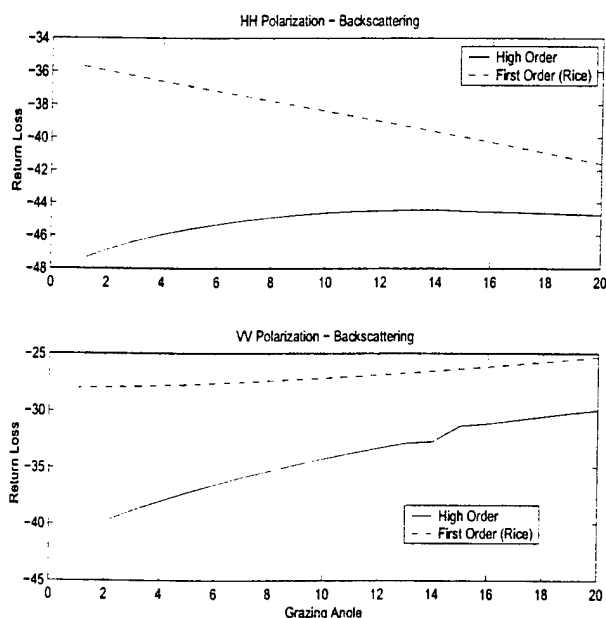
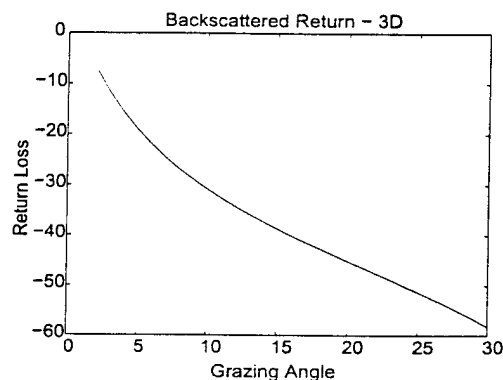


Figure 1: Scattered fields for low to very low grazing angles for the simulated hydrodynamic surface shown above: high-order full double precision accurate results (solid line) compared to the first order calculation akin to Rice's theory (dashed line).

This surface resulted from the nonlinear interaction of an initial configuration consisting of a long wave (24 cm wavelength) and a rapidly varying short wave

or "roughness" (3 cm wavelength). The long wave slope is $ka = 0.2$, which corresponds to a maximum height of 0.76 cm. In Figure 1 we show the corresponding backscattering at low to very low grazing angles. The high order perturbation method described in Section 3 produces the scattered field for this problem with double precision accuracy for an incident plane wave down to 1° grazing in both polarizations. In Figure 1 we also provide a comparison of the accurate results provided by the high order method to those given by the corresponding first order Rice theory. Note the large errors in the predictions of the first order approach.

Our final example is the two-dimensional biperiodic surface depicted below. The corresponding backscattering returns, which are plotted in the following graph, were computed by the boundary variations code with full double precision accuracy.



Acknowledgement and Disclaimer: Effort sponsored by the Air Force Office of Scientific Research, Air Force Materials Command, USAF, under grant numbers F49620-96-1-0008, F49620-99-1-0010 and F49620-99-1-0193, from DARPA, and through NSF contracts No. DMS-9523292 and DMS-9816802). The US Government is authorized to

reproduce and distribute reprints for governmental purposes notwithstanding any copyright notation thereon. The views and conclusions contained herein are those of the authors and should not be interpreted as necessarily representing the official policies or endorsements, either expressed or implied, of the Air Force Office of Scientific Research or the US Government.

References

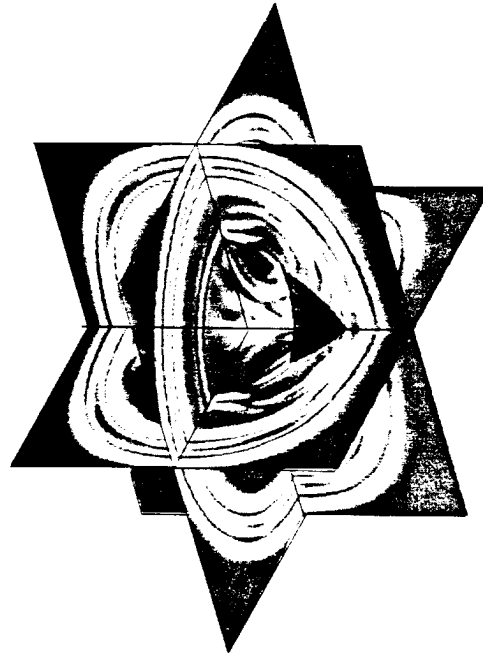
- [1] G. R. Valenzuela, *Theories for the interaction of electromagnetic and oceanic waves - A review*, Boundary-layer Meteor. **13** (1978), 61-85.
- [2] A.G. Voronovich, *Wave scattering from rough surfaces*, Springer-Verlag, Berlin, 1994.
- [3] A.B. Shmelev, *Wave scattering by statistically uneven surfaces*, Soviet Physics uspekhi, Vol 15, 2, pp 173-183, Sept. 1972.
- [4] B.F. Kuryanov, *The scattering of sound at a rough surface with two types of irregularity*, Soviet Physics-Acoustic, Vol 8, 3, pp 252-257, Jan. 1963.
- [5] S.T. McDaniel and A.D. Gorman *An examination of the composite-roughness scattering model*, J. Acoust. Soc. Am., Vol 73, 5, pp 1476-1486, 1983.
- [6] Galybin N.N., *Backscattering of sound by a disturbed sea surface*, Soviet Physics-Acoustic, Vol 22, pp 193-197, 1976.
- [7] N. Bleistein and R.A. Handelsman, *Asymptotic expansions of integrals*, Dover Publications, New York, 1986.
- [8] M. Abramowitz and I. Stegun *Handbook of mathematical functions with formulas, graphs, and mathematical tables*, US Dept Commerce, June, 1964.
- [9] B. Kinsman, *Wind waves, their generation and propagation on the ocean surface*, Englewood Cliffs, N.J., Prentice-Hall, 1965.
- [10] M.S. Longuet-Higgins and E.D. Cokelet *The deformation of steep surface waves on water: I a numerical method of computation*, Proc. R. Soc. Lond. A, **350**, (1976), 1-26.
- [11] G. V. Anand and M. K. George, *Normal mode sound propagation in an ocean with sinusoidal surface waves*, J. Acoust. Soc. Am. **80** (1986), 238-243.
- [12] G. V. Anand and M. K. George, *Normal mode sound propagation in an ocean with random narrow-band surface waves*, J. Acoust. Soc. Am. **94** (1993), 279-292.
- [13] G. A. Baker and P. Graves-Morris, *Padé Approximants, 2nd edition*, Encyclopedia of Mathematics and its Applications **59**, Cambridge University Press, Cambridge (1996).
- [14] O. P. Bruno and F. Reitich, *Solution of a boundary value problem for Helmholtz equation via variation of the boundary into the complex domain*, Proc. Roy. Soc. Edinburgh **122A** (1992), 317-340.
- [15] O. P. Bruno and F. Reitich, *Numerical solution of diffraction problems: a method of variation of boundaries*, J. Opt. Soc. Amer. A **10** (1993), 1168-1175.
- [16] O. P. Bruno and F. Reitich, *Numerical solution of diffraction problems: a method of variation of boundaries II. Dielectric gratings, Padé approximants and singularities*, J. Opt. Soc. Amer. A **10** (1993), 2307-2316.
- [17] O. P. Bruno and F. Reitich, *Numerical solution of diffraction problems: a method of variation of boundaries III. Doubly periodic gratings*, J. Opt. Soc. Amer. A **10** (1993), 2551-2562.
- [18] O. P. Bruno and F. Reitich, *Approximation of analytic functions: a method of enhanced convergence*, Math. Comp. **63** (1994), 195-213.
- [19] J. J. Greffet, *Scattering of electromagnetic waves by rough dielectric surfaces*, Phys. Rev. B **37** (1988), 6436-6441.

- [20] J. J. Greffet, C. Baylard and P. Versaavel, *Diffraction of electromagnetic waves by crossed gratings: a series solution*, Opt. Lett. **17** (1992), 1740-1742.
- [21] J. J. Greffet and Z. Maassarani, *Scattering of electromagnetic waves by a grating: a numerical evaluation of the iterative-series solution*, J. Opt. Soc. Am. A **7** (1990), 1483-1493.
- [22] E. Y. Harper and F. M. Labianca, *Perturbation theory for scattering of sound from a point source by a moving rough surface in the presence of refraction*, J. Acoust. Soc. Am. **57** (1975), 1044-1051.
- [23] E. Y. Harper and F. M. Labianca, *Scattering of sound from a point source by a rough surface progressing over an isovelocity ocean*, J. Acoust. Soc. Am. **58** (1975), 349-364.
- [24] D. R. Jackson, D. P. Winebrenner and A. Ishimaru, *Comparison of perturbation theories for rough-surface scattering*, J. Acoust. Soc. Am. **83** (1988), 961-969.
- [25] W. A. Kuperman and F. Ingenito, *Attenuation of the coherent component of sound propagating in shallow water with rough boundaries*, J. Acoust. Soc. Am. **61** (1977), 1178-1187.
New York (1968).
- [26] Y. Liu, S. J. Frasier and R. E McIntosh, *Measurement and classification of low-grazing-angle radar sea spikes*, IEEE Trans. Ant. Prop. **46** (1998), 27-40.
- [27] C. Lopez, F. J. Yndurain and N. Garcia, *Iterative series for calculating the scattering of waves from hard corrugated surfaces*, Phys. Rev. B **18** (1978), 970-972.
- [28] A. A. Maradudin, *Iterative solutions for electromagnetic scattering by gratings*, J. Opt. Soc. Am. **73** (1983), 759-764.
- [29] D. Maystre, *Rigorous vector theories of diffraction gratings*, in *Progress in Optics*, E. Wolf ed., North Holland, Amsterdam (1984), 3-67.
- [30] D. Maystre, and M. Nevière, *Electromagnetic theory of crossed gratings*, J. Optics **9** (1978), 301-306.
- [31] A. H. Nayfeh and O. R. Asfar, *Parallel-plate waveguide with sinusoidally perturbed boundaries*, J. Appl. Phys. **45** (1974), 4797-4800.
- [32] W. H. Peake, *Theory of radar return from terrain*, IRE Nat'l Conv. **7** (1959), 27-41.
- [33] W.J. Pierson and L. Moskowitz *A proposed spectral form for fully developed wind seas based on the similarity theory of S.A. Kitaigorodskii*, J. Geo. Res. **69** (1964), 5181-5190.
- [34] Lord Rayleigh, *The theory of sound*, Vol. 2, Dover, New York (1945).
- [35] S. O. Rice, *Reflection of electromagnetic waves from slightly rough surfaces*, Comm. Pure Appl. Math. **4** (1951), 351-378.
- [36] J. Roginsky, *Derivation of closed-form expressions for the T matrices of Rayleigh-Rice and extinction-theorem perturbation theories*, J. Acoust. Soc. Am. **90** (1991), 1130-1137.
- [37] A. Sei, O. Bruno and M. Caponi, *Study of polarization dependent scattering anomalies with applications to oceanic scattering*, Radio Sci. **34** (1999) 385-411.
- [38] N. C. Skaropoulos and D. P. Chrissoulidis, *General perturbative solution to wave scattering from a soft random cylindrical surface*, J. Acoust. Soc. Amer. **106** (1999), 596-604.
- [39] Talbot, D., Titchener, J. B. and Willis, J. R., *The reflection of electromagnetic waves from very rough interfaces*, Wave Motion **12** (1990), 245-260.
- [40] A. Wirgin, *Scattering from hard and soft corrugated surfaces: Iterative corrections to the Kirchhoff approximation through the extinction theorem*, J. Acoust. Soc. Am. **85** (1989), 670-679.

Appendix A4:

High-Order High Frequency solutions of rough surface scattering problem, Fifth
International Conference on Mathematical and Numerical Aspects of Wave Propagation,
Santiago de Compostella, Spain, July 2000.

FIFTH INTERNATIONAL CONFERENCE ON
MATHEMATICAL AND
NUMERICAL ASPECTS
OF WAVE PROPAGATION



Edited by

Alfredo Bermúdez,
Dolores Gómez,
Christophe Hazard,
Patrick Joly, and
Jean E. Roberts

siam

 **INRIA**

High Order High Frequency Solutions of Rough Surface Scattering Problems

Oscar Bruno

Applied Mathematics, Caltech, Pasadena, California

Alain Sei

Ocean Technology Department, TRW, Redondo Beach, California

Maria Caponi

Ocean Technology Department, TRW, Redondo Beach, California

1 Introduction

The electromagnetic scattering from the surface of the ocean and other rough surfaces plays an important role in a wide range of applications, including SAR imaging, remote sensing, scattering from terrain, non destructive testing in optics, etc. The analysis of the scattering processes involved in these applications poses a rather challenging scientific problem as it requires description and understanding of diffraction by complicated multiple-scales surfaces [1]. Computationally, the main difficulty arises from the multiple-scale nature of the scattering surfaces, whose spectrum spans a wide range of lengthscales. In fact, known techniques have been developed to treat limiting cases. For example, the high frequency case, in which the wavelength λ of the incident radiation is much smaller than the surface lengthscales, can be handled by asymptotic methods such as geometrical optics or the Kirchhoff approximation. On the other hand, resonant problems where the incident radiation is of the order of the surface scale are treated by perturbation methods, typically first or second order expansions in the height h of the surface (cf. [2, 3]). However, when a multitude of scales is present on the surface none of the techniques above is adequate, and attempts to combine them in a so-called two-scale approaches ([4, 2]) have been given. The results provided by these methods are not always satisfactory — precisely as a result of the limitations imposed by the low orders of approximation used in both, the high-frequency approximation and the small perturbation methods.

Our approach to multi-scale scattering is based on use of expansions of *very high order* in both parameters λ and h . Such extensions require rather complex mathematical treatments, including complex variable theory and analytic continuation. The resulting approach expands substantially on the range of applicability over low order methods, and can be used in some of the most challenging cases arising in applications. In this paper we focus on one of our high order expansions, namely a high-order perturbation expansion in the wavelength λ . Perturbation series of very high-order in h , have been introduced and used elsewhere ([6, 7]); the combined algorithms are currently under development.

The presentation in this paper focuses on the two-dimensional problem of scattering from a perfectly conducting rough surface of a transverse electric polarized wave (TE). The scattered field created by an incident plane wave impinging on the rough surface solves Helmholtz's equation with a Dirichlet boundary condition. As is known [2] the scattered field can be computed from the surface current density ν induced on the surface $f(x)$ by the incident plane wave. The function ν solves the integral equation

$$(1) \quad \frac{\nu(x, k)}{2} - \frac{i}{4} \int_{-\infty}^{+\infty} h(k M M') g(x, x') \nu(x', k) dx' = -e^{i\alpha x - i\beta f(x)}$$

where

$$MM' = \sqrt{(x' - x)^2 + (f(x') - f(x))^2} \quad h(t) = tH_1^1(t) \quad H_1^1 \text{ Hankel function}$$

$$g(x, x') = \frac{f(x') - f(x) - (x' - x)f'(x')}{MM'^2} \quad \alpha = k \sin(\theta_{inc}) \quad \beta = k \cos(\theta_{inc}).$$

To solve this equation we use an asymptotic expansion of high order around $k = \infty$. Our asymptotic expansion results from the ansatz

$$(2) \quad \nu(x, k) = e^{i\alpha x - i\beta f(x)} \sum_{n=0}^{+\infty} \frac{\nu_n(x)}{k^n}$$

From equations (1) and (2) we obtain

$$(3) \quad \sum_{n=0}^{+\infty} \frac{1}{k^n} \left(\nu_n(x) - \frac{i}{2} I^n(x, k) \right) = -2$$

where

$$I^n(x, k) = \int_{-\infty}^{+\infty} h(kMM') g(x, x') e^{i\alpha(x' - x) - i\beta(f(x') - f(x))} \nu_n(x') dx'$$

To obtain the coefficients $\nu_n(x)$ we must produce the asymptotic expansion of $I^n(x, k)$ in powers of $1/k$. To do this we use two separate integration regions and we define

$$I_-^n(x, k) = \int_{-\infty}^x h(kMM') g(x, x') e^{i\alpha(x' - x) - i\beta(f(x') - f(x))} \nu_n(x') dx'$$

$$I_+^n(x, k) = \int_x^{+\infty} h(kMM') g(x, x') e^{i\alpha(x' - x) - i\beta(f(x') - f(x))} \nu_n(x') dx'$$

2 Asymptotic expansion of $I_+^n(x, k)$

We focus first on an asymptotic expansion for $I_+^n(x, k)$. Using $t = x' - x$ we can write

$$(4) \quad I_+^n(x, k) = \int_0^{+\infty} h(k\phi_+(x, t)) g(x, x+t) e^{i\alpha t - i\beta(f(x+t) - f(x))} \nu_n(x+t) dt$$

where

$$\phi_+(x, t) = \sqrt{t^2 + (f(x+t) - f(x))^2}.$$

For the simplest treatment we present here we assume that $f(x)$ satisfies the condition

$$\phi'_+(x, t) = \frac{\partial \phi_+(x, t)}{\partial t} > 0 \quad \text{for } t \geq 0$$

so that the map $t \mapsto \phi_+(x, t)$ is invertible; this condition is generally satisfied by rough surfaces considered in practice. Then setting

$$u = \phi_+(x, t) \quad \Longleftrightarrow \quad t = \phi_+^{-1}(x, u)$$

we can rewrite equation (4) in the form

$$I_+^n(x, k) = \int_0^{+\infty} h(ku) \frac{g(x, x + \phi_+^{-1}(x, u))}{\phi'_+(x, \phi_+^{-1}(x, u))} \nu_n(x + \phi_+^{-1}(x, u)) e^{i\alpha \phi_+^{-1}(x, u) - i\beta(f(x + \phi_+^{-1}(x, u)) - f(x))} du$$

or, calling

$$(5) \quad F_n^+(x, u) = \frac{g(x, x + \phi_+^{-1}(x, u))}{\phi_+'(x, \phi_+^{-1}(x, u))} \nu_n(x + \phi_+^{-1}(x, u))$$

$$\psi^+(x, u) = (f(x + \phi_+^{-1}(x, u)) - f(x)) \cos(\theta_{inc}) - \phi_+^{-1}(x, u) \sin(\theta_{inc}),$$

$$I_+^n(x, k) = \int_0^{+\infty} h(ku) F_n^+(x, u) e^{-ik\psi^+(x, u)} du.$$

We can now use the Taylor series of the map $u \mapsto F_n^+(x, u)$ around $u = 0$

$$F_n^+(x, u) = \sum_{m=0}^{+\infty} \frac{\partial^m F_n^+(x, 0)}{\partial u^m} \frac{u^m}{m!} = \sum_{m=0}^{+\infty} p_{n,m}^+(x) u^m \quad p_{n,m}^+(x) = \frac{1}{m!} \frac{\partial^m F_n^+(x, 0)}{\partial u^m}$$

to express $I_+^n(x, k)$ in the form

$$(6) \quad \begin{aligned} I_+^n(x, k) &= \sum_{m=0}^{+\infty} p_{n,m}^+(x) \int_0^{+\infty} u^m h(ku) e^{-ik\psi^+(x, u)} du \\ &= \sum_{m=0}^{+\infty} \frac{p_{n,m}^+(x)}{k^{m+1}} \int_0^{+\infty} v^m h(v) e^{-ik\psi^+(x, \frac{v}{k})} dv = \sum_{m=0}^{+\infty} \frac{p_{n,m}^+(x)}{k^{m+1}} A^+(k, m, x) \end{aligned}$$

where we have set

$$(7) \quad A^+(k, m, x) = \int_0^{+\infty} v^m h(v) e^{-ik\psi^+(x, \frac{v}{k})} dv.$$

(These non-convergent integrals must be re-interpreted by means of analytic continuation -- in a manner similar to that use in the definition and manipulation of Mellin transforms. We do not provide details about this analytic continuation procedure here; see [8] for a complete treatment in the case of the Mellin transform.)

To complete our expansion of $I_+^n(x, k)$ we need to produce a corresponding expansion of the quantity $A^+(k, m, x)$ in powers of $1/k$. With $\varepsilon = 1/k$ we call

$$(8) \quad \tilde{A}^+(\varepsilon, m, x) = A^+(k, m, x) = \int_0^{+\infty} v^m h(v) e^{-i\psi^+(x, \varepsilon v)/\varepsilon} dv.$$

By evaluation of the successive derivatives of $\tilde{A}^+(\varepsilon, m, x)$ with respect to ε at $\varepsilon = 0$ it is easy to check that the coefficients of the Taylor series of $\tilde{A}^+(\varepsilon, m, x)$ with respect to ε can be obtained directly if all the integrals in the sequence

$$\tilde{A}^+(0, m, x) = \int_0^{+\infty} v^m h(v) e^{-i\frac{\partial \psi^+}{\partial u}(x, 0)} dv,$$

are known; for example, the first two such derivatives are given by (with $\psi_n^+(x) = \frac{\partial^n \psi^+}{\partial u^n}(x, u=0)$)

$$\begin{aligned} \left. \frac{\partial \tilde{A}^+(\varepsilon, m, x)}{\partial \varepsilon} \right|_{\varepsilon=0} &= -i \frac{\psi_2^+(x)}{2} \tilde{A}^+(0, m+2, x) \\ \left. \frac{\partial^2 \tilde{A}^+(\varepsilon, m, x)}{\partial \varepsilon^2} \right|_{\varepsilon=0} &= -i \frac{\psi_3^+(x)}{3} \tilde{A}^+(0, m+3, x) - \frac{(\psi_2^+)^2(x)}{4} \tilde{A}^+(0, m+4, x). \end{aligned}$$

Using equations (6) and (8) the expansion for $I_+^n(x, k)$ results; clearly, the expansion of $I_-^n(x, k)$ can be obtained through a similar derivation. The combined expansion for $I^n(x, k)$ involves combinations of

quantities such as $p_{n,m}^+(x)$, $\psi_\ell^+(x)$, $p_{n,m}^-(x)$, $\psi_\ell^-(x)$, $\bar{A}^+(0, m, x)$, $\bar{A}^-(0, m, x)$. It can be shown that all of these quantities — and therefore the integrals $\bar{A}^\pm(0, m, x)$ for all m — can be obtained from the integrals

$$\int_0^{+\infty} v^{m+1} H_1^1(v) \cos(av) dv \quad \text{if } m \text{ even}$$

$$\int_0^{+\infty} v^{m+1} H_1^1(v) \sin(av) dv \quad \text{if } m \text{ odd}$$

for which closed form formulas are available [5].

3 Numerical results

To test the accuracy of our numerical procedure we compared our results to a highly accurate boundary variation code (cf. [6]) in a region (in wavelength) where the two algorithms were very accurate as shown below. Note that these two methods are substantially different in nature: one is a high order expansion in λ whereas the other is a high order expansion in the height h of the profile.

All our results are for normal incidence illumination. The results listed in the columns Order 0-17 are the relative errors for each scattered energy (efficiency) listed.

We start with the simplest example namely a sinusoidal profile $f(x) = \frac{h}{2} \cos(2\pi x)$. In this example we have $h = 0.025$ and $\lambda = 0.025$.




Scattering Direction #	Scattered Energy	Order 0	Order 1	Order 3	Order 5	Order 9	Order 11
0	4.843033211037387e-02	1.9e-3	4.8e-6	1.9e-8	4.2e-11	1.6e-15	0.0e-16
1	4.533269321280629e-02	2.3e-3	2.4e-6	8.3e-9	2.4e-11	1.8e-15	0.0e-16
2	8.263582066556663e-02	8.3e-4	3.0e-6	1.3e-8	3.5e-11	3.4e-16	0.0e-16
3	1.032017750281185e-03	1.8e-2	7.4e-5	3.7e-8	1.3e-10	9.7e-15	1.0e-15
4	1.019744820363490e-01	1.0e-3	1.3e-6	7.1e-10	1.6e-12	0.0e-16	0.0e-16
5	1.396970992023250e-01	1.2e-4	3.4e-6	5.1e-9	8.7e-12	0.0e-16	0.0e-16
6	7.578492663719054e-02	7.9e-4	6.5e-6	1.3e-8	2.6e-11	3.7e-16	0.0e-16
7	2.361867030378681e-02	1.3e-3	1.0e-5	2.3e-8	5.5e-11	8.8e-16	0.0e-16

Our next example is given by the profile $f(x) = \frac{h}{2}(\cos(2\pi x) + \cos(4\pi x))$. In this example we have $h = 0.01$ and $\lambda = 0.025$.



Scattering Direction #	Scattered Energy	Order 0	Order 1	Order 5	Order 9	Order 11	Order 15
0	1.983702874853860e-01	1.4e-3	6.7e-6	6.3e-10	1.8e-13	5.0e-15	0.0e-16
1	2.125625186015414e-02	4.3e-3	7.3e-6	8.6e-10	4.6e-14	4.9e-16	0.0e-16
2	5.109656298137152e-02	4.2e-3	5.3e-6	1.3e-9	3.5e-14	6.9e-15	0.0e-16
3	1.350594564861170e-01	1.1e-3	3.0e-6	1.8e-10	5.1e-14	6.9e-16	0.0e-16
4	1.670755436364386e-02	4.3e-3	9.2e-6	1.5e-9	1.8e-13	0.0e-14	0.0e-16
5	1.041839113172000e-01	8.7e-4	1.1e-5	4.7e-10	3.8e-14	0.0e-16	0.0e-16
6	3.029977474761340e-02	7.6e-4	1.1e-5	4.8e-10	1.0e-15	2.0e-15	0.0e-16
7	2.828409217693459e-02	2.5e-3	3.2e-5	1.8e-9	3.5e-14	4.6e-15	6.1e-16

Our last example is third order "Stokes" wave (cf. [9]) given by $f(x) = \frac{h}{2}(-\cos(2\pi x) + 0.35 \cos(4\pi x) - 0.035 \cos(6\pi x))$. Here $h = 0.03$ and $\lambda = 0.025$.



Scattering Direction #	Scattered Energy	Order 0	Order 1	Order 5	Order 9	Order 13	Order 17
0	1.168946586556380e-01	1.1e-3	2.1e-6	1.0e-9	1.8e-12	8.5e-15	0.0e-16
1	1.259788401686170e-01	1.1e-3	1.0e-5	9.0e-10	5.8e-13	7.9e-15	0.0e-16
2	7.407393363864252e-03	3.2e-3	2.7e-5	3.6e-9	1.9e-12	9.6e-15	0.0e-16
3	2.657137880809774e-02	5.1e-3	1.8e-5	1.3e-9	4.1e-13	1.4e-14	1.0e-15
4	4.889524445075034e-02	2.5e-5	1.7e-5	1.9e-9	2.4e-13	9.9e-16	2.8e-16
5	1.497662001023263e-02	4.7e-3	2.7e-5	3.6e-9	1.4e-12	1.3e-14	0.0e-16
6	1.617786430146189e-03	1.4e-2	5.9e-6	2.0e-9	9.0e-13	2.8e-14	1.9e-15
7	2.523077976253081e-02	5.4e-3	6.9e-6	6.7e-10	1.1e-12	2.8e-14	0.0e-16

Our implementation of this method is very efficient. All the functions considered are decomposed in their Fourier series, in particular no discretization points on the surface are used. The largest run time is 22 sec for the order 17 calculation presented in the table above on a DEC Alpha workstation (500MHz). A more typical run for the order 11 calculation presented in the second example took 3 seconds.

References

- [1] G.R. Valenzuela, *Theories for the interaction of electromagnetic and oceanic waves - A review*, Boundary-layer Meteor. **13**, 61-85, 1978.
- [2] A.G. Voronovich, *Wave scattering from rough surfaces*, Springer-Verlag, Berlin, 1994.
- [3] A.B. Shmelev, *Wave scattering by statistically uneven surfaces*. Soviet Physics uspekhi, Vol 15, 2, pp 173-183, Sept. 1972.
- [4] B.F. Kuryanov, *The scattering of sound at a rough surface with two types of irregularity*, Soviet Physics-Acoustic, Vol 8, 3, pp 252-257, Jan. 1963.
- [5] M. Abramowitz and I. Stegun *Handbook of mathematical functions with formulas, graphs, and mathematical tables*, US Dept Commerce, June, 1964.
- [6] O. Bruno and F. Reitich, *Numerical solution of diffraction problems: a method of variation of boundaries I, II, III*, J. Opt. Soc. A **10**, 1168-1175, 2307-2316, 2551-2562, 1993.
- [7] A. Sei, O.P. Bruno and M. Caponi, *Study of polarization scattering anomalies with application to oceanic scattering* Radio Science, Vol 34, No 2, pp385-411, March 1999.
- [8] N. Bleistein and R.A. Handelsman, *Asymptotic expansions of integrals*. Dover Publications, New York, 1986.
- [9] B. Kinsman, *Wind waves, their generation and propagation on the ocean surface*, Englewood Cliffs, N.J., Prentice-Hall, 1965.

Appendix A5:

An innovative high-order method for electromagnetic scattering from rough surfaces,
National Radio Science Meeting, Boulder, Colorado, January 2000.

**NATIONAL ACADEMIES OF SCIENCES AND ENGINEERING
NATIONAL RESEARCH COUNCIL
of the
UNITED STATES OF AMERICA**

**UNITED STATES NATIONAL COMMITTEE
International Union of Radio Science**



National Radio Science Meeting
4-8 January 2000

Sponsored by USNC/URSI

University of Colorado
Boulder, Colorado
U.S.A.

B/F2-6
15:00AN INNOVATIVE HIGH-ORDER METHOD FOR ELECTRO-
MAGNETIC SCATTERING FROM ROUGH SURFACES

Oscar Bruno
Caltech
Pasadena, CA 91125
Maria Caponi
TRW
Redondo Beach, CA 90278
Alain Sei*
TRW
Redondo Beach, CA 90278

We present an innovative algorithm for the computation of electromagnetic scattering from rough surfaces, with emphasis on ocean scattering applications. Our new method couples a high-order boundary variation method with an approach based on high-order, high-frequency asymptotic expansions of singular integrals.

To solve a scattering problem on a rough surface — composed of a smooth swell of general shape underlying a rough, highly oscillatory layer — we view the roughness as perturbation of the swell. The boundary variations method, used extensively in previous studies (Sei et al., *Radio Science*, **34**, 385-411, 1999, Bruno O. and Reitich F., *J. Opt. Soc. A.*, **10**, 2551-2562, 1993), allows us to evaluate the scattered field from such rough surfaces by means of analytic continuation of an associated perturbation series of *high order* (Bruno O. and Reitich F., *Proc. R. Soc. Edinburgh. A*, **122**, 317-340, 1992).

The evaluation of each one of the coefficients in this perturbation expansion requires the solution of a scattering problem on a smooth surface with highly oscillatory boundary conditions. The solution of this notoriously difficult problem is computed efficiently and accurately by means of a new, high-order, high-frequency asymptotic expansion for the surface currents. Our high-frequency solver, which is designed to apply in the small wavelength regime — in which geometrical optics and the Kirchoff approximation are frequently used —, should be applicable to a wide range of scattering problems. Unlike the geometrical optics type expansions where amplitudes can become unbounded (at caustics), our high frequency algorithm is entirely rigorous and highly accurate.

This presentation will describe our approach to the general rough surface problem with a detailed discussion on the high-frequency solver. Numerical results in a variety of cases will be presented, demonstrating the accuracy and computational efficiency of our new methods.

Appendix B1:

US Patent application: *High-Order High-Frequency rough surface scattering solver*

CERTIFICATE OF MAILING

Express Mail Mailing Label No. EK745231604US

Date of Deposit September 29, 2000

I hereby certify that this paper or fee is being deposited with the United States Postal Service "Express Mail Post Office to Addressee" service under 37 CFR 1.10 on the date indicated above and is addressed to the Assistant Commissioner of Patents and Trademarks, Washington, DC 20231.

Mailer Lynn E. Cabiles

(print)

Mailer *Lynn E. Cabiles*

(signature)

**HIGH-ORDER HIGH-FREQUENCY ROUGH SURFACE
SCATTERING SOLVER**

This invention was made with Government support under F49620-99-C-0014 awarded by AFOSR/DARPA. The Government has certain rights in this invention.

BACKGROUND OF THE INVENTION

5 1. Field of the Invention

The present invention relates generally to scattering processes, and in particular to computation of electromagnetic scattered fields from multiple scale geometries.

2. Discussion of the Related Art

10 Electromagnetic scattering from rough surfaces such as the surface of the ocean plays an important role in a wide range of applications including imaging, remote sensing, and detection. The analysis of the scattering processes involved in these applications poses a rather challenging scientific problem that

requires description and understanding of diffraction by complicated surfaces. Computationally, the main difficulty arises from the multiple-scale nature of the scattering surfaces, whose spectrum spans a wide range of lengthscales. A number of techniques have been developed to treat associated limiting cases.

- 5 For example, the high frequency case, in which the wavelength, λ , of the incident radiation is much smaller than the surface lengthscales can be handled by asymptotic methods such as geometrical optics or physical optics approximations. On the other hand, resonant problems where the incident radiation is of the order of the surface scale are treated by perturbation methods,
- 10 typically first or second order expansions in the height, h , of the surface.

However, when a multitude of scales is present on the surface, none of the techniques described above either alone or in combination in so-called two-scale approaches is adequate. The two-scale models imply a splitting of the surface into a large scale and a small scale. Typically, a first order

15 approximation in wavelength is used to treat the smooth components of the surface, and a first order in surface height is used to deal with the rough components of the surface. The results provided by these methods are not satisfactory precisely as a result of limitations imposed by the low orders of approximation used in both, the high-frequency approximation method and the

20 small perturbation method.

SUMMARY OF THE INVENTION

The present invention provides a rough surface scattering method and solver for efficiently computing electromagnetic scattered fields resulting from an incident wave being reflected from a slowly varying surface (high frequency
5 case). The claimed approach to multi-scale scattering is based on the use of expansions of *high order* in parameter λ . The resulting high-order perturbation expansion approach expands substantially on the range of applicability over low order methods, and can be used in some of the most challenging cases arising in applications. A surface current is induced by the incident wave. The surface
10 current is determined by solving a surface current integral equation. A surface current ansatz is substituted into the surface current integral equation, wherein a surface current series expansion is formed having a high frequency order. The surface current series expansion includes an oscillatory factor and surface current coefficients to be determined. An asymptotic expansion of the oscillatory
15 integral is produced such that a Taylor series including a non-convergent integral is formed. The non-convergent integral is re-interpreted by means of analytic continuation. The re-interpreted non-convergent integral is inserted into the Taylor series to solve for the surface current coefficients. The surface current coefficients are inserted into the surface current series expansion and the
20 surface current is obtained by summing the power series in λ with the known surface current coefficients. Finally, the scattered field is computed based upon the solved surface current, by quadratures.

For a more complete understanding of the invention, its objects and advantages, reference may be had to the following specification and to the accompanying drawings.

5

BRIEF DESCRIPTION OF THE DRAWINGS

Figure 1 illustrates a flow diagram of a method for computing scattered fields in accordance with the teachings of the invention; and

Figure 2 illustrates a transverse electric polarized wave (TE) impinging on a rough surface.

10

DETAILED DESCRIPTION OF THE PREFERRED EMBODIMENT

Referring to Figure 1, a method of computing a scattered field according to the present invention is shown. The method is based on the use of expansions of *high order* in the parameter λ . Such extensions require rather complex mathematical treatments, including complex variable theory and analytic continuation. The resulting approach expands substantially on the range of applicability over low order methods, and can be used in some of the most challenging cases arising in applications. Here, we focus on a high-order perturbation expansion in the wavelength λ .

1. Introduction

20

With additional reference to Figure 2, a transverse electric polarized wave (TE) 12, with electric field, E , pointing out of the figure, impinging on a rough surface 10 is illustrated. The method is particularly suitable for two-dimensional

problems of scattering from a perfectly conducting rough surface 10 of a transverse electric polarized wave (TE) 12. A scattered field created by the incident plane wave 12 impinging on the rough surface 10 solves Helmholtz's equation with a Dirichlet boundary condition. The scattered field can be
 5 computed from the surface current density, v , 14 induced on the rough surface $f(x)$ 10 by the incident plane wave 12 by integrating the solved surface current against the Green's function. See, *Wave scattering from rough surfaces*, by A.G. Voronovich, Springer-Verlag, Berlin, 1994, which is hereby incorporated by reference. The function v solves the integral equation:

$$10 \quad (1) \quad \frac{v(x, k)}{2} - \frac{i}{4} \int_{-\infty}^{\infty} h(kMM') g(x, x') v(x', k) dx' = -e^{i\alpha x - i\beta f(x)}, \text{ step 20,}$$

where

$$MM' = \sqrt{(x' - x)^2 + (f(x') - f(x))^2} \quad h(t) = tH_1^1(t) \quad H_1^1 \text{ Hankel function}$$

$$g(x, x') = \frac{f(x') - f(x) - (x' - x)f'(x')}{MM'^2} \quad \alpha = k \sin(\theta_{inc}) \quad \beta = k \cos(\theta_{inc}).$$

15 To solve this equation, an asymptotic expansion of high order around $k = \infty$ is used. The asymptotic expansion results from the ansatz

From equations (1) and (2) we obtain the following equation for the surface current coefficients;

$$(3) \quad \sum_{n=0}^{+\infty} \frac{1}{k^n} \left(v_n(x) - \frac{i}{2} I''(x, k) \right) = -2, \text{ step 24.}$$

where

$$5 \quad I''(x, k) = \int_{-\infty}^{+\infty} h(kMM') g(x, x') e^{i\alpha(x'-x) - i\beta(f(x') - f(x))} v_n(x') dx'.$$

To obtain the coefficients $v_n(x)$ we produce the asymptotic expansion of $I''(x, k)$, an oscillatory integral, in powers of $1/k$, step 26. To do this we use two separate integration regions which we define below. However using a single integration region or multiple integration regions is within the scope of the invention.

$$10 \quad I''_-(x, k) = \int_{-\infty}^x h(kMM') g(x, x') e^{i\alpha(x'-x) - i\beta(f(x') - f(x))} v_n(x') dx'$$

$$I''_+(x, k) = \int_x^{+\infty} h(kMM') g(x, x') e^{i\alpha(x'-x) - i\beta(f(x') - f(x))} v_n(x') dx'$$

2. Asymptotic expansion of $I_+^n(x, k)$

We focus on an asymptotic expansion for $I_+^n(x, k)$. Using $t = x' - x$ we can write

$$(4) \quad I_+^n(x, k) = \int_0^{+\infty} h(k\phi_+(x, t))g(x, x+t)e^{i\alpha t - i\beta(f(x+t) - f(x))}v_n(x+t)dt$$

5 where

$$\phi_+(x, t) = \sqrt{t^2 + (f(x+t) - f(x))^2}.$$

For the simplest treatment we present here we assume that $f(x)$ satisfies the condition

$$\phi'_+(x, t) = \frac{\partial \phi_+(x, t)}{\partial t} > 0 \quad \text{for } t \geq 0$$

10 so that the map $t \mapsto \phi_+(x, t)$ is invertible; this condition is generally satisfied by rough surfaces considered in practice. Then setting

$$u = \phi_+(x, t) \quad \Leftrightarrow \quad t = \phi_+^{-1}(x, u)$$

we can rewrite equation (4) in the form

$$I_+''(x, k) = \int_0^{+\infty} h(ku) \frac{g(x, x + \phi_+^{-1}(x, u))}{\phi_+'(x, \phi_+^{-1}(x, u))} v_n(x + \phi_+^{-1}(x, u)) e^{i\alpha\phi_+^{-1}(x, u) - i\beta(f(x + \phi_+^{-1}(x, u)) - f(x))} du$$

or, calling

$$F_n^+(x, u) = \frac{g(x, x + \phi_+^{-1}(x, u))}{\phi_+'(x, \phi_+^{-1}(x, u))} v_n(x + \phi_+^{-1}(x, u))$$

(5)

$$5 \quad \psi_+(x, u) = (f(x + \phi_+^{-1}(x, u)) - f(x)) \cos(\theta_{inc}) - \phi_+^{-1}(x, u) \sin(\theta_{inc}),$$

$$I_+''(x, k) = \int_0^{+\infty} h(ku) F_n^+(x, u) e^{-ik\psi_+(x, u)} du.$$

We can now use the Taylor series of the map $u \mapsto F_n^+(x, u)$ around $u = 0$

$$F_n^+(x, u) = \sum_{m=0}^{+\infty} \frac{\partial^m F_n^+(x, 0)}{\partial u^m} \frac{u^m}{m!} = \sum_{m=0}^{+\infty} p_{n,m}^+(x) u^m \quad p_{n,m}^+(x) = \frac{1}{m!} \frac{\partial^m F_n^+(x, 0)}{\partial u^m}$$

to express $I_+''(x, k)$ in the form

$$10 \quad I_+''(x, k) = \sum_{m=0}^{+\infty} p_{n,m}^+(x) \int_0^{+\infty} u^m h(ku) e^{-ik\psi_+(x, u)} du$$

(6)

$$I_+^n(x, k) = \sum_{m=0}^{+\infty} \frac{p_{n,m}^+(x)}{k^{m+1}} \int_0^{\infty} v^m h(v) e^{-ik\psi^+\left(x, \frac{v}{k}\right)} dv = \sum_{m=0}^{+\infty} \frac{p_{n,m}^+(x)}{k^{m+1}} A^+(k, m, x), \text{ step 28}$$

where we have set

$$(7) \quad A^+(k, m, x) = \int_0^{\infty} v^m h(v) e^{-ik\psi^+\left(x, \frac{v}{k}\right)} dv$$

These non-convergent integrals are re-interpreted by means of analytic continuation – in a manner similar to that used in the definition and manipulation of Mellin transforms. See *Asymptotic expansions of integrals* (hereby incorporated by reference), by N. Bleistein and R.A. Handelsman, Dover Publications, New York, 1986, for a complete treatment of this analytic continuation procedure in the case of the Mellin transform, step 30.

To complete our expansion of $I_+^n(x, k)$ we produce a corresponding expansion of the quantity $A^+(k, m, x)$ in powers of $1/k$. With $\varepsilon = 1/k$ we call

$$(8) \quad \tilde{A}^+(\varepsilon, m, x) = A^+(k, m, x) = \int_0^{\infty} v^m h(v) e^{-i\psi^+(x, \varepsilon v)/\varepsilon} dv.$$

By evaluation of the successive derivatives of $\tilde{A}^+(\varepsilon, m, x)$ with respect to ε at $\varepsilon = 0$ it is easy to check that the coefficients of the Taylor series of $\tilde{A}^+(\varepsilon, m, x)$ with respect to ε can be obtained directly if the integrals in the sequence

$$\tilde{A}^+(0, m, x) = \int_0^\infty v^m h(v) e^{-i \frac{\partial \psi^+}{\partial u}(x, 0)} dv,$$

are known. For example, the first two such derivatives are given by

$$\left(\text{with } \psi_n^+(x) = \frac{\partial n \psi^+}{\partial u^n}(x, u=0) \right)$$

$$\left. \frac{\partial \tilde{A}^+(\varepsilon, m, x)}{\partial \varepsilon} \right|_{\varepsilon=0} = -i \frac{\psi_2^+(x)}{2} \tilde{A}^+(0, m+2, x)$$

$$5 \quad \left. \frac{\partial^2 \tilde{A}^+(\varepsilon, m, x)}{\partial \varepsilon^2} \right|_{\varepsilon=0} = -i \frac{\psi_3^+(x)}{3} \tilde{A}^+(0, m+3, x) - \frac{(\psi_2^+)^2(x)}{4} \tilde{A}^+(0, m+4, x).$$

Using equations (6) and (8) the expansion for $I_+^n(x, k)$ results. The expansion of $I_-^n(x, k)$ is obtained through a similar derivation. The combined expansion for $I^n(x, k)$ involves the combinations of quantities such as $p_{n,m}^+(x)$, $\psi_\ell^+(x)$, $p_{n,m}^-(x)$, $\psi_\ell^-(x)$, $\tilde{A}^+(0, m, x)$, $\tilde{A}^-(0, m, x)$. It can be shown that the

10 integrals $\tilde{A}^\pm(0, m, x)$ for all m – can be obtained from the integrals

$$\int_0^\infty v^{m+1} H_1^1(v) \cos(av) dv \quad \text{if } m \text{ even}$$

$$\int_0^{\infty} v^{m+1} H_1^{(1)}(v) \sin(av) dv \quad \text{if } m \text{ odd}$$

for which closed form formulas are available in *Handbook of mathematical functions with formulas, graphs, and mathematical tables*, by M. Abramowitz and

- 5 I. Stegun, US Dept Commerce, June, 1964, which is hereby incorporated by reference, step 32.

Next, the high frequency order for the computation is selected, step 34. The scope of the invention includes a high frequency order that is 2 or greater. Those skilled in the art will readily recognize that selection of the high frequency
10 order involves a trade-off between computation speed and accuracy which will vary depending on the particular application.

Finally, having determined the surface current coefficients, the surface current is computed with formula (2) for, and the scattered field is computed by integrating the solved surface current against Green's function, step 36.

15 3. Numerical results

To test the accuracy of the procedure we compared our results to a highly accurate boundary variation code in a region (in wavelength) where the two algorithms were very accurate as shown below. See, *Numerical solution of diffraction problems: a method of variation of boundaries I, II, III*, by O. Bruno and
20 F. Reitich, J. Opt. Soc. A 10, 1168-1175, 2307-2316, 2551-2562, 1993. Note that these two methods are substantially different in nature: ours is a high order

that these two methods are substantially different in nature: ours is a high order expansion in λ whereas the other is a high order expansion in the height h of the profile.


All our results are for normal incidence illumination. The results listed in
5 the columns Order 0-17 are the relative errors for each scattered energy (efficiency) listed.

We start with the simplest example namely a sinusoidal profile

$f(x) = \frac{h}{2} \cos(2\pi x)$. In this example we have $h = 0.025$ and $\lambda = 0.025$.

Scattering Direction #	Scattered Energy	Order 0	Order 1	Order 3	Order 5	Order 9	Order 11
0	4.843033211037387e-02	1.9e-3	4.8e-6	1.9e-8	4.2e-11	1.6e-15	0.0e-16
1	4.533269321280629e-02	2.3e-3	2.4e-6	8.3e-9	2.4e-11	1.8e-15	0.0e-16
2	8.263582066556663e-02	8.3e-4	3.0e-6	1.3e-8	3.5e-11	3.4e-16	0.0e-16
3	1.032017750281185e-03	1.8e-2	7.4e-5	3.7e-8	1.3e-10	9.7e-15	1.0e-15
4	1.019744820363490e-01	1.0e-3	1.3e-6	7.1e-10	1.6e-12	0.0e-16	0.0e-16
5	1.396970992023250e-01	1.2e-4	3.4e-6	5.1e-9	8.7e-12	0.0e-16	0.0e-16
6	7.578492663719054e-02	7.9e-4	6.5e-6	1.3e-8	2.6e-11	3.7e-16	0.0e-16
7	2.361867030378681e-02	1.3e-3	1.0e-5	2.3e-8	5.5e-11	8.8e-16	0.0e-16

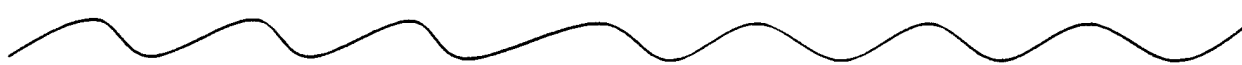
Our next example is given by the profile $f(x) = \frac{h}{2} (\cos(2\pi x) + \cos(4\pi x))$. In this
10 example we have $h = 0.01$ and $\lambda = 0.025$.



Scattering Direction #	Scattered Energy	Order 0	Order 1	Order 5	Order 9	Order 11	Order 15
0	1.983702874853860e-01	1.4e-3	6.7e-6	6.3e-10	1.8e-13	5.0e-15	0.0e-16
1	2.125625186015414e-02	4.3e-3	7.3e-6	8.6e-10	4.6e-14	4.9e-16	0.0e-16
2	5.109656298137152e-02	4.2e-3	5.3e-6	1.3e-9	3.5e-14	6.9e-15	0.0e-16
3	1.350594564861170e-01	1.1e-3	3.0e-6	1.8e-10	5.1e-14	6.9e-16	0.0e-16
4	1.670755436364386e-02	4.3e-3	928e-6	1.5e-9	1.8e-13	0.0e-14	0.0e-16
5	1.041839113172000e-01	8.7e-4	1.1e-5	4.7e-10	3.8e-14	0.0e-16	0.0e-16
6	3.029977474761340e-02	7.6e-4	1.1e-5	4.8e-10	1.0e-15	2.0e-15	0.0e-16
7	2.828409217693459e-02	2.5e-3	3.2e-5	1.8e-9	3.5e-14	4.6e-15	6.1e-16

Our last example is a third order "Stokes" wave (cf. [9]) given by

$$f(x) = \frac{h}{2} (-\cos(2\pi x) + 0.35 \cos(4\pi x) - 0.035 \cos(6\pi x)). \text{ Here } h = 0.03 \text{ and } \lambda = 0.025.$$



Scattering Direction #	Scattered Energy	Order 0	Order 1	Order 5	Order 9	Order 13	Order 17
0	1.168946586556380e-01	1.1e-3	2.1e-6	1.0e-9	1.8e-12	8.5e-15	0.0e-16
1	1.259788401686170e-01	1.1e-3	1.0e-5	9.0e-10	5.8e-13	7.9e-15	0.0e-16
2	7.407393363864252e-03	3.2e-3	2.7e-5	3.6e-9	1.9e-12	9.6e-15	0.0e-16
3	2.657137880809774e-02	5.1e-3	1.8e-5	1.3e-9	4.1e-13	1.4e-14	1.0e-15
4	4.889524445075034e-02	2.5e-5	1.7e-5	1.9e-9	2.4e-13	9.9e-16	2.8e-16
5	1.497662001023263e-02	4.7e-3	2.7e-5	3.6e-9	1.4e-12	1.3e-14	0.0e-16
6	1.617786430146189e-03	1.4e-2	5.9e-6	2.0e-9	9.0e-13	2.8e-14	1.9e-15
7	2.523077976253081e-02	5.4e-3	6.9e-6	6.7e-10	1.1e-12	2.8e-14	0.0e-16

Our implementation of this method is very efficient. All the functions considered are decomposed in their Fourier series. The largest run time is 22 sec for the order 17 calculation presented in the table above on a DEC Alpha workstation (600MHz). A more typical run for the order 11 calculation presented
5 in the second example took 3 seconds.

Thus it will be appreciated from the above that as a result of the present invention, a method for computing a scattered field resulting from an incident wave being reflected from a rough surface is provided by which the principal objectives, among others, are completely fulfilled. It will be equally apparent and
10 is contemplated that modification and/or changes may be made in the illustrated embodiment without departure from the invention. Accordingly, it is expressly intended that the foregoing description and accompanying drawings are illustrative of preferred embodiments only, not limiting, and that the true spirit and scope of the present invention will be determined by reference to the appended
15 claims and their legal equivalent.

CLAIMSWhat is claimed is:

- 1 1. A method of computing a scattered field resulting from an incident
- 2 wave being reflected from a rough surface, a surface current being induced by
- 3 the incident wave, comprising the steps of:
- 4 representing the surface current as high-order high-frequency
- 5 expansion;
- 6 substituting a surface current ansatz into the surface current
- 7 integral equation, wherein a surface current series expansion is formed having a
- 8 high frequency order, the surface current series expansion including an
- 9 oscillatory integral and surface current coefficients;
- 10 producing an asymptotic expansion of the oscillatory integral;
- 11 evaluating the asymptotic expansion for the surface current
- 12 coefficients;
- 13 inserting the surface current coefficients into the surface current
- 14 series expansion;
- 15 evaluating the surface current series expansion for the surface
- 16 current; and
- 17 computing the scattered field based upon the solved surface
- 18 current.

1 2. The method of Claim 1 wherein the step of producing an
2 asymptotic expansion includes the steps of:
3 forming a Taylor series that includes a non-convergent integral;
4 re-interpreting the non-convergent integral by means of analytic
5 continuation; and
6 inserting the re-interpreted non-convergent integrals into the Taylor
7 series to solve for the surface current coefficients.

1 3. The method of Claim 2 wherein the step of producing an asymptotic
2 expansion further includes the step of dividing the oscillatory integral into split
3 integrals covering separate integration regions.

1 4. The method of Claim 1 wherein the selected high frequency order
2 is preferably 20.

1 5. The method of Claim 2 further comprising the step of solving the re-
2 interpreted non-convergent integral using a closed form formula.

1 6. The method of Claim 2 further comprising the step of solving the re-
2 interpret non-convergent integral using numerical analysis.

1 7. The method of Claim 1 wherein the step of computing the scattered
2 field includes integrating the solved surface current against Green's function.

1 8. The method of Claim 1 wherein the oscillatory integral is

$$2 \quad I^n(x, k) = \int_{-\infty}^{+\infty} h(kMM') g(x, x') e^{i\alpha(x'-x) - i\beta(f(x') - f(x))} v_n(x') dx',$$

$$3 \quad \text{where; } MM' = \sqrt{(x'-x)^2 + (f(x') - f(x))^2} \quad h(t) = tH_1^1(t) \quad H_1^1 \text{ Hankel function}$$

$$4 \quad g(x, x') = \frac{f(x') - f(x) - (x' - x)f'(x')}{MM'^2} \quad \alpha = k \sin(\theta_{inc}) \quad \beta = k \cos(\theta_{inc}).$$

1 9. The method of Claim 2 wherein the Taylor series is

$$2 \quad I_+^n(x, k) = \sum_{m=0}^{+\infty} \frac{P_{n,m}^+(x)}{k^{m+1}} A + (k, m, x)$$

1 10. A method of computing a scattered field resulting from an incident
2 wave being reflected from a rough surface having a characteristic lengthscale, a
3 surface current being induced by the incident wave, the incident wave having a
4 wavelength less than the rough surface lengthscale, comprising the steps of:

5 representing the surface current as a high-order high-frequency
6 expansion;

7 substituting a surface current ansatz into the surface current
8 integral equation, wherein a surface current series expansion is formed having a
9 high frequency order, the surface current series expansion including an
10 oscillatory integral and surface current coefficients;

11 producing an asymptotic expansion of the oscillatory integral such
 12 that a Taylor series including a non-convergent integral is formed;
 13 re-interpreting the non-convergent integral by means of analytic
 14 continuation;
 15 inserting the re-interpreted non-convergent integrals into the Taylor
 16 series to solve for the surface current coefficients;
 17 inserting the surface current coefficients into the surface current
 18 series expansion;
 19 evaluating the surface current series expansion for the surface
 20 current; and
 21 integrating the solved surface current against Green's function,
 22 whereby the scattered field is determined.

1 11. The method of Claim 10 wherein the step of producing an
 2 asymptotic expansion further includes the step of dividing the oscillatory integral
 3 into split integrals covering separate integration regions.

1 12. The method of Claim 10 wherein the high frequency order is at
 2 least about three.

1 13. The method of Claim 10 further comprising the step of solving the
 2 re-interpreted non-convergent integral using a closed form formula.

1 14. The method of Claim 10 wherein the Taylor series is

2
$$I_+^n(x, k) = \sum_{m=0}^{+\infty} \frac{p_{n,m}^+(x)}{k^{m+1}} A + (k, m, x).$$

1 15. The method of Claim 10 further comprising the step of solving the
2 re-interpreted non-convergent integral using a closed form formula.

1 16. The method of Claim 15 wherein the closed form formula is

2
$$\int_0^{+\infty} v^{m+1} H_1^1(v) \cos(av) dv \quad \text{if } m \text{ even}$$

3 and

4
$$\int_0^{+\infty} v^{m+1} H_1^1(v) \sin(av) dv \quad \text{if } m \text{ odd.}$$

1 17. A solver for computing a scattered field resulting from an incident
2 wave being reflected from a rough surface having a characteristic lengthscale, a
3 surface current being induced by the incident wave, the incident wave having a
4 wavelength less than the rough surface lengthscale, comprising:

5 means for representing the surface current as a high-order high-
6 frequency expansion;

7 means for substituting a surface current ansatz into the surface
8 current integral equation, wherein a surface current series expansion is formed
9 having a high frequency order, the surface current series expansion including an
10 oscillatory integral and surface current coefficients;

11 means for producing an asymptotic expansion of the oscillatory
 12 integral such that a Taylor series including a non-convergent integral is formed;
 13 means for re-interpreting the non-convergent integral by means of
 14 analytic continuation;
 15 means for inserting the re-interpreted non-convergent integrals into
 16 the Taylor series to solve for the surface current coefficients;
 17 means for inserting the surface current coefficients into the surface
 18 current series expansion;
 19 means for evaluating the surface current series expansion for the
 20 surface current; and
 21 means for integrating the solved surface current against Green's
 22 function, whereby the scattered field is determined.

1 18. The solver of Claim 17 wherein the high frequency order is at least
 2 about three.

1 19. The solver of Claim 17 further comprising means for dividing the
 2 oscillatory integral into split integrals covering separate integration regions.

HIGH-ORDER HIGH-FREQUENCY ROUGH SURFACE SCATTERING SOLVER

ABSTRACT OF THE DISCLOSURE

The present invention provides a rough surface scattering method and solver for efficiently computing electromagnetic scattered fields resulting from an incident wave (12) being reflected from a surface slowly varying on the scale of the wavelength (10). The wavelength claimed approach to high-frequency scattering is based on the use of expansions of *high order* in parameter λ , wavelength of the incident radiation. The resulting high-order expansion approach expands substantially on the range of applicability over low order methods, and can be used in some of the most challenging cases arising in applications. The surface current (14) induced by the incident wave (12) is represented as a high-order high-frequency expansion (20). The surface current ansatz is substituted into the surface current integral equation (22), wherein a surface current series expansion is formed (24) having a high frequency order. The surface current series expansion includes an oscillatory integral and surface current coefficients. An asymptotic expansion of the oscillatory integral is produced having a Taylor series (26). The Taylor series is evaluated and the surface current coefficients (32) determined. The surface current coefficients are inserted into the surface current series expansion. The surface current series expansion is evaluated to yield the surface current (36). Finally, the scattered field is computed based upon the solved surface current (36).

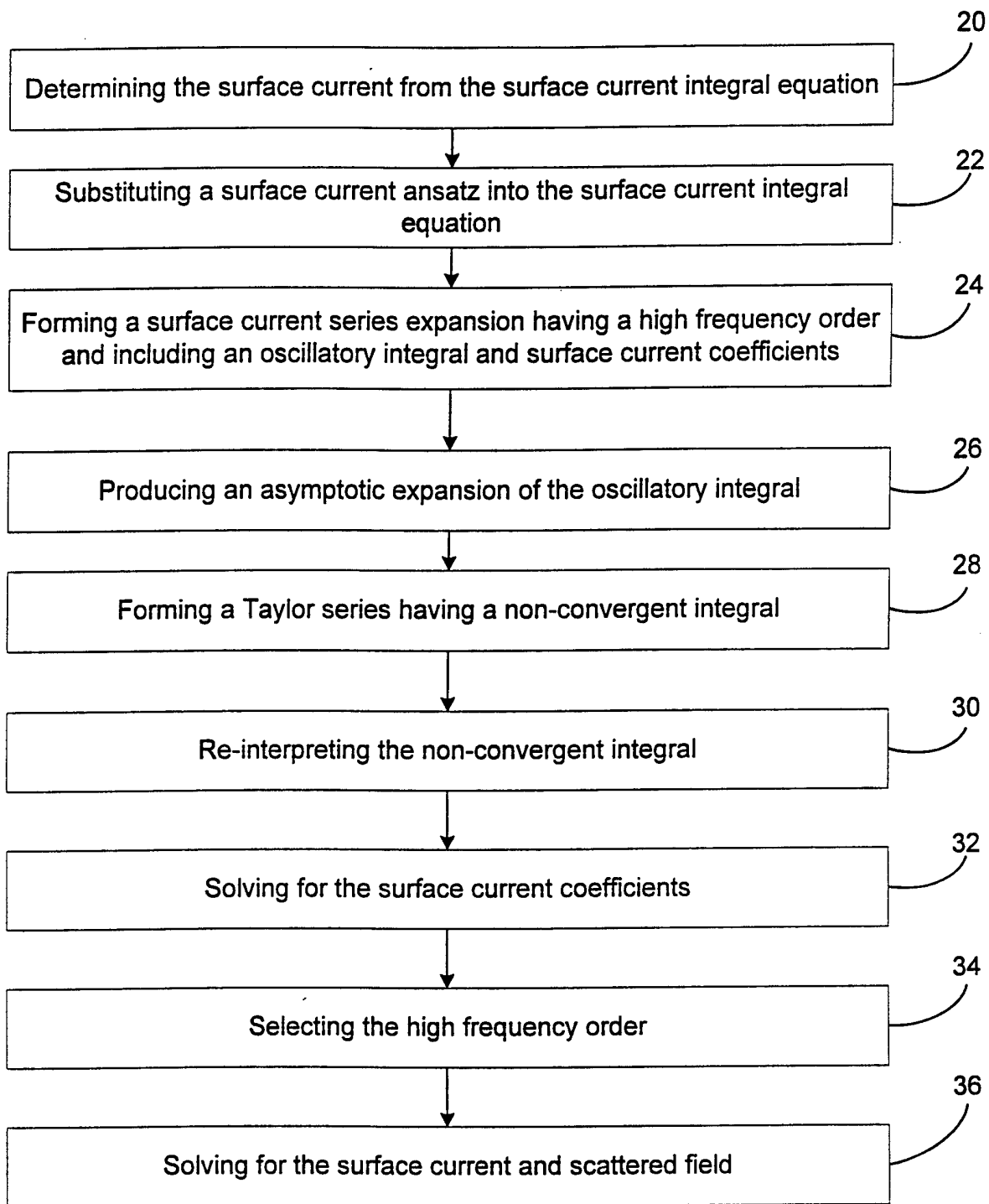


FIG. 1

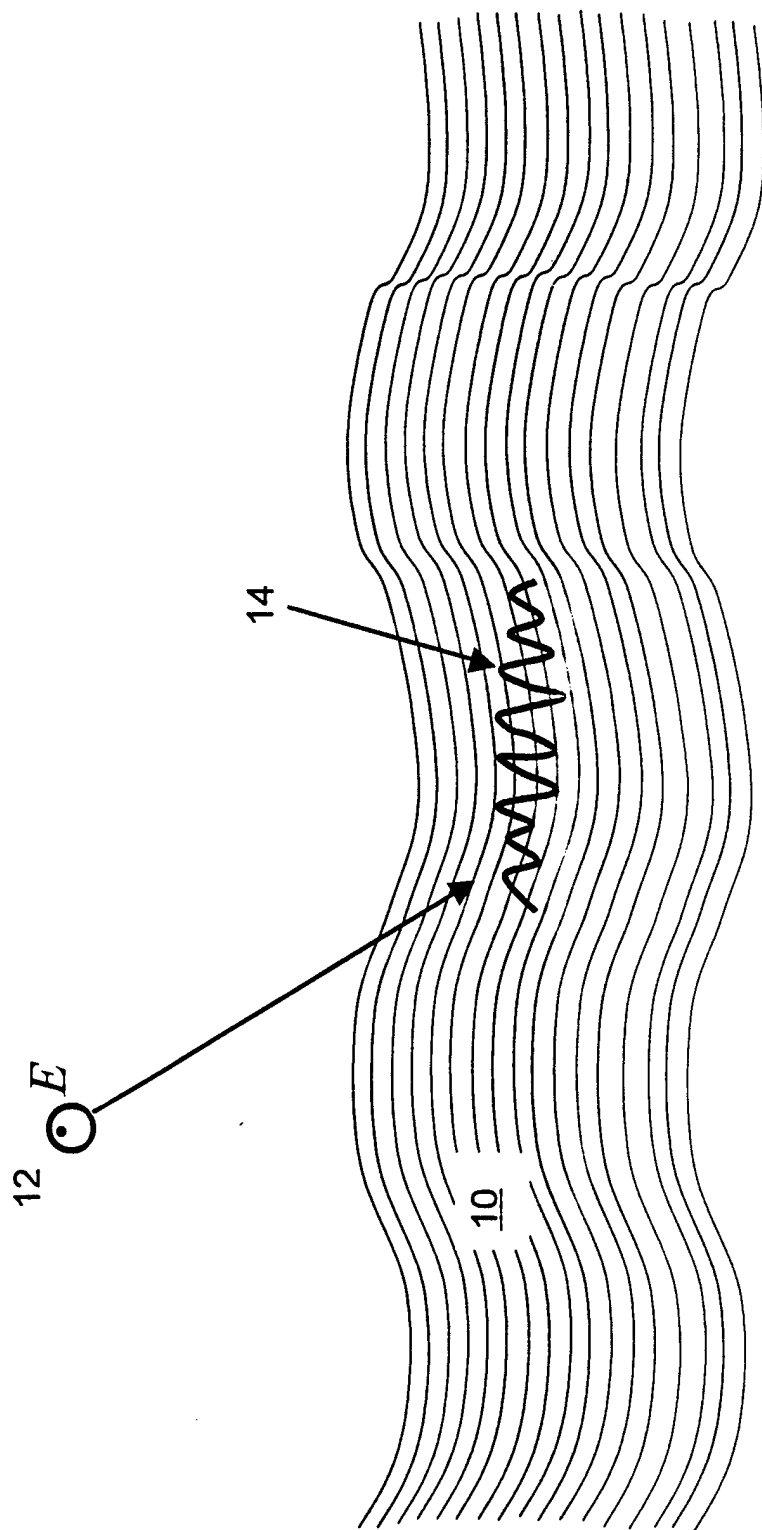


FIG. 2

Appendix C1

Electromagnetic Scattering from Multiple Scale Geometries

Contract Number: F49620-99-C-0014
Progress Report for the period: March 01-99 - July 31-99

PI: Maria Caponi
Email: mcaconi@amelia.sp.trw.com
Phone: 310-812-0079
Fax: 310-814-2359

TRW, Inc;
Ocean Technology Department
R1-1008
Redondo Beach, California 90278

2 Program Objectives:

The statement of work objectives for the first year of this program is:

Development and initial implementation of a new approach to calculate scattering from multiple scale surfaces containing large curvature and small-scale corrugations.

Initial numerical calculations for simple 2-D two scale geometries relevant to ocean applications.

Objective 1 includes:

1.a Development of a very accurate algorithm to solve high-frequency scattering problems on a smooth non-planar surface.

1.b Development of the integrated algorithm that treats the short scale surface variations (roughness) as perturbations of the long scale modulations.

3. Status of effort:

A new algorithm has been developed and implemented, and is currently being tested to calculate the scattering return from smooth, slowly varying, arbitrary surfaces (the high-frequency scattering problem) (Objective 1.a). The algorithm relies on an integral equation formulation and makes use of an innovative high-order high-frequency rigorous asymptotics expansion of the singular integrals. The method includes *all* multiple scattering terms with *no iterations* of the integral equation. The initial calculations to *third order* have been validated by comparison with a previously developed boundary variation method in the overlap region of validity. The results show an improvement of 5 orders of magnitude over Kirchhoff (0th order). Higher order calculations are currently being implemented. The integrated algorithm to calculate the scattering from short scale roughness on long scale swell surfaces (Objective 1.b) has been formulated. Initial implementation will start once the high-frequency algorithm is validated to arbitrary orders.

4. Accomplishments/New Findings

During the initial 5 months of this project the following significant research has been accomplished:

The innovative algorithm proposed at the beginning of this project to compute the scattering return from multi-scale surfaces has been formulated in detail. The algorithm consists of two main elements: A) A boundary variation method that reduces the multi-scale problem to a sequence of high-frequency scattering problems on a smooth surface. B) A new high-order, high frequency method.

The high-frequency part of this algorithm, which entails the highly accurate calculation of the scattering return from surfaces with characteristic scales larger than the radiation wavelength has been implemented and successfully validated to third order. Results that are 5 orders of

magnitude more accurate than Kirchhoff (0th order) have been obtained, demonstrating the advantages of the new method.

The implementation of the high- frequency algorithm is based on an ingenious asymptotic expansion of the highly singular integrals and on the analytic continuation of the divergent integrals. A numerically efficient version of the algorithm was found to compute accurately these expansions to *all* orders. High accuracy is crucial for this method since it will be used repeatedly to solve the general problem.

These initial results are critical to an accurate calculation of the scattering return from multiple scale surfaces, in particular for ocean surveillance applications. For example, recent experimental results have shown polarization losses of the order of -80 dB for high horizontal to vertical polarization ratios ($HH/VV > 1$) that can not be predicted with standard scattering models. The algorithm developed in this program will have enough accuracy to predict those large losses. Further, once validated, this algorithm will be able to predict radar returns not only for ocean but also for terrain relevant missions where multi-scale surfaces play a dominant role in the characteristics of the return.

5 Personnel Supported:

Dr. Alain Sei, TRW: (supported by this program ~ 65% of his time); Dr. Maria Caponi, TRW: (supported by this program <5% of her time); Dr. Oscar Bruno, MathSys and Caltech (Technical services, supporter by this program <10% of his time)

6 Publications: None on current contract period.

7 Interactions/Transitions:

Participation/presentation: Poster and VG at ACMP DARPA PI meeting. S.F. June 30-July1, 1999.

Transitions: the algorithm being developed is planned to be used in conjunction with the TRW hydrodynamic codes to obtain a predictive model of ocean radar returns. The results from this combination code will be relevant to Navy applications.

8 New Discoveries: A new method to solve the high-frequency scattering problem with high accuracy (16 digits)

9 Honors/Awards: None during current contract period

Appendix C2

Electromagnetic Scattering from Multiple Scale Geometries

Contract Number: F49620-99-C-0014
Progress Report for the period: July 31- 99 - July 31- 00

PI: Maria Caponi
Email: mcaconi@amelia.sp.trw.com
Phone: 310-812-0079
Fax: 310-814-2359

TRW, Inc;
Ocean Technology Department
R1-1008
Redondo Beach, California 90278

2. Program Objectives:

The statement of work objectives for the second year of this program were:

Parametric investigations with 2-D multi-scale code for surfaces relevant to ocean remote sensing applications

Development and initial implementation of new approach to 3-D surfaces.

These objectives have been revised to:

Validation of the 2-D high-order high-frequency code for large scale surfaces and its use in parametric investigations relevant to ocean remote sensing applications.

Formulation and implementation of the 2-D multi-scale algorithm.

Objective 1 includes

1.a. Efficient implementation of the high-frequency algorithm to arbitrary order.

Objective 2 includes:

2.a. Development of coupling between the high frequency and the boundary variation methods, including innovative use of Cauchy-Kowalesky argument for computation of high order normal derivatives.

2.b. Treatments of high-order normal derivatives through the use of Helmholtz's equation second order normal derivatives and high-order tangential derivatives to avoid hyper-singular integrals.

The revision of the objectives was due in part to the need for a more efficient and accurate implementation of the high-frequency algorithm than the one carried out during the first year of this contract. The original implementation was not easily amenable to very high order expansions therefore limiting the range and accuracy of application of the method. However, the repeated use of the high-frequency code in the final multiple scale algorithm requires double digit accuracy to arbitrary orders. The new implementation uses subtle and intensive algebraic treatments that result in a very efficient and innovative algorithm, currently being considered for a patent application. However, this revised implementation delayed the coding of the final multi-scale algorithm. Further delay also resulted from extensive validations of the results.

3. Status of effort:

The new high-order-high frequency algorithm has been extended to arbitrary order and accuracy. This extension relies on the development of a library of subroutines for the efficient algebraic treatment of infinite Taylor-Fourier series. The code has been validated by comparison with the method of variation of boundaries in the overlap region in wavelengths where both methods are valid. The code has been exercised for numerous configurations, machine precision accuracy was reached in cpu times of seconds in all cases (Rev. objective 1). A detailed formulation of the multiple-scale algorithm including an innovative coupling of the

new high-order high frequency method and the boundary variation method has been completed and implemented. The details of the method have been documented. The complete Fortran implementation of the integrated algorithm is expected in the next few weeks. Currently, each segment of the Fortran code is being carefully tested and verified (Rev. objective 2). Afterwards, careful parametric investigations relevant to ocean remote sensing will be performed.

4. Accomplishments/New Findings

During the last year the following significant accomplishments have been reached in this project:

- 1 A library of subroutines for the efficient algebraic treatment of infinite Taylor-Fourier series was completed. These series were introduced specifically by us to meet the accuracy and efficiency demands of this project.
- 2 Full double precision agreement was obtained between the high-order high-frequency method and the boundary variation method for numerous and varied examples throughout the overlap region in wavelengths where both methods are valid. Computing times of the order of seconds on a 600MHz desktop workstation were achieved in all cases. The high-frequency code was also validated and exercised in the high-frequency regime (wavelength < surface scale length) for configurations of interest to ocean remote sensing where the boundary variation code failed.
- 3 The details of this highly innovative high-frequency algorithm are currently being considered by TRW for a patent application.
- 4 The high frequency algorithm has been integrated with the method of variation of boundaries to yield a highly accurate and efficient multiple-scale solver. The high order nature of the algorithm requires an inventive use of the Cauchy-Kowalevsky argument. A method has been derived for the evaluation of the necessary high-order normal derivatives, (which would normally give rise to hyper-singular integrals) through the use of the Helmholtz equation, the second normal derivative and the high-order tangential derivatives. These tangential derivatives, in turn, are computed through an application of the Taylor-Fourier algebra mentioned in 1 above. The second normal derivative is computed directly by manipulations of the kernel singularities.

This integrated code, currently being tested, is expected to be the most efficient and accurate solver for the computation of scattered waves from multi-scale rough surfaces. A code with these characteristics is necessary for current ocean and terrain remote sensing applications, given the small scattering returns relative to the incident field.

5. Personnel Supported:

Dr. Alain Sei, TRW: (supported by this program ~ 65% of his time);

Dr. Maria Caponi, TRW: (supported by this program < 5% of her time);

6 Publications:

The results of these investigations are documented in the following papers:

O. Bruno, A. Sei, and M. Caponi; "*High order, high frequency solvers for rough surface scattering problems*". In Proceedings of the 2001 IEEE AP-S International symposium and USNC/URSI National Radio Science meeting, July 2001, Boston, Massachusetts, USA.

A. Sei, M. Caponi and O. Bruno, "*Polarization Ratios Anomalies of 3D Rough Surface Scattering as Second Order Effects*". in Proceedings of the 2001 IEEE AP-S International symposium and USNC/URSI National Radio Science meeting, July 2001, Boston, Massachusetts, USA.

7 Interactions/Transitions:

Participation/presentation:

Participation in the AFOSR Electromagnetic workshop, San Antonio, Jan 2001.

Presentation to DARPA PI meeting Washington D.C., April 2001.

Transitions:

A detailed study of polarization anomalies has been performed in 3D using the previously developed method of variation of boundaries. This study is still on-going and a statistical study similar to the one performed last year in two dimensions is envisioned. This study is of interest a particular Navy customer.

Discussion with the government are on going for application of these methods to problems of interest to the Navy, this is expected to result in a transition follow on project. This follow on project will include the use of the numerical code in conjunction with the TRW hydrodynamic codes to calculate the time evolution of radar return from evolving relevant ocean surfaces and the appropriate calculation of the associate Doppler spectrum in both the TE (H) and the TM (V) polarization. In addition experimental validation of the algorithm will be carried out using the TRW testing facilities.

8 New Discoveries:

A new method to solve multi-scale scattering problems under TE polarization has been developed implemented and validated.

A new method to solve high-frequency scattering problems under TM polarization with machine precision accuracy has been implemented and validated.

9 Honors/Awards:

None this year.



Dr. Oscar Bruno, MathSys and Caltech (Technical services, supported by this program < 10% of his time)

6. Publications:

The investigations and results of this program are documented in the following papers:

O. Bruno, M. Caponi and A. Sei; "*An innovative high-order method for electromagnetic scattering from rough surfaces.*" In Proceedings of the National Radio Science Meeting, 4-8 January, 2000, Univ. of Colorado, Boulder, USA

O. Bruno, A. Sei and M. Caponi, "*Rigorous multi-scale solver for rough-surface scattering problems: high-order-high-frequency and variation of boundaries*". To appear in Proceedings of the NATO meeting on Low Grazing Angle Clutter: Its characterization, measurement and application. April 2000, Laurel, Maryland, USA.

O. Bruno, A. Sei, and M. Caponi; "*High order, high frequency solution of rough surface scattering problems*". In Proceedings of the fifth international conference on mathematical and numerical aspects of wave propagation, Santiago de Compostella, Spain, July 2000, pp. 477-481.

O. Bruno, A. Sei and M. Caponi; "*High order high frequency solutions of rough surface scattering problem*", in final preparation, to be send for publication to Radio Science, Aug. 2000.

A claim has been recently sent to the TRW lawyers (July 2000) to obtain permission to file a patent on the invention of the high frequency high order algorithm for solution of rough surface scattering problems.

7. Interactions/Transitions:

Participation/presentation:

Poster presentation in AFOSR San Antonio Electromagnetic Workshop, Jan. 2000.

Presentation to DARPA PI meeting Washington D.C., April 2000.

Transitions: the algorithm being developed is intended to be used in conjunction with the TRW hydrodynamic codes to obtain a predictive model of ocean radar returns. The results from this combined code will be extremely relevant to Navy applications. In the mean time, a tailored version of the boundary variation method code has been used to perform a statistical study of the polarized backscattering returns associated with ocean spectra characteristic of near breaking long waves for a particular Navy customer. This study, still ongoing, will be extended to larger spectral bandwidths once the multi-scale code is completely implemented and validated.

8. New Discoveries:

A new method to compute the high-frequency scattering problem to arbitrary orders with machine precision has been implemented.

A new method to solve the multi-scale scattering problems has been developed and implemented.

9. Honors/Awards:

Dr A. Sei chaired the three sessions on scattering at the fifth international conference the mathematical and numerical aspects of wave propagation, Santiago de Compostella, Spain, July 2000.

Appendix C3

Electromagnetic Scattering from Multiple Scale Geometries

Contract Number: F49620-99-C-0014

Progress Report for the period: July 31- 00 - July 31- 01

PI: Maria Caponi

Email: mcaconi@amelia.sp.trw.com

Phone: 310-812-0079

Fax: 310-814-2359

TRW, Inc;

Ocean Technology Department

R1-1008

Redondo Beach, California 90278

2. Program Objectives:

The statement of work objectives for the third year of this program were:

Detailed parametric investigations for 3-D surfaces relevant to applications of interest. (E.g. 2 and 3 scale modulated wave geometries with different modulations and/or scales in each dimension).

For the first half of the third year, these objectives have been revised to:

Implementation and validation of the 2-D TE multi-scale code for surfaces including a range of scales and its use in parametric investigations relevant to ocean remote sensing applications.

Formulation of the 2-D TM multi-scale algorithm.

The goal for the rest of the third year of this program is to implement the TM multiscale algorithm and exercise it in conjunction with the multiscale TE

Objective 2 includes

2. 1. Formulation and implementation of the high-frequency algorithm to arbitrary order under TM polarization.
2. 2. Development of coupling between the high frequency and the boundary variation methods, including innovative use of Cauchy-Kowalesky argument for computation of high order normal derivatives in the TM case.
- 2.3. Treatment of high-order normal derivatives through the use of Helmholtz's equation, second order normal derivatives and high-order tangential derivatives to avoid hyper-singular integrals. This involves implementing the Neumann to Dirichlet map and its tangential derivatives.
- 2.4. Integration of previous modules for a general fully accurate TM multi-scale scattering code and parametric studies relevant to oceanic scattering.

The revision of the objectives was a requirement for a more efficient and accurate implementation of the high-frequency algorithm. The original implementation was not amenable to very high order expansions therefore limiting the range and accuracy of application of the method. However, the repeated use of the high-frequency code in the final multiple scale algorithm requires double digit accuracy to arbitrary orders.

3. Status of effort:

The essential modules for the **TE multi-scale algorithm** (high-order high-frequency solver, Dirichlet to Neumann map implementation) have been integrated to yield a highly accurate and efficient code. Extensive optimization and validation of the code have been done by comparison with the method of variation of boundaries in the overlap region in wavelengths where both methods yield accurate results. The code has been exercised for numerous configurations, machine precision accuracy was reached in cpu times of minutes in all cases (**objective 1**). A

detailed formulation of the **high-order high frequency solver in the TM** case has been documented and implemented. This solver has been optimized and extensively validated by comparison with the method of variation of boundaries in the overlap region in wavelengths where both methods yield accurate results. In all cases CPU times of the order of seconds yield full double precision accuracy (**objective 2.1**).

The **multiscale TM algorithm**, involving the **coupling** between the high-frequency TM algorithm and the boundary variation methods as well as the treatment of high-order normal derivatives (and its crucial part the Neumann to Dirichlet map) have been formulated and documented (**objective 2.2 and 2.3**). The Fortran implementation of the integrated algorithm is expected to be completed in the next few months. By the end of this third year the code will be exercised and careful parametric investigations relevant to ocean remote sensing will be performed.

4. Accomplishments/New Findings

During the last year the following significant accomplishments have been reached in this project:

- 5 Full double precision agreement was obtained between our new multi-scale method under TE polarization and the boundary variation method for numerous and varied examples throughout the overlap region in wavelengths where both methods are valid. Computing times of the order of minutes on a 600MHz desktop workstation were achieved in all cases.
- 6 The high-order high frequency algorithm has been formulated and implemented for the TM case. The code was validated by comparison with the method of variation of boundary (in the region of overlapping validity) for numerous examples. On a 600MHz desktop workstation, full double precision accuracy was achieved in CPU times of seconds.

Our current **TE multi-scale solver** (as well as the shortly expected TM multi-scale solver) is the most efficient and accurate solver for the computation of scattered waves from multi-scale rough surfaces. A code with such high accuracy requirements (full double precision) and speed is a necessary tool for the study of current ocean and terrain remote sensing applications, given the small scattering returns relative to the incident field.

The formulation of the **multiscale TM algorithm** has been completed and is in the process of implementation.

5 Personnel Supported:

Dr. Alain Sei, TRW: (supported by this program ~ 70% of his time);

Dr. Maria Caponi, TRW: (supported by this program < 1% of her time);

Dr. Oscar Bruno, MathSys and Caltech (Technical services, supported by this program < 10% of his time)

Appendix C4

Electromagnetic Scattering from Multiple Scale Geometries

Contract Number: F49620-99-C-0014

Progress Report for the period: July 31- 01 - December 31- 01

PI: Maria Caponi

Email: mcaconi@amelia.sp.trw.com

Phone: 310-812-0079

Fax: 310-814-2359

TRW, Inc;

Ocean Technology Department

R1-1008

Redondo Beach, California 90278

2. Program Objectives:

The statement of work objectives for the third year of this program were modified in the progress report for the period 07/31/00 – 07/31/01 (see appendix below). They consisted of the two following objectives:

Implementation and validation of the 2-D TE multi-scale code for surfaces including a range of scales and its use in parametric investigations relevant to ocean remote sensing applications.
Formulation of the 2-D TM multi-scale algorithm.

The goal for the rest of the third year of this program is to implement the TM multiscale algorithm and exercise it in conjunction with the multiscale TE

Objective 2 includes

2. 1. Formulation and implementation of the high-frequency algorithm to arbitrary order under TM polarization.

2. 2. Development of coupling between the high frequency and the boundary variation methods, including innovative use of Cauchy-Kowalesky argument for computation of high order normal derivatives in the TM case.

2.3. Treatment of high-order normal derivatives through the use of Helmholtz's equation, second order normal derivatives and high-order tangential derivatives to avoid hyper-singular integrals. This involves implementing the Neumann to Dirichlet map and its tangential derivatives.

2.4. Integration of previous modules for a general fully accurate TM multi-scale scattering code and parametric studies relevant to oceanic scattering.

3. Status of effort:

The objectives 1, 2.1 and 2.2 were accomplished last year. In the period August 1st 2001, December 31st 2001 objectives 2.2 and 2.3 were implemented and tested. The implementation of the Neumann to Dirichlet map (similar to the implementation of the Dirichlet to Neumann map) yielded full double precision agreement with the method of variation of boundaries. The tests used a shallow surface where Rayleigh hypothesis holds. This meant that the Rayleigh series expansion (Plane wave expansion) of the scattered field converged uniformly and absolutely on the surface. Therefore the Neumann to Dirichlet map could be computed by direct differentiation of the Rayleigh series.

The derivation and implementation of the general right hand side for an arbitrary order was then tested first in the case of a plane to arbitrary high order, where the method of variation of boundaries yielded the reference solution in closed form. Then the general right hand side was tested for orders up to 5 by comparison of the numerical results from our code to an algebraic

manipulator (Maple). Again in this case full double precision agreement was obtained (**Objective 2.3**). The integration of the Neumann to Dirichlet module, the computation of the general right hand side and the high frequency solver was then the final step towards a general multiscale scattering solver in TM polarization. The implementation was completed and testing showed that accuracy of 9 to 10 digits was achieved in configuration similar to those tested in the TE case (**Objective 2.4**). The testing and debugging of the code however had to be interrupted in December due to lack of funding.

4. Accomplishments/New Findings

During the last six months of this project, the following significant accomplishments have been reached:

- 7 Full double precision agreement of the computation of the Neumann to Dirichlet map was obtained between our method based on single layer potentials and the Rayleigh series expansion.
- 8 The general right hand side for the general high frequency problem in TM polarization was successfully tested against the method of variation of boundary (in the case of a plane) and against an algebraic manipulator (Maple) for a general configuration up to order 5.
- 9 The general multi-scale solver in TM polarization was integrated and gave results with accuracy of 9 to 10 digits in general configurations in CPU times of minutes. Further improvement in the accuracy had to stop however due to lack of funding.

5 Personnel Supported:

Dr. Alain Sei, TRW: (supported by this program ~ 70% of his time);

Dr. Maria Caponi, TRW: (supported by this program < 1% of her time);

Dr. Oscar Bruno, MathSys and Caltech (Technical services, supported by this program < 10% of his time)

6 Publications:

None this period

7 Interactions/Transitions:

None this period

8 New Discoveries:

A new method to solve multi-scale scattering problems under TM polarization has been developed implemented and validated.

9 Honors/Awards: None this year.